The role of mouse zinc-sensing GPR39 receptor in memory functions associated with Alzheimer's disease

by

Michał Rychlik

a PhD thesis

written under the supervision of

Professor Katarzyna Młyniec

at the Department of Pharmacobiology,

Faculty of Pharmacy,

Jagiellonian University Medical College

Cracow, 2021

Table of contents

List of abbreviations

2-AG - 2-Arachidonoylglycerol

Actb - actin beta

AD - Alzheimer's disease

AMPAR - α-amino-3-hydroxy-5-methyl-4-isoxazolepropionic acid receptor

ApoE-ε4 - apolipoprotein E-ε4

APP - amyloid precursor protein

Aβ - amyloid beta

BDNF - brain-derived neurotropic factor

CA - cornu ammonis

CI - consolodation interfereance

Clu - clusterin

CREB - cAMP response element binding protein

ELM - episodic-like memory

ERK 1/2 - extracellular signal-regulated kinase 1/2

GABA - γ-aminobutyric acid

GABAA1 - gamma-aminobutyric acid type A receptor alpha 1

GABAB3 - gamma-aminobutyric acid type A receptor subunit beta3

Gabra5 - gamma-aminobutyric acid type A receptor subunit alpha5

Gabrb3 - gamma-aminobutyric acid type A receptor subunit beta3

Gabrg2 - gamma-aminobutyric acid type A receptor subunit gamma2

GluA2 - glutamate ionotropic receptor AMPA type subunit 2

Gpx1 - glutathione peroxidase 1

Gria1-4 - glutamate ionotropic receptor AMPA type subunit 1-4

Gria2 - glutamate ionotropic receptor AMPA type subunit 2

Grin1 - glutamate ionotropic receptor NMDA type subunit 1

Grin2a - glutamate ionotropic receptor NMDA type subunit 2A

Grin2b - glutamate ionotropic receptor NMDA type subunit 2B

GSK-3b - glycogen synthase kinase 3b

HET - heterozygote

ip - intraperitoneal

ISI - inter-stage interval

KCC2 - potassium/chloride cotransporter 2

KO - knockout

LTD - long-term depression

LTP - long-term potentiation

Mapk1-3 - mitogen-activated protein kinase 1-3 (ERK1/2)

Mapt - microtubule associated protein tau

MCI - mild cognitive impairment

MF - mossy fibres

mPFC - medial prefrontal cortex

Mtor - mechanistic target of rapamycin kinase

MWM - Morris water maze

NFT - neurofibrillary tangles

NMDAR - *N*-methyl-D-aspartate receptor

OD - old displaced object

OS - old stationary object

PAM - positive allosteric modulator

PCR - polymerase chain reaction

PET - positron emission tomography

PLC - phospholipase C

PM - procedural memory

PP - perforant pathway

PP2A - protein phosphatase 2A

PR1 - parameter measuring temporal order memory (ELM test)

PR2 - parameter measuring spatial location memory (ELM test)

PR3 - parameter measuring integrated spatiotemporal memory (ELM test)

qRT-PCR - quantitative real-time polymerase chain reaction

RD - recent displaced object

RS - recent stationary object

SC - Schaffer collaterals

SDS - sodium dodecyl sulphate

SDS-PAGE - SDS-Polyacrylamide Electrophoresis

Slc12a5 - solute carrier family 12 member 5 (KCC2)

SM - spatial memory

TrkB - tyrosine receptor kinase B

WT - wild-type

ZnT3 - zinc transporter 3

Abstract

In the mammalian brains synaptic zinc acts as a neuromodulator and a neurotransmitter. Synapses are also where toxic forms of amyloid beta (Aβ) are formed, which is the first step of a pathological cascade leading to Alzheimer's dementia (AD) in humans. Evidence gathered over the span of last 25 years shows that synaptic zinc exacerbates the effects of Aβ; and, that by binding zinc Aβ disrupts the physiological functions of the ion. One of the most understudied physiological functions in this regard is neurotransmission through the zincergic GPR39 receptor.

The main aim of this work was to establish whether GPR39 modulates memory in mice, especially: an analogue of declarative memory affected in early stages of AD in humans i.e. episodic memory. Secondly, the effects of both acute and chronic pharmacological manipulations of GPR39 with its agonist (TC-G 1008) on declarative memory of mice were investigated; as well as, the effect of GPR39 knock-out (KO) on the action of memantine – a drug used in pharmacotherapy of AD. Lastly, the procognitive potential of both drugs was tested in a model of neurodegeneration – the constitutive heterozygous KO of brain-derived neurotropic factor (*Bdnf*). The battery of behavioral tests used in this work consisted of the episodic-like memory (ELM) test, the Morris Water Maze (MWM) and the modified rota-rod test of procedural memory. In order to explore the molecular underpinnings of GPR39 activity in the hippocampus, *ex vivo* measurements of selected proteins (Western blotting) and mRNA (qRT-PCR) were conducted.

Genetic and acute pharmacological manipulations of the GPR39 suggest the receptor is functionally involved in declarative, but not procedural memory of mice. Chronic TC-G 1008, however, did not affect neither ELM, nor spatial memory. No clear effect of acute memnatine was observed, while chronic memantine had a tendency to improve the spatial component of ELM in both wild-type and KO male mice; as well as, disrupted spatial memory of GPR39 KO mice in the MWM. Mice with lower expression of BDNF displayed an impairment (but not loss of function) of spatial memory in the MWM, which was unaffected by either TC-G 1008 or memantine administered chronically. The results of *ex vivo* molecular experiments point to both excitatory and inhibitory neurotransmission as being affected by GPR39 manipulations, but the pattern of the observed changes does not offer a clear mechanistic explanation of the behavioral results.

Introduction

1. Alzheimer's disease

Epidemiology

It is estimated that around 60-70% of dementias worldwide are of Alzheimer's type (Prince *et al.*, 2015). In 2015 this amounted to 28-33 million people of the 47 million affected by dementia - figures that will have tripled until 2050 (*ibidem*). Around 98-99% of Alzheimer's disease (AD) patients are over 60 years of age and aging seems to be the most important factor for the development of AD. The remaining 1-2% of AD cases are observed in people aged 30-60, and this early onset AD is closely linked to genetic factors, such as mutations in the amyloid precursor protein (APP) and presenilins 1 and 2 genes (*ibidem*). Thus, early onset AD runs in around 520 families spread all over the world (Ebenezer, 2015) and is often referred to as familial AD. Regardless of the leading cause, life-style related factors such as diet, physical exercise, educational attainment, obesity and diabetes also heavily influence the risk of AD development, which corresponds to the fact that 60% of people with dementia live in low and middle income countries (Prince *et al.*, 2015). Lastly, gender has been shown to affect both the risk of AD and the course of the disease (Podcasy and Epperson, 2016). Old women (>65 years of age) are: almost twice as prone to the development of AD as old men; display faster progression of the clinical symptoms and neuropathology; and – at the same time - have a longer life span during the course of AD, with female sex being a predictor of longevity in patients with a good response to pharmacotherapy (*ibidem*).

History and current definition

In 1901 Alois Alzheimer - a German psychiatrist and neuropathologist - examined a 51 year old Auguste Deter, who was admitted to an asylum in Frankfurt after her husband had become worried by progressive changes in her behavior over the course of the previous year (Maurer, Volk and Gerbaldo, 1997). These would include jealousy, loss of memory and disorientation (*ibidem*). Further examination revealed that the woman suffered from auditory hallucinations, delusions, anxiety and psychosocial deficits. The symptoms were commonly observed by the physician, albeit in much older patients, therefore Alzheimer became highly interested in Augustes' "presenile dementia" and requested her to remain in the asylum, until her death 5 years later, in order to study the patient's brain *postmortem* (*ibidem*). A detailed description of both clinical symptoms and neuropathological changes of this new form of

dementia was presented in 1906 at a conference in Tubingen, published the following year, and made famous as "Alzheimer's disease" by Emil Kraeplin, who included it in the 8th edition of his Handbook of Psychiatry in 1910 (*ibidem*). Apart from indications of brain loss, such as enlarged sulci, Alzheimer observed histopathological changes that to this day remain the main factor for differential diagnosis of the disorder from other causes of dementia (Jack *et al.*, 2018): extracellular neuritic plaques and intracellular neurofibrillary tangles (NFTs).

It is only recently that these defining biomarkers of AD have become possible to reliably quantify *in vivo*, and throughout the 20th century, as well as at the beginning of the 21st century, a definite diagnosis of AD could be made only *postmortem*. Nonetheless, AD existed as a clinical entity diagnosed *antemortem* and was defined by various symptoms that changed over the course of 100 years since Alzheimer's original description (Knopman, Petersen and Jack, 2019). Up until 1970's, AD was thought to be a form of presenile dementia, similar to the condition of Auguste Deter (*ibidem*). This changed in the 1980's, when cognitive impairment at any age caused by neuritic plaques and NFTs was considered AD. Since neuropathology could be evaluated only *postmortem*, a diagnostic term of "probable AD" was used and defined as an acquired, progressively worsening amnestic disorder, with functional consequences in daily life (*ibidem*). Around 80% of individuals diagnosed with probable AD exhibited AD neuropathology, as did around 30% without clinical symptoms of the disorder (*ibidem*). With the development of more sensitive neuropsychological diagnostic tools in the 1990's, it became apparent that decline in cognition can be detected before functional impairment in daily life. Hence, a new category of mild cognitive impairment (MCI) was established and considered a prodromal phase of AD (*ibidem*). Subsequently, it was discovered that around 30% of MCI individuals, who go on to develop symptoms of dementia, have no indication of AD-like neuropathology (*ibidem*). Moreover, another level of complexity was introduced by concurrent developments in basic molecular research of AD.

In the 1980's the amyloid beta (Aβ) protein was identified as the core of extracellular neuritic plaques, which additionally consist of degenerating dendrites and axons until these prats of neurons are destroyed by microglial cells (Glenner and Wong, 1984). The Aβ peptide was found to consist of 39 to 43 amino acids and to be a part of a larger protein of 695 amino acids, named amyloid precursor protein (APP), as APP was discovered in the course of investigating Aβ (Hardy and Selokoe, 2002). The gene encoding APP is located at chromosome 21, trisomy of which causes Downs syndrome that is characterized by neuropathology similar to AD (*ibidem*). In the early 1990's it was discovered that: 1) Aβ is a normal product of APP metabolism; 2) Aβ production is enhanced by mutations of presenilin 1 and 2 genes, which

encode parts of the γ-secretase protease responsible for the cleavage of APP; 3) genetic mutations of *APP* that lead to AD are located at sites where the protein is cleaved by α-, β- and γ-secretases; 4) mutations in a gene encoding apolipoprotein E (ApoE-ε4), responsible for phospholipid clearance, are a risk factor for AD (Hardy and Selokoe, 2002; Selkoe and Hardy, 2016).

Taken together, these studies led to the development of the "amyloid cascade" hypothesis of AD, which states that abnormal deposition of fibrillary Aβ in the extracellular space, due to either its overproduction, decreased clearance, or both, subsequently - over the course of many years - leads to neuropathological changes and dementia (Hardy and Higgins, 1992). With the introduction of ^{11}C Pittsburgh compound B positron emission tomography (PET) in the early 2000's, which enabled measurement of Aβ deposits in human brains *in vivo* (Klunk *et al.*, 2004), the amyloid cascade hypothesis was weakened by a confirmation of earlier *postmortem* studies showing little or no correlation between the levels of Aβ plaques in the brain, and cognitive disturbances (Ingelsson *et al.*, 2004, Villemagne *et al.*, 2011). Simultaneously, a correlation of dementia with the levels of NFTs was observed (Ingelsson *et al.*, 2004; Villemagne *et al.*, 2014). Since NFTs are also a histopathological hallmark of other neurodegenerative disorders that lead to cognitive decline, such as fronto-temporal dementia, it became clear that Aβ plaques in AD "(…) lead to many downstream cellular and molecular changes (e.g., microgliosis, neuritic dystrophy, tangles, etc.) that are more proximate to and causative of neuronal dysfunction" (Selkoe and Hardy, 2016).

A large body of research into soluble, nonfibrillar forms of Aβ was prompted by the discovery of high neurotoxicity of Aβ oligomers (dimers, trimers) in 1998 (Lambert *et al.*, 1998). These studies, conducted over the course of last 20 years, have shown that Aβ oligomers are responsible for the majority of the neuropathology observed in AD, including: synaptic plasticity dysfunction, microglia hyperactivation, loss of synaptic connections, receptor redistribution, oxidative stress, and – finally – hyperphosphorylation of the Tau protein, which leads to the formation of NFTs (reviewed in: Cline *et al.*, 2018). Therefore, it can be stated that the first step of the amyloid cascade hypothesis i.e. abnormal APP processing into Aβ, remains a highly probable distal cause of AD, but establishing a link between Aβ, NFTs, neuropathology and clinical symptoms of AD is an ongoing endeavor.

In 2018 this matter was recognized by the National Institute on Aging and Alzheimer's Association workgroups (Jack *et al.*, 2018), which redefined their previous, widely-accepted, conceptualization of AD as a clinical-pathologic construct (McKhann *et al.*, 2011). The new proposal is a research framework for a disease defined by a certain profile of biomarkers

independent from clinical symptoms, which will eventually lead to solutions that can be adopted in clinical practice (Jack *et al.*, 2018). This novel approach was inspired by substantial progress made since 2011 in validating AD-specific biomarkers and expanding their measurement techniques in humans, which includes: confirmation that Aβ PET scans yield results similar to *postmortem* measurements; confirmation of $A\beta_{42}$ or $A\beta_{42}/A\beta_{40}$ ratio in cerebrospinal fluid as a valid proxy of Aβ brain pathology; and, the development of pathologic Tau (i.e. paired helical filaments) PET scans (Jack *et al.*, 2018). Moreover, methods commonly used in AD research to evaluate neurodegeneration have been verified as not specific for AD. These include: magnetic resonance imaging of structural changes; fluorodeoxyglucose PET imaging of brain metabolism; and, the measurement of total Tau in cerebrospinal fluid (*ibidem*).

Therefore, the National Institute on Aging and Alzheimer's Association workgroups' proposal was to restrict the term AD to individuals with abnormal markers of amyloidosis (A, these include: high Aβ PET levels or low levels of $A\beta_{42}$ or $A\beta_{42}/A\beta_{40}$ ratio in cerebrospinal fluid), *and* abnormal markers of tauopathy (T, which includes: high pathologic Tau PET levels or elevated levels of phosphorylated Tau in cerebrospinal fluid) (*ibidem*). Individuals with biomarker evidence of amyloidosis (A+), but without abnormal tauopathy biomarkers (T-) would be classified as "Alzheimer's pathologic change", and regarded an earlier phase of "Alzheimer's continuum", with the later phase (A+T+) being AD. With the addition of the abovementioned 3 biomarkers of neurodegeneration (N), that are not specific for AD diagnosis, but are helpful in evaluating the progression of the disease, the workgroup adopted the AT(N) biomarker grouping system (Jack *et al.*, 2016) into a broad classification system of research participants. Based on their biomarker profile, an individual can be classified as "normal" (A-T-(N)-), being on "Alzheimer's continuum" (**A+**T+/-(N)+/-) or "suspected non-Alzheimer's pathophysiology" (SNAP, **A-** and either T+ or (N)+ or both T and (N) +). This classification will be used in the next section in order to pinpoint a memory dysfunction that, to this date, has the most solid empiric background to be associated with AD.

Amnestic symptoms of Alzheimer's disease

The National Institute on Aging and Alzheimer's Association deliberately abandoned clinical symptoms of a multidomain amnestic dementia in order to focus on the neuropathologic changes that actually define AD as one of the causes of dementia. By adapting this approach it became possible for researchers to search for cognitive correlates of Alzheimer's continuum in an unbiased manner. One finding, which stems from studies utilizing the AT(N) classification conducted so far, is that neuropsychological episodic memory measures are sensitive to the

presence of the "A" biomarker in cognitively normal adults (Burnham *et al.*, 2019), as well as individuals reporting subjective concerns about their cognition, but without any functional impairment in daily life (Jutten *et al.*, 2021). This is in line with a previous meta-analysis of the relationship between Aβ biomarkers and various cognitive domains in cognitively normal older adults, where only episodic memory was correlated with Aβ PET levels (Hedden *et al.*, 2013).

Moreover, it has recently been shown that episodic memory may be used to predict the progression of AD (Moscoso *et al.*, 2019; McCollum *et al.*, 2021). Within a group of individuals with MCI, the A+T+(N+) (i.e. AD) biomarker profile is characterized by worse baseline episodic memory, smaller posterior hippocampal volume, thinner cortex, and steeper longitudinal decline than A+T-(N+) profile (i.e. Alzheimer's and concomitant suspected non-AD pathologic change) (McCollum *et al.*, 2021). Another study confirmed that episodic memory can be used to predict progression from early to late MCI only in A+T+(N+) individuals, and that no changes in episodic memory are observed between early and late MCI in A+T-(N+) participants (Moscoso *et al.*, 2019). Combined with the abovementioned results from cognitively normal adults, it seems that a decline in episodic memory corresponds to a progression from normal, to Alzheimer's pathologic change, to AD biomarker profile, with "A" being more important at earlier, while "T" at the latter stages (Fig. 1).

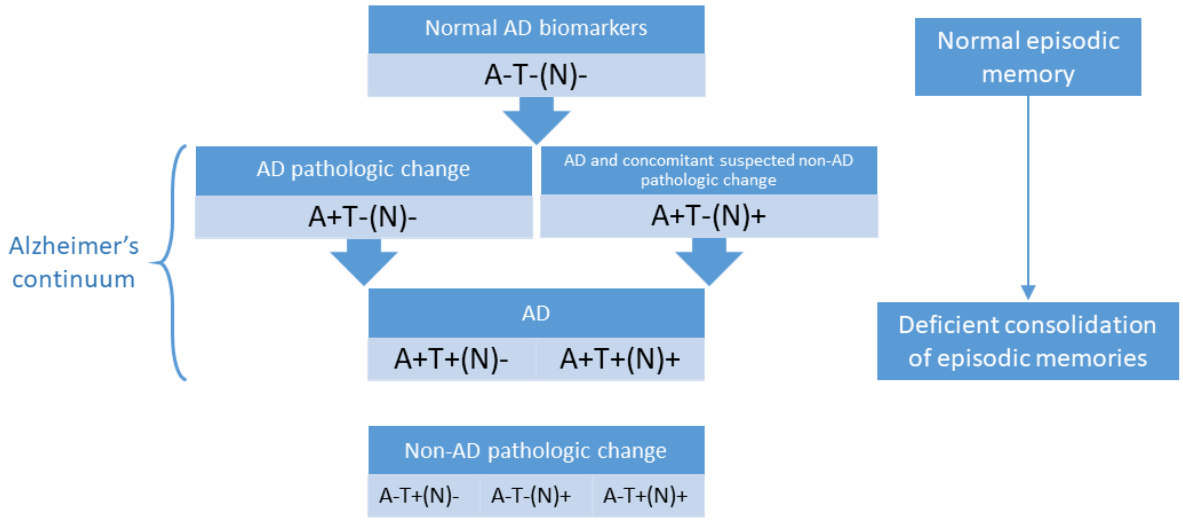

Fig. 1. Summary of the AT(N) classification (based on: Jack *et al.*, 2018) in relation to neuropsychological episodic memory test results. Aβ deposits are inversely related to episodic memory function in cognitively normal adults, while pathological Tau protein is a crucial component of episodic memory decline during Alzheimer's continuum (see text for explanation).

The implication that episodic memory may be a cognitive marker of Alzheimer's continuum is important both for the clinic and for potential back-translation to basic and

preclinical research. With regard to the former, given the scarcity of biomarker testing in a clinical setting and lack of disease-modifying treatments for AD, other tools for initial, scalable screening of individuals at risk of AD are a must in order to apply preventive treatment. This issue has become of even more importance since the recent approval of aducanumab for medical use in the USA in June 2021, which opens the avenue to target Aβ aggregates pharmacologically in asymptomatic individuals in order to halt the buildup of AD neuropathology. Moreover, in cases where MCI is already present, deficits of episodic memory could be used for initial differential neuropsychological diagnosis of AD against other forms of dementia (Economou, Routsis and Papageorgiou, 2015; Xu *et al.*, 2018), before biomarker confirmation of the disease. Neuropsychological studies also highlight the fact that AD patients display a deficit in consolidation of episodic memory i.e. transferring the information to long-term memory (Economou, Routsis and Papageorgiou, 2015), pointing to late long-term potentiation (LTP) as a potential cellular target for pharmacotherapy.

Regarding basic and preclinical research, over the course of last 20 years multiple lines of evidence have supported the notion, that other mammals and birds possess functional equivalents of human episodic memory, which are often termed episodic-like memory (ELM). Several methods to probe ELM in laboratory rodents have been established and not only improved our understanding of the neurobiology of ELM, but also enabled preclinical pharmacological manipulations of ELM to be tested (for a review see: Chao *et al.*, 2020). Therefore, the second section of this work (entitled *Episodic memory*) will cover episodic memory and ELM in more detail to elucidate aspects of the topic relevant for this work.

Zinc and Alzheimer's disease

A connection between zinc and Alzheimer's disease was proposed as early as 1981, based solely on the fact that most of the transcription enzymes utilize zinc ions (Zn^{2+}) as a cofactor (Burnet, 1981). Today we know that around 10% of human proteome contains a zinc-binding domain (Andreini *et al.*, 2006), and that multiple roles this biometal plays in the human body include regulation of the immune, digestive, endocrine, reproductive and nervous systems. The concentration of zinc in the brain is estimated at around 150 μM/L, which makes it the highest of all organs, and translates to the fact that around 70% of proteins in the brain utilize zinc as a structural component (Portbury and Adlard, 2017). The majority of the ion (85-90%) remains bound to proteins, but the remaining 10-15% constitutes a pool of "free", chelatable Zn^{2+}, which resides in: pico- to low nano-molar concentrations in the cytosol (Granzotto, Canzoniero and Sensi, 2020); low nanomolar (5-25 nM) concentrations in the extracellular fluid

(Frederickson *et al.*, 2006); and, low micromolar concentrations (<10 μM) (Vergnano *et al.*, 2014) in the synapse during neurotransmission (Pan *et al.*, 2011; Perez-Rosello *et al.*, 2013, 2015; Kalappa *et al.*, 2015). Synapses are where Aβ aggregates are formed and it has been shown that both the levels of Aβ deposits and their toxicity are dependent on neuronal activity (Bero *et al.*, 2011, 2012). Around the time amyloid cascade hypothesis was formulated (Hardy and Higgins, 1992) it was discovered that Zn^{2+} causes rapid aggregation of human Aβ at concentrations as low as 300 nM (Bush *et al.*, 1994). Zn^{2+} had no effect on aggregation of the rodent form of Aβ at concentrations of up to 25 μM, which was speculated to explain the lack of amyloidosis in aged mice and rats, in spite of physiological production of Aβ in rodent brains (*ibidem*).

Since then it has been confirmed that Zn^{2+} release from presynaptic terminals is necessary for rapid oligomerization of Aβ, as well as subsequent toxic and functional disturbances in the synapse (Deshpande *et al.*, 2009; Lee *et al.*, 2018). These include the disruption of LTP (Lee *et al.*, 2018), which is one of the best-studied neurophysiological mechanisms behind memory formation. Compared to wild-type animals, in hippocampal slices of mice devoid of synaptic Zn^{2+} (due to knockout of ZnT3 – a membrane transporter responsible for loading presynaptic terminals with Zn^{2+}) human Aβ oligomer formation is highly reduced (Deshpande *et al.*, 2009). Moreover, *in vivo* experiments show, that human Aβ alone is insufficient to cause both LTP and memory impairments after injection to rats' hippocampus, and that these effects of Aβ are observed only in the presence of Zn^{2+} (Takeda *et al.*, 2017). Similarly, human Aβ neurotoxicity in rat hippocampal slices was dependent on synaptic Zn^{2+} release, which was higher – and therefore more detrimental - in both aged and female animals (Datki *et al.*, 2020). Therefore, zinc-induced neurotoxicity and disruption of synaptic plasticity by Aβ might be possible mechanisms behind age and female sex being risk factors for AD development. Other mechanisms by which Zn^{2+} could exacerbate the effects of amyloidosis include: increased processing of APP into Aβ; and, shielding Aβ from degradation (Wang and Wang, 2017).

Zn^{2+} acts as a neuromodulator of glutamate, GABA and glycine receptors (Frederickson and Moncrieff, 1994; Birinyi *et al.*, 2001; Wang *et al.*, 2002), as well as a neurotransmitter trough a zinc-specific metabotropic GPR39 receptor (Holst *et al.*, 2007; Yasuda *et al.*, 2007). Due to its high affinity to Zn^{2+}, Aβ could interfere with zincergic neuromodulation/neurotransmission by sequestering Zn^{2+} from the synapse. Because of the inhibitory neuromodulation of glutamatergic *N*-methyl-D-aspartate receptors (NMDARs) and α-amino-3-hydroxy-5-methyl-4-isoxazolepropionic acid receptors (AMPARs) by Zn^{2+}, it has

been hypothesized that neuronal hyperactivity observed during early stages of AD (Busche and Konnerth, 2015) could be caused by depletion of Zn^{2+} by Aβ from the synapse (Granzotto, Canzoniero and Sensi, 2020). Moreover, the GPR39 has been shown to be a necessary component of glutamate release inhibition *via* the 2-AG endocannabinoid in zincergic synapses of the dorsal cochlear nucleus (Perez-Rosello *et al.*, 2013), and of the inhibitory action of $GABA_A$ receptors *via* upregulation of potassium/chloride cotransporter 2 (KCC2) in the hippocampus (Chorin *et al.*, 2011; Gilad *et al.*, 2015), but the role of Zn^{2+} in AD-related neuronal hyperactivity remains to be experimentally verified.

The effects of Zn^{2+} sequestration by Aβ were investigated *in vitro* with regard to GPR39's involvement in response to oxidative stress (Dittmer *et al.*, 2008) in human neuroblastoma cells and mouse cortical neurons (Abramovitch-Dahan *et al.*, 2016). Pretreatment with Aβ caused a decrease in Zn^{2+}-GPR39-mediated calcium (Ca^{2+}) and clusterin release into the cytosol, as well as a decrease in extracellular signal-regulated kinase 1/2 (ERK 1/2) phosphorylation (*ibidem*). Mutations in the gene encoding clusterin are a significant risk factor for progression from MCI to AD (Lacour *et al.*, 2017) and the protein is involved in neuronal response to oxidative insults (Foster *et al.*, 2019), which are a well-recognized consequence of AD neuropathology (Cheignon *et al.*, 2018).

Furthermore, another line of evidence links Zn^{2+} to NFTs. Numerous *in vitro* cell line studies have shown that at low micromolar concentrations Zn^{2+} causes phosphorylation and aggregation of the Tau protein (Mo *et al.*, 2009; Hu *et al.*, 2017) through activation of ERK1/2, glycogen synthase kinase (GSK)-3b and P70S6 kinase (An *et al.*, 2005; Pei *et al.*, 2006), or inhibition of protein phosphatase 2A (PP2A) (Sun *et al.*, 2012; Xiong *et al.*, 2013). Moreover, not only does Zn^{2+} significantly accelerates pathological aggregation of Tau, but it also exacerbates the neurotoxicity of the resultant NFTs (Hu *et al.*, 2017). The increase of intracellular Zn^{2+} levels, necessary for the initiation of the abovementioned mechanisms, can be achieved either by influx of extracellular Zn^{2+} through voltage-gated calcium channels or Ca^{2+} and Zn^{2+} permeable AMPARs lacking the GluA2 subunit, or by recruitment of Zn^{2+} from intracellular stores (Granzotto, Canzoniero and Sensi, 2020). The latter is often a consequence of Ca^{2+} influx, which can additionally be caused by overactivation of the NMDARs – one of the main causes of excitotoxicity (Zhou *et al.*, 2013). Aβ oligomers have been shown not only to directly activate NMDARs (Texidó *et al.*, 2011), but also potentiate the release of glutamate (Kabogo *et al.*, 2010), which would further activate NMDARs and Ca^{2+} and Zn^{2+} permeable AMPARs (especially with inhibitory neuromodulation of Zn^{2+} weakened due to sequestration by Aβ). The neurotoxicity of the latter mechanism of Aβ action has been confirmed in neuronal

cell lines and hippocampal slices (Alberdi *et al.*, 2010). Therefore, based on the results of basic research, it is possible that in humans Zn^{2+}-induced oligomerization of Aβ can lead to extra- and intra-cellular Zn^{2+} dyshomeostasis and cause both of the pathophysiological changes that define AD.

To date, there is only one real-time imaging investigation of human brain Zn^{2+} levels in AD (DeGrado *et al.*, 2016). PET imaging of Zn^{2+} clearance (^{63}Zn-zinc citrate), amyloidosis (^{11}C-Pittsburgh Compound B) and neurodegeneration (^{18}F-fluorodeoxyglucose) revealed slower ^{63}Zn clearance in AD patients compared to healthy controls, which correlated with amyloidosis and neurodegeneration measures in cortical regions commonly affected by AD (DeGrado *et al.*, 2016). It has to be noted, that the differences in clearance rates were not accompanied by differences in total ^{63}Zn uptake (*ibidem*), which could explain the negative results of a meta-analysis of *postmortem* Zn^{2+} levels comparisons in the neocortex of AD and healthy individuals (Schrag *et al.*, 2011), as well as the substantial heterogeneity of results of studies of *postmortem* brain Zn^{2+} levels in AD in general (Portbury and Adlard, 2017). DeGrado *et al.* study highlights the possibility that Zn^{2+}-Aβ interaction may exert its pathological effect on neurons at a short timescale – a property that could explain the long development of AD neuropathology and symptoms. Moreover, if episodic memory was among functions physiologically dependent on synaptic Zn^{2+}, the fast dynamic of Zn^{2+}-Aβ interaction could explain why this particular mnemonic function is affected at a very early phase of AD development.

2. Episodic memory

Memory can be broadly defined as a property of living systems to acquire or create, store, use and dispose of information about their internal and/or external environment. A framework commonly used to categorize animal memory subsystems differentiates explicit (Schacter, 1987) or declarative (Squire, 1992) memory from implicit (Schacter, 1987) or non-declarative/procedural (Squire, 1992) memory. Declarative memory can be further subdivided into semantic and episodic information systems (Tulving, 1983). Semantic information is concerned with facts and rules that are devoid of the context in which they were acquired/encoded, and strong associations exist between the units of information (*ibidem*). In contrast, episodic memories convey information about single experiences and the context in which they were encoded, and the associations between single memories have to be weaker (*ibidem*). Within a single episodic memory, strong associations between three types of information have to be made: 1) the content of an event, termed “what?”; 2) the spatial location

of the event, termed “where?”; and, the temporal sequence of different events, termed “when?”. It is assumed that successful inhibition of interference (i.e. pattern separation) between similar spatial and/or temporal aspects of different events is required for both encoding and retrieval of an episodic memory, and that such memories must be encoded rapidly (Kesner, 2016; Sugar and Moser, 2019). An opposite process of detecting similarity between a sensory cue and stored memory of an episode (i.e. pattern completion) is additionally required for retrieval (*ibidem*). These processes were first postulated by computational models of the hippocampus – a structure which later was experimentally confirmed to be critically involved in pattern separation and completion (Yassa and Stark, 2011).

Neuroanatomy of episodic memory

Neuroimaging studies in humans consistently report, that encoding and consolidation of episodic memories is associated with network activity of the following areas: hippocampus, parahippocampal gyrus, retrosplenial/posterior cingulate cortex and medial prefrontal cortex (mPFC) (Dede and Smith, 2016). Additionally, connectivity between these structures changes with the age of episodic memory. Damage of either hippocampus, parahippocampal gyrus or retrosplenial/posterior cingulate cortex in humans leads to temporally-graded retrograde amnesia (*ibidem*) i.e. a condition, where older memories are still retrievable, while fresh memories are not; and, anterograde amnesia (*ibidem*), where new episodic information is quickly forgotten/is not consolidated into long-term memory. The encoding deficits are global when hippocampus is affected, and restricted to visual aspects of memory in case of retrosplenial cortex (*ibidem*). The activity of all three structures is also necessary in tasks that demand pattern separation, further supporting their role in rapid encoding of episodes (Leal and Yassa, 2018). The mPFC is responsible for self-referential aspect of episodic memory (Dede and Smith, 2016) and pattern completion in humans (Leal and Yassa, 2018), while in rodents it plays a more executive role (ex. working memory, decision-making) (Kesner, 2016).

Global deficits in encoding episodes after hippocampal damage are in line with neuroanatomical wiring of the hippocampus, which has bidirectional connections with the polymodal association areas of the frontal, temporal and parietal lobes (Schultz and Engelhardt, 2014). In primates these connections constitute the majority of corticohippocampal connections, while in rodents most of the connected cortical areas are primary and convey less processed, unimodal information (Lisman and Redish, 2018). Rodent hippocampus is also better interconnected with its contralateral counterpart *via* commissural/associational fibers than primate hippocampus (Schultz and Engelhardt, 2014). These anatomical differences

highlight the evolutionary change from subcortical to cortical processing in primates and humans compared to rodents (Lisman and Redish, 2018). Among the subcortical structures reciprocally connected with the hippocampus are: 1) the amygdaloid complex; 2) septal nuclei; 3) the striatum; 4) hypothalamus (*via* mammillary bodies); 5) and thalamus (Schultz and Engelhardt, 2014). Hippocampus also receives monoaminergic modulatory projections from the raphe nuclei (serotonin), locus coeruleus (noradrenalin) and ventral tegmental area (dopamine) (*ibidem*), as well as cholinergic and GABAergic neuromodulation from the medial septal nucleus that plays a key role in keeping the theta rhythm (Tsanov, 2015). The noradrenergic, dopaminergic and cholinergic modulation of hippocampal functions is reduced

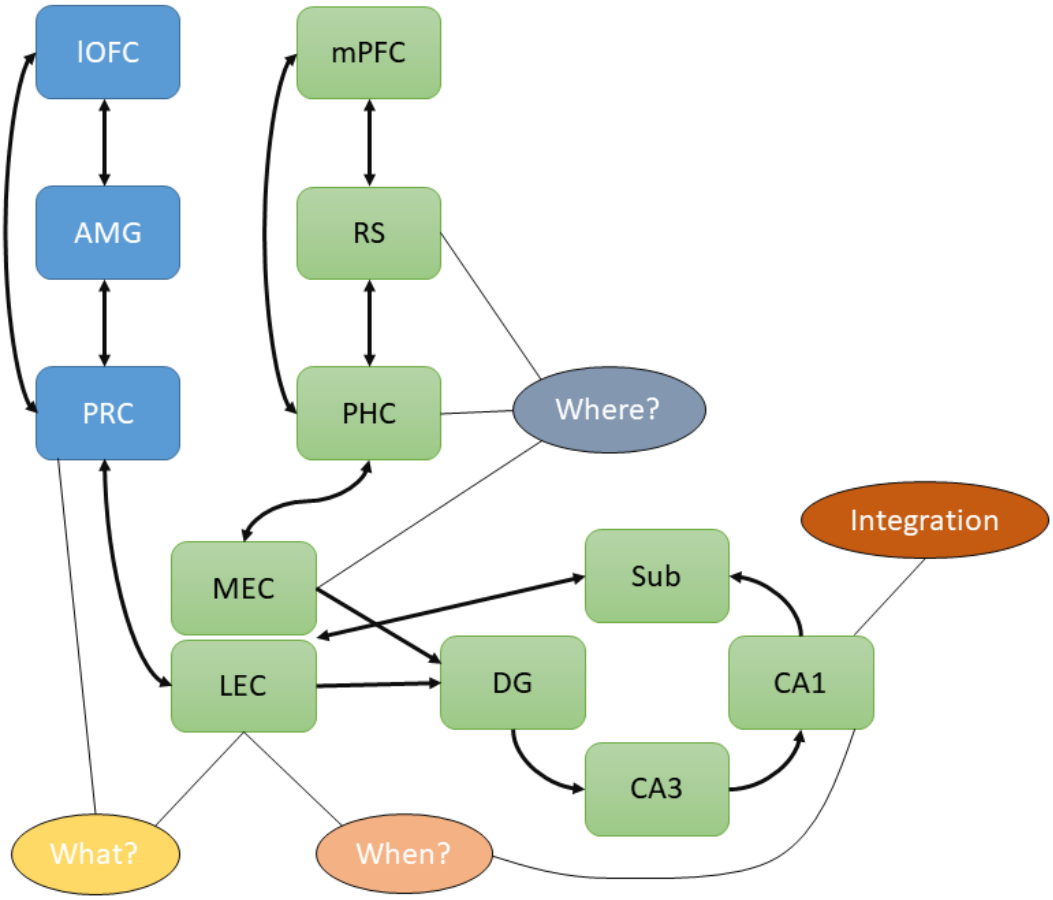

Fig. 2. Simplified representation of the connections (black arrows) between structures that initially process the 3 key components of episodic memory i.e. "what?", "when?" and "where?", before conveying this information to hippocampus proper (CA3 and CA1). Highlighted in green are the structures implicated as crucial for episodic memory in human studies. The information that CA1 integrates all 3 components comes from rodent studies (Chao *et al.*, 2017; see text for explanation). *AMG* - amygdala; *CA1* - cornu ammonis 1 field; *CA3* - cornu ammonis 3 field; *DG* - dentate gyrus; *LEC* - lateral entorhinal cortex; *MEC* - medial entorhinal cortex; *PHC* - parahippocampal cortex; *PRC* - perirhinal cortex; *RS* - retrosplenial cortex; *Sub* - subiculum; *lOFC* - lateral orbitofrontal cortex; *mPFC* - medial prefrontal cortex. Connectivity pattern in the figure drawn based on: Ritchey, Libby and Ranganath, 2015.

with age and may underlie the decline in episodic memory observed in older animals and humans (Leal and Yassa, 2015).

Since the seminal work of O'Keefe and Nadel, who discovered neurons firing in correlation with the position of a rat in an open field (i.e. "place cells"), the hippocampus was endowed with the role of providing a spatial cognitive map for episodic memories (O'Keefe and Nadel, 1978). An important development of this idea came with the discovery of neurons in the medial entorhinal cortex, the activity of which covered the whole open field in equal intervals. When treated as vertexes and connected, the locations of a neuron's activity created a triangular grid (Sugar and Moser, 2019). Together, "place cells" and "grid cells" provide an efficient system of coding the "where?" component of episodic memory. More recent studies revealed, that both types of space-encoding neurons are capable of coding relative time on a short timescale i.e. the progression of events within an episode (Sugar and Moser, 2019). Moreover, population activity of cells in the CA1 area of the hippocampus and around 20% of neurons in the lateral entorhinal cortex have been shown to code time at longer timescales (ex. between episodes) and provide time tags at the whole temporal spectrum (i.e. within and between episodes), respectively (*ibidem*). Apart from participating in coding the "when?" component of episodic memory, the lateral entorhinal cortex together with perirhinal cortex transmits sensory cues to the hippocampus, which constitute the "what?" component (*ibidem*).

The different computations performed within the hippocampus seem segregated between its dentate gyrus, CA3 and CA1 fields that span the coronal plane of the structure (Figure 3). The dentate gyrus, which receives input from the entorhinal cortex *via* perforant pathway (PP), performs pattern separation, which relies on generation of new neurons, as well as the sparsity of mossy fibers (MF) projections of dentate gyrus to the CA3 field (Yassa and Stark, 2011). The CA3 field performs both pattern separation and completion depending on how big a difference in the sensory cues was detected, with smaller differences biasing the network towards pattern completion, while pattern separation being more probable in case of bigger differences (*ibidem*). Pattern completion relies on the auto-associative connections of the CA3 neurons, which become strengthened with age in rodents (Leal and Yassa, 2015). This mechanism may underlie the mnemonic rigidity of both aged rodents and humans, who require larger dissimilarity between sensory cues for successful pattern separation to occur, and display a tendency towards pattern completion in their CA3 fields (*ibidem*). Moreover, the mossy fibers – CA3 (MF-CA3) pathway is necessary for encoding, while a direct projection from the entorhinal cortex *via* PP to the CA3 is responsible for retrieval (Yassa and Stark, 2011). The

latter pathway has been shown to be weakened with age in both rats and humans (Leal and Yassa, 2015). Apart from temporal coding at longer timescales mentioned above, the CA1 field: switches between encoding and retrieval by comparing the Schaffer collaterals (SC) inputs from the CA3 area with the direct PP projections from the entorhinal cortex; and, does not exhibit neither pattern separation nor completion (Leal and Yassa, 2018). With respect to aging, the neurons in the CA1 area are more susceptible (than CA3 neurons) to synaptic plasticity dysfunctions, that cause age-related memory encoding impairments (Leal and Yassa, 2015). Zinc regulates synaptic plasticity in both areas (Pan *et al.*, 2011; Anderson *et al.*, 2015), albeit by different mechanisms, which will be shortly discussed in the next section (for a more thorough review, see: Rychlik and Mlyniec, 2019).

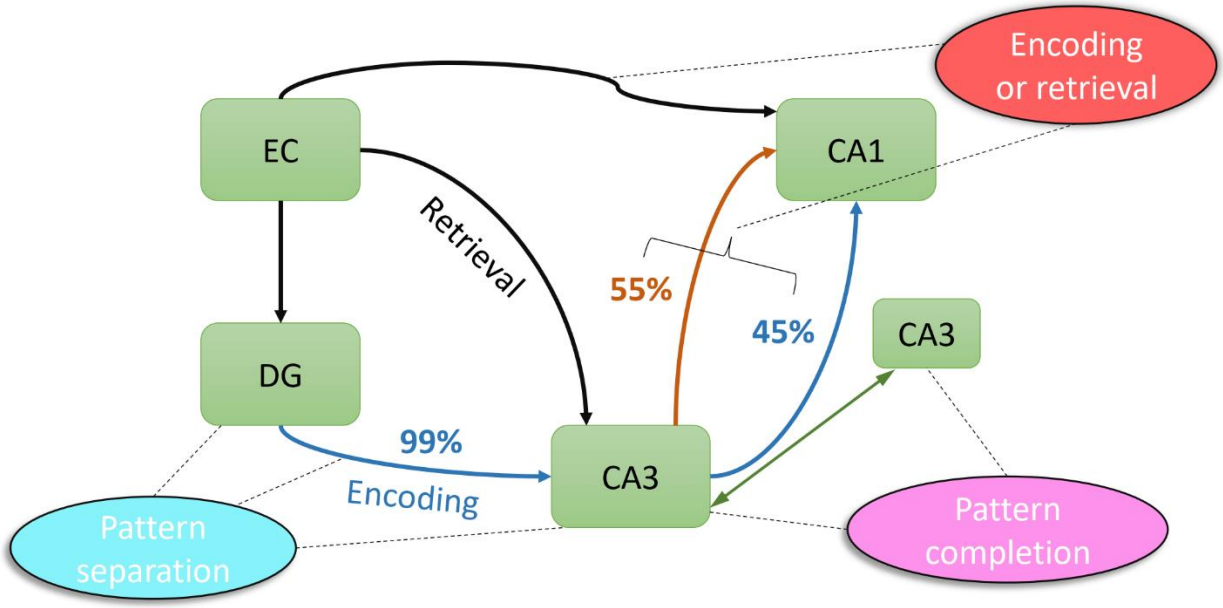

Fig. 3. Structure-function mapping of hippocampal areas and their connections. Black arrows: perforant pathways; blue arrows: glutamatergico-zincergic projections, mossy fibres (DG-CA3) and Schaffer collaterals (CA3-CA1); red arrow: non-zincergic Schaffer collaterals; green arrow: associative connections. *EC* – entorhinal cortex; *DG* – dentate gyrus; *CA3* - cornu ammonis 3 field; *CA1* - cornu ammonis 1 field.

Recently, a set of experiments utilizing a behavioral object-recognition task for rodents, capable of simultaneous measurement of spatial and temporal components, as well as their integration into ELM (for a detailed description of the test, see: the *Behavioral tests* section of this work; for a review of the experiments, see: Chao *et al.*, 2020), elucidated the role of hippocampal fields in rodent ELM. Disconnection of the CA3 area and mPFC impaired the

"where?" and "when?" components, as well as their integration (De Souza Silva *et al.*, 2016), while disconnection of the CA1 area, which is downstream to CA3 in information processing, disrupted only spatiotemporal integration, sparing the temporal and spatial components (Chao *et al.*, 2017). Since spatiotemporal integration component measured with this task can be present in rodents regardless of the other two (Belblidia *et al.*, 2015), the CA1-mPFC seems to be responsible for higher order interaction between fundamental aspects of ELM, which are processed within the CA3 area. As previously stated, CA1 field is also the area more prone to abnormal LTP as a result of aging, which is one of the factors behind episodic memory decline in humans. It also has to be noted that the disconnection of either CA1 or CA3 areas had no effect on object novelty recognition, temporal order and spatial location memory, when these functions were measured separately (De Souza Silva *et al.*, 2016; Chao *et al.*, 2017).

Lastly, it is worth mentioning the differences in precision and type of material encoded by the anterior/ventral and posterior/dorsal segments of the hippocampus. In both rodents and humans, the anterior/ventral section engages in coding more robust and general information, while the posterior/dorsal section is concerned with fine visuospatial details of an event (Sekeres, Winocur and Moscovitch, 2018). This can be exemplified by the size of place fields of place cells in both sections – place cells in the anterior part cover whole environments, whereas place cells in the posterior part display the "classic" localized activity (Sugar and Moser, 2019). The proportion of both sections differs considerably between rodents and humans. In the latter species the anterior part became enlarged, possibly in order to handle the higher-order information it receives from polymodal association cortical areas (Lisman and Redish, 2018). However, episodic memories may critically depend on the posterior section in humans, as evidenced by the association of a decline in episodic memory with lower posterior hippocampal volume in MCI individuals with AD biomarker profile (A+T+(N+)) compared to MCI individuals with Alzheimer's pathologic change profile (A+T-(N+)) (McCollum *et al.*, 2021).

The role of zinc in the hippocampus

A wealth of evidence gathered over the span of last 20 years strongly supports the idea that, on top of being an allosteric neuromodulator, synaptic Zn^{2+} acts as a classic neurotransmitter (McAllister and Dyck, 2017; Aizenman, 2019). These include: 1) presence of chelatable Zn^{2+} in presynaptic terminals; 2) a mechanism for transporting Zn^{2+} into synaptic vesicles *via* the ZnT3 transporter, the deletion of which causes a complete loss of synaptic Zn^{2+}; 3) the release of Zn^{2+} from presynaptic neurons in an activity-dependent manner, and the ability

of synaptic Zn^{2+} to cross the synapse and interact with receptors of the postsynaptic membrane; 4) the ability of synaptic Zn^{2+} to specifically and directly activate a metabotropic zinc-sensing GPR39 receptor; 5) the removal of synaptic Zn^{2+} from the synaptic cleft *via* ZIP transporters into astrocytes, pre- or post-synaptic neurons, and diffusion of Zn^{2+} to extra-synaptic sites, which results in termination of the activity of Zn^{2+} in the synapse (summarized in: Aizenman, 2019).

All of the abovementioned mechanisms have been proven to operate in hippocampal MF-CA3 and SC-CA1 glutamatergic synapses. It is also known, that – at least in the murine hippocampus - synaptic Zn^{2+} is present at all of the MF-CA3 synapses and at around 45% of the SC-CA1 synapses (Sindreu *et al.*, 2003). Moreover, while all of the pyramidal neurons of the CA3 field express AMPARs at similar levels, the postsynaptic sites of non-zincergic synapses of the CA1 area express ~40% more AMPARs than postsynaptic sites of CA1's zincergic synapses (*ibidem*). Since Zn^{2+} inhibits postsynaptic AMPAR currents after a single presynaptic action potential (Kalappa *et al.*, 2015), non-zincergic synapses of the CA1 field could be responsive to stimuli of lower intensity than zincergic synapses, which would provide a mechanism for segragation of inputs from the CA3 to the CA1 areas of the hippocampus (Figure 3).

Another mechanistic difference supported by synaptic Zn^{2+} in the MF-CA3 and SC-CA1 synapses is directly linked to the physiological basis of learning and memory. As mentioned in the previous section, synaptic Zn^{2+} participates in synaptic plasticity by influencing LTP (Pan *et al.*, 2011; Vergnano *et al.*, 2014; Kalappa *et al.*, 2015). In general, the strengthening of a synapse *via* LTP can be divided into NMDAR-dependent/associative and NMDAR-independent/non-associative. The former mechanism requires the presynaptic neuron to fire before the postsynaptic neuron, and is utilized in SC-CA1 synapses (Lüscher *et al.*, 2012), while the latter is independent of the timing of these events and is characteristic of MF-CA3 synapses (Nicoll and Schmitz, 2005). Postsynaptic NMDARs are critical for associative LTP, because these ion channels are sensitive to both binding of their primary ligand (glutamate) and depolarization of postsynaptic membrane caused by activation of another glutamate receptor – the AMPAR. Simultaneous occurrence of both events causes an expulsion of Mg^{2+}, which blocks the NMDAR channel, and subsequent influx of Ca^{2+} into the postsynaptic neuron. This in turn sensitizes the postsynaptic cell to glutamate *via* recruitment of AMPARs into the postsynaptic membrane. Following a series of action potentials, a phasic rise of Zn^{2+} in the synapse inhibits the GluN2A-containing NMDARs, and interferes with associative LTP induction at MF-CA3 (Pan *et al.*, 2011; Vergnano *et al.*, 2014) and SC-CA1 (Vergnano *et al.*,

2014) synapses. Moreover, synaptic Zn^{2+} is necessary for non-associative LTP at MF-CA3, since lack of the ion blocks an increase of neurotransmitters' release probability from presynaptic terminals (Pan *et al.*, 2011) – the main mechanism behind this form of synaptic plasticity. Therefore, at MF-CA3 synapses synaptic Zn^{2+} is critical for a shift towards non-associative LTP and its expression, while at SC-CA1 synapses the ion may further segregate the inputs from CA3, by demoting associative LTP at zincergic subpopulation of these projections.

The functional consequences of the latter mechanism remain to be elucidated, but it is known that optimal influx of synaptic Zn^{2+} into the postsynaptic neuron is a crucial component of LTP at SC-CA1 synapses (Takeda *et al.*, 2015), while LTP at PP-CA1 synapses requires the release of Zn^{2+} from intracellular stores (Tamano, Nishio and Takeda, 2017). Chelation of the ion at either SC-CA1 or PP-CA1 synapses disrupts both LTP and the behavioral expression of memory (object novelty recognition) in rats (Takeda *et al.*, 2015; Tamano, Nishio and Takeda, 2017). Zn^{2+} also mediates rapid encoding of episodic-like contextual fear memory at the MF-CA3 synapses (Ceccom *et al.*, 2014), and its function is restricted to the CA3 pyramidal neurons, as the ion has no effect on the MF-CA3 interneurons (Pan, Zhao and McNamara, 2019) or on the plasticity of commissural/associational fibers of CA3 fields (Lu *et al.*, 2000). This means that within the rodent CA3 area, Zn^{2+} is necessary for fast learning to occur, but it might be less important for the precision of memory (which in rodents depends on MF-CA3 interneurons: Ruediger *et al.*, 2011) and for pattern completion or coding of the temporal order of episodes (which in rodents depend on CA3 commissural/associational fibers: Inoue and Watanabe, 2014; Cox *et al.*, 2019). Synaptic Zn^{2+} released from MFs also regulates LTP of pyramidal neurons that receive PP inputs, by facilitating their intrinsic excitability following Zn^{2+}'s heterosynaptic influx (Eom *et al.*, 2019). Therefore, within the CA3 field Zn^{2+} should participate in pattern separation during MF-dependent encoding, but also influence the PP-dependent retrieval, by strengthening time-locked activation of MF and PP inputs to CA3.

A recent *in vivo* study of juvenile rats showed that early-life Zn^{2+} deficiency causes an impairment, while Zn^{2+} supplementation causes an improvement of object novelty recognition, and that this corresponds to hippocampal GPR39 downregulation and upregulation, respectively (Chen *et al.*, 2019). GPR39 is responsible for ~25% of the increase of intracellular Ca^{2+} levels due to metabotropic receptors' activation of CA3 pyramidal neurons in response to MF stimulation (Besser *et al.*, 2009). This leads to ERK1/2 phosphorylation and affects the intrinsic excitability of neurons by upregulating KCC2, which maintains the inhibitory effect of the $GABA_A$ receptor (Chorin *et al.*, 2011). Successful postsynaptic inhibition of hippocampal

pyramidal neurons is necessary for the preservation of memory in aging animals (Tran, Gallagher and Kirkwood, 2018), and therefore the inhibitory action of GPR39 may play a role in senescence-related memory maintanance or impairment. As previously mentioned, Aβ attenuates the ligand-mediated activity of GPR39 in hippocampal neurons (Abramovitch-Dahan *et al.*, 2016), and exacerbates the aging-related overexcitability of these cells. Moreover, the elderly aged >60 have a Zn^{2+} intake of less than 50% of their daily allowance, due to senescence-related mechanisms (Mocchegiani *et al.*, 2013). However, because of the neurotoxic effects of Zn^{2+}-Aβ interaction described in the *Zinc and Alzheimer's disease* section of this work, as well as the complex effects of the ion on hippocampal neurons, Zn^{2+} supplementation in individuals with Alzheimer's pathologic change might not be an optimal solution.

Lastly, the brain-derived neurotropic factor (BDNF) is a protein with crucial roles in neuronal survival, synapse formation and synaptic plasticity, and is consistently found to be decreased in serum (Ng *et al.*, 2019; Xie *et al.*, 2020) and cerebrospinal fluid (Du *et al.*, 2018) of AD patients at advanced stages of the disease. A similar tendency is found in *postmortem* studies of AD hippocampus and neocortex, although the results are less consistent (Du *et al.*, 2018). For some time it was assumed that the $Val_{66}Met$ polymorphism in the *Bdnf* gene could be a risk factor for AD, but a recent meta-analysis, which included potential confounding factors in the model, found no association in this regard (Zhao *et al.*, 2018). It is therefore probable that the decrease of BDNF levels, rather than its genetic malfunction, is an element of AD neuropathology cascade. Zn^{2+} regulates BDNF levels in the hippocampus by: 1) promoting the maturation of the protein through activation of MMP-9 metalloproteinase (Yoo *et al.*, 2016); and, 2) promoting the expression of the *Bdnf* gene (Sowa-Kućma *et al.*, 2008), possibly through the activation of the cAMP response element binding (CREB) transcription factor by a GPR39-dependent signaling cascade (Mlyniec *et al.*, 2015). The first mechanism depends on intracellular Zn^{2+}, and – paradoxically – genetic depletion of synaptic Zn^{2+} increases intracellular Zn^{2+} levels, enhances MMP-9 activity and BDNF expression and maturation (Yoo *et al.*, 2016); and, *in vivo* studies suggest that this effect may be restricted to females (McAllister *et al.*, 2020). The second, GPR39-dependent mechanism, possibly relies on the constitutive activity of the receptor, as no effect on BDNF levels in the hippocampus was found when GPR39 was chronically activated with its agonist (Starowicz *et al.*, 2019). Synaptic Zn^{2+} can still modulate BDNF signaling at the MF-CA3 synapse by direct transactivation of the tyrosine receptor kinase B (TrkB) (Huang *et al.*, 2008), which preferentially binds BDNF as an agonist, but the ion does not affect the levels of TrkB in the hippocampus (McAllister *et al.*, 2020).

In summary, a multitude of neurobiological mechanisms support a claim that synaptic and intracellular Zn^{2+} play a vital role in the hippocampus. Behaviorally, these translate to modulation of spatial learning and memory (Adlard *et al.*, 2010), object novelty recognition (Takeda *et al.*, 2015; Chen *et al.*, 2019) and contextual fear conditioning (Ceccom *et al.*, 2014) in rodents, but the role of zincergic neurotransmission in a pirmary hippocampal function of episodic memory and ELM is yet to be studied.

Aims of the study

The general aim of these studies was to determine the role of GPR39 in hippocampus-dependent memory functions. The first aim of this work was to establish whether GPR39 modulates ELM in rodents, and if its action is specific for this type of declarative memory. Secondly, the possibility of pharmacological modulation of GPR39-dependent types of memory was explored, and whether the receptor was necessary for the procognitive effects of a drug used in AD pharmacotherapy. Lastly, the effects of pharmacological manipulations of GPR39 on cognitive deficits caused by neuropathological changes observed in the course of AD (i.e. BDNF deficits) were explored. Significant behavioral findings were followed by *ex vivo* studies of hippocampal mRNAs related to excitatory/glutamatergic or inhibitory/GABAergic neurotransmission, signaling pathways, oxidative stress and neuroprotection. Hippocampal levels of selected proteins were also studied.

Materials and Methods

1. Animals

Two types of genetically modified C57BL/6J mice were used in the experiments: GPR39 knockout (KO) and BDNF heterozygotes (HET), with their age-matched WT littermates that served as control animals for the effects of genetic manipulations. During the experiments, all animals were housed in the Animal Facility of the Faculty of Pharmacy, Jagiellonian University Medical College (JUMC) in Cracow, Poland in a temperature- (22±1°C) and humidity-(55±10%) controlled air-conditioned room under a 12-hour light/dark cycle (lights on at 8.00 AM). Mice were maintained on a standard breeding-class diet (Altromin 1314, Germany) with a zinc content of 85 mg/kg of dry chow. Food and water were provided *ad libitum*. The status of animals was assessed daily based on standard behavioral and physiological health markers. After behavioral testing all animals were sacrificed by decapitation and their hippocampi

harvested using standard isolation procedures in order to assess the levels of mRNA and proteins of selected targets. Isolation was performed either 24 h (Experiments 1, 2, 8, 9) or 7 days (Experiment 5) after the last test. All of the experimental procedures were conducted according to the National Institute of Health Animal Care and Use Committee guidelines and approved by the 1st Local Ethical Committee in Cracow.

GPR39 KO mice

The GPR39 KO mice were originally generated by Deltagen, Inc. by means of homologous recombination, which exchanged the nucleotides 278 – 647 of the open reading frame in the first exon of the *Gpr39* gene (Holst *et al.*, 2009). These mice were bred in the Animal Facility of the Faculty of Pharmacy, JUMC. The litters of HET breeding pairs, which consisted of WT, GPR39 KO and HET littermates, were genotyped by means of standard PCR methods, with the following primers used to amplify DNA fragments isolated from a tail biopsy: forward KO – 5' TACCAAGGTCCTCGCTCTGT; reverse KO – 5' TGAACTCCGGGTTTCACTTC; forward WT – 5' TCATCGATCACAGCCATGTT; reverse WT – 5' ACTCGATACCCATGGCAAAG. After reaching puberty (P25-30), all animals were single-housed in transparent T-2 type cages without environment enrichment (fresh sawdust and nesting material were provided weekly), in order for the housing conditions to remain consistent with our previous studies. At the time of experiments, mice weighed 30-50 g and were either 4–7, 11–12 or 18–20 months old, representing three developmental stages: adult, middle-aged and old, respectively. Both male and female GPR39 KO and WT mice were used in the experiments.

BDNF HET mice

The use of BDNF HET, as opposed BDNF KO mice, was based on the fact that constitutive KO of the *Bdnf* gene results in severe coordination and motoric deficits, along with sensory ganglia degeneration and high mortality rates i.e. most of such animals fail to live through the second postnatal week (Ernfors, Lee and Jaenisch, 1994). The BDNF HET mice, which retain normal neurodevelopment and lifespan, while exhibiting ~50% lower expression of BDNF, were generated using the CRISPR/Cas9 method and bred in the Mouse Genome Engineering Facility, International Institute of Molecular and Cell Biology in Warsaw, Poland. In order to truncate all known *Bdnf* transcripts and prevent successful BDNF protein translation, a knock-in strategy was used. A KO cassette consisting of 3xSTOP codons and a BamHI restriction site was inserted in the open reading frame of exon 2 of the *Bdnf* gene. The following

primers were used to amplify DNA fragments isolated from either tail or ear biopsy using standard PCR: forward - 5' TCCCCGAGAAAGAAAGTTC; reverse - 5' TAGACATGTTTGCGGCATC. After arriving at the Animal Facility of the Faculty of Pharmacy, JUMC, all animals were single-housed in transparent T-3 type cages with environment enrichment (wooden blocks, paper tunnels). At the time of experiments the mice weighed 25-40 g and were 3–5 months old. Only male BDNF HET and WT mice were used in the experiments.

2. Behavioral tests

All behavioral procedures were performed during the light phase of the light/dark cycle, between 9.00 AM and 5.00 PM. We conducted the tests in a space openly connected to the habitat area, behind a partition wall which separated the experimental area from the cage racks. The experimental area had a separate light source independent of the light/dark cycle. The experiments were designed so that mice representing different independent variables (i.e. age, genotype, treatment) were evenly distributed throughout the workday and each individual animal was handled/tested at the same time(s) of the day. Prior to the experimental procedures, all animals were habituated to the experimenters for at least 7 days in order to reduce stress to a minimum. A habituation session consisted of handling for 2 minutes and – in the case of mice undergoing intraperitoneal (*ip*) injections – additionally performing a standard dorsal grip and gently touching the ventral side of the mouse. For acute drug treatments, 2 mock saline injections were performed over the span of 2 days preceding the first testing day. White noise was played during all of the tests to occlude background sounds. In order to prevent olfactory distractors/cues, the boxes and objects used for the ELM test and the rotarod apparatus were cleaned with 10% alcohol (Extance and Goudie, 1981) after each trial and dried with paper towels.

Episodic-like memory (ELM) test

The general concept of the “what-where-when” ELM test was described and validated by Dere *et al.* (Dere, Huston and De Souza Silva, 2005b, 2005a). The task combines spatial (Ennaceur, Neave and Aggleton, 1997) and temporal (Mitchell and Laiacona, 1998) versions of the object novelty recognition test into one task consisting of 3 stages (5 minutes per stage, Fig. 4). At each of the stages, mice are presented with 4 objects located beside the walls of an open-field box. Two types of objects (A and B, in quadruplicate) are used in the task. During the 1st (exposition) trial, a mouse is allowed to freely explore 4 copies of object A randomly

placed at 4 of the 8 possible locations in the box. Following an inter-stage interval (ISI), the animal explores 4 copies of object B positioned in a different spatial configuration (2nd trial). After another ISI, a test (3rd) trial is performed, where 2 copies of objects A (old objects) and B (recent objects) are presented together. One copy of each object type is shifted to a location in which it was not encountered in its original exposition trial (displaced objects), while the other copy remains in its original location (stationary objects). Thus, there are 4 categories of objects in the test trial: old stationary (OS), old displaced (OD), recent stationary (RS) and recent displaced (RD). Time (s) spent exploring each of the objects is recorded, and parameters (PRs) measuring the temporal order (PR1), spatial location (PR2) and integrated spatiotemporal (PR3) memory are calculated according to the following formulae:

$$PR1 = \frac{OS}{OS+RS}; \qquad PR2 = \frac{RD}{RD+RS}; \qquad PR3 = \frac{OD}{OD+OS}$$

We conducted the ELM test in 2 sets of white boxes (30 x 30 x 40 cm) with 2 visual spatial cues (a black square and a cross) at the top of adjacent walls, under dim, indirect lighting (8 lux at the center of the box). Independent variables were always counterbalanced between the box sets, as was the order of types of objects presented in the first 2 exposition trials within a box set. Over the course of 5 days preceding the ELM test, mice were habituated to their respective open-field boxes. A habituation session consisted of placing an animal in an empty box and allowing free exploration for 5 minutes. On the fifth day a single object different from the ones used in the ELM task was presented in the center in order to reduce anxiety during testing the following day.

Objects had similar height (~12 cm), but differed in shape, color and texture, and were immobilized with double-sided tape in order to prevent mice from displacing them. Pilot experiments were conducted in order to confirm that mice were able to discriminate between the objects and did not have innate preferences for any particular object type. Two types of objects were used in experiments 1, 2, 8 and 9, and 4 types in experiments 3–7.

The ISI was set to 60 minutes in the standard ELM test version. In the consolidation interference (CI) version an ISI of 5 minutes was used. A pilot experiment of the ELM CI version confirmed that 9–10-month-old male mice do not develop ELM when the ISI is reduced to 5 minutes (one-sample *t*-tests, *PR1*, $t_{(7)} = 0.56$, NS; *PR2*, $t_{(7)} = 0.03$, NS; *PR3*, $t_{(7)} = 0.36$, NS). The same animals displayed spatial (one-sample *t*-test, *PR2*, $t_{(7)} = 2.4$, $p = 0.048$) and integrated spatiotemporal (one-sample *t*-test, *PR3*, $t_{(7)} = 2.77$, $p = 0.028$) components of ELM under 60-

minute ISIs, with a trend towards a significant difference in the spatiotemporal component between testing conditions (paired-samples *t*-test of *PR3*, $t_{(7)} = 2.12$, $p = 0.072$).

The behavior was recorded for later analysis by cameras (DMK 22AUC03, ImagingSource, Germany or HD LiveCam, Creative!) suspended above the open-field boxes and connected to a laptop computer equipped with Any-maze tracking software (Stoelting, UK). Exploration time (s) was automatically registered when the snout of an animal entered a 2-cm zone surrounding an object, with the exception of events when this occurred incidentally while a mouse was passively sitting next to the object, in which case a manual correction was made. Whenever a mouse failed to explore all objects during the first 2 exposition trials or whenever its total exploration time in a trial was lower than 5 s, it was excluded from the analysis.

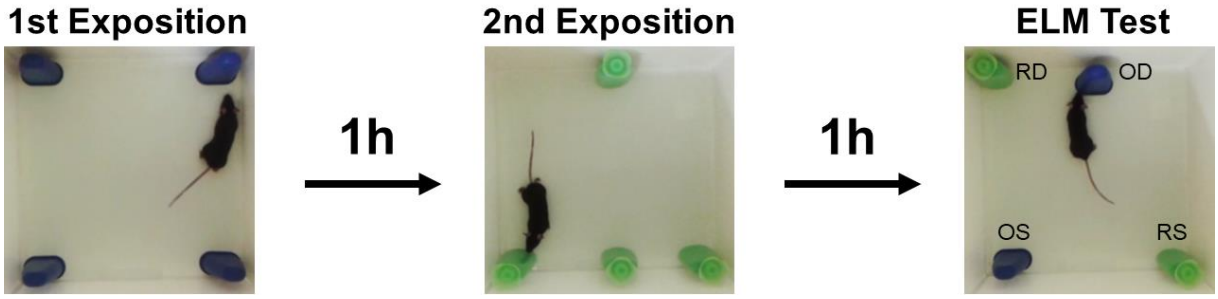

Fig. 4. ELM test design. In the consolidation interference version of the test a 5 min inter-stage interval (ISI) is used instead of 1h ISI.

Morris water maze spatial memory (SM) test

The Morris water maze (MWM) test was performed according to a previously described protocol (Vorhees and Williams, 2006) in its basic form – that is, only learning (over 5-7 days) and long-term memory 24 h after the last training day were assessed. The general aim of the task is for an animal to learn and remember the location of an escape platform hidden in a circular pool filled with water. In order to navigate itself, the animal has to use distal spatial cues, since the interior of the pool (i.e. the wall and water surface) is uniform in all directions.

We used a circular water tank (diameter: 105 cm at water surface level) made of black plastic, and a circular PVC platform (diameter: 9 cm) covered with anti-skid material for better traction. The ratio of search area to the platform area was 135:1. The pool was divided into virtual quadrants, with the platform submerged 1 cm below water surface in the middle of the SE quadrant. The water (21–22°C) was colored with white non-toxic tempera paint (Primo, Italy). Distal visual cues were placed outside the pool in the N, E, S and W directions to aid navigation. A source of light from the side of the pool was used to avoid reflections on the

water, and a camera (DMK 22AUC03) connected to a laptop computer was suspended above the pool for online analysis of animals' behavior. The experimenter was not present during swimming, and monitored mice on the computer screen behind a partition wall.

Mice were trained for 5-7 days (4 trials per day). Each trial (60 s) started when a mouse was gently placed in the water facing the pool wall, and was terminated when the animal mounted the platform. In the event of a failed trial, mice were directed to the platform by an experimenter. Animals were allowed to remain on the platform for 15 s after a trial. For each mouse, we used the following start positions in a pseudorandom order that changed between days: N, W, NE, SW. Mice remained in their home-cages during the time needed for all other animals to complete a particular trial. Non-performers were excluded from analyses. These mice were defined as: not searching for the platform for 3 days in a row, while passively floating in the pool and failing to find the platform. Speed, cumulative distance from the platform and latency to reach the platform were measured during the training sessions.

The probe trial (30 s) was conducted 24 h after the last training trial. Mice were placed in a novel NW start position in the pool devoid of the platform. Cumulative distance from the former location of the platform, percentage of time spent in the SW (platform) quadrant, and number of platform zone crossings were measured to assess long-term spatial memory (SM).

Rotarod test of procedural memory (PM)

To assess procedural memory (PM), we used a version of the accelerating rotarod test, which was previously described by Dere et al. (Dere *et al.*, 2008). Standard rotarod equipment (Panlab/Harvard Apparatus, LE8200, Spain), with mechanical fall sensors and a rubber-covered rotating rod (diameter: 3 cm) elevated 20 cm above the sensors, was set to accelerate from 4 to 40 rpm in 5 minutes. Mice were first trained for 3 days (3 trials per day) by placing them on the rod and allowing to walk until they fell. If an animal failed to walk, and fell immediately, the timer was reset and the mouse was placed back on the rod for up to 5 times in one trial. In between the trials, mice stayed in their home cages for the time necessary to complete the task by the remaining animals. After a 4-day retention-delay, mice were given another 3 trials, and time (s) to fall was measured. PM was evaluated by comparing mean time to fall during the third day of training with the mean time to fall after 4 days of retention.

3. *Ex vivo* molecular studies

Quantitative Real-Time Polymerase Chain Reaction

One of the harvested hippocampi was placed in RNAlater stabilizing solution (Invitrogen, USA) immediately after isolation and stored on ice until frozen in -20°C. The RNA was isolated from samples with the use of TRIzol method. In short: samples were homogenized mechanically (Tissue Ruptor) and chemically (20 min. of incubation in 1mL TRI reagent); phases separated by addition 0.2 mL of chloroform and centrifugation; RNA was precipitated by addition of 1:1 of isopropyl alcohol to water phase and centrifugation; RNA pellet was washed with 95% ethyl alcohol; and, redissolved in RNase-free water. Subsequently, the RNA containing solution was: purified from any residual genomic DNA with Turbo DNA-free kit (Invitrogen, USA); mRNA concentration was measured with Quant-iT RiboGreen kit (Invitrogen, USA) and normalized to 1 ng/μL; and, reverse-transcribed to complimentary DNA with High-Capacity cDNA Reverse Transcription kit with RNase inhibitor (Applied Biosystems, USA). All kit-based procedures were performed according to the manufacturers' instructions.

The quantitative real-time polymerase chain reaction (qRT-PCR) measurement of target mRNA was performed with the use of TaqMan probes and Fast Advanced Master Mix (Applied Biosystems, USA) in a QuantStudio 3 Real-Time PCR System (Applied Biosystems, USA). Relative expression was measured in all experiments in a duplex setup, with the second target in each sample being *Actb* (cat. no. Mm02619580_g1), which served as a reference gene and was verified to be stable across experimental groups in separate experiments. For large experimental groups a subset of up to 11 samples/animals was used, based on behavioral tests' data, so that the mean and variance of subsets were representative of these data distribution estimators in experimental groups. The targets of interest were functionally associated with: excitatory/glutamatergic neurotransmission (*Gria1* (cat. no. Mm00433753_m1), *Gria2* (cat. no. Mm00442822_m1), *Gria3* (cat. no. Mm00497506_m1), *Gria4* (cat. no. Mm00444754_m1), *Grin1* (cat. no. Mm00433790_m1), *Grin2a* (cat. no. Mm00433802_m1), *Grin2b* (cat. no. Mm00433820_m1); inhibitory/GABAergic neurotransmission (*Gabra5* (Mm00621092_m1), *Gabrb3* (cat. no. Mm00433473_m1), *Gabrg2* (cat. no. Mm00433489_m1), *Slc12a5* (cat. no. Mm00803929_m1); and, neuronal survival/plasticity/remodeling (*Clu* (cat. no. Mm01197002_m1), *Gpx1* (cat. no. Mm00656767_g1), *Gpr39* (cat. no. Mm01308380_s1), *Bdnf* (cat. no. Mm04230607_s1), *Creb1* (cat. no. Mm00501607_m1), *Gsk3b* (cat. no.

Mm00444911_m1), *Mapk1* (cat. no. Mm00442479_m1), *Mapk3* (cat. no. Mm01973540_g1), *Mtor* (cat. no. Mm00444968_m1), *Mapt* (cat. no. Mm00521992_m1).

Western Blotting

One of the harvested hippocampi was immediately frozen on dry ice and stored in −80°C. Samples were homogenized mechanically in 2% sodium dodecyl sulphate (SDS), centrifuged, and total protein concentration was measured in the supernatant with BCA Protein Assay Kit (Thermo Fisher Scientific, USA) in order to normalize the sample concentration. Samples were loaded onto Mini Criterion™ Stain-Free Gels (Bio-Rad, USA) in equal amounts per well (20-50 μg) and subjected to SDS-Polyacrylamide Electrophoresis (SDS-PAGE, 200 V, 45 min.). The gels were activated with UV light in ChemiDoc MP Imaging System (Bio-Rad, USA) and samples transferred onto PVDF membranes with the use of Trans-Blot Turbo Transfer System (Bio-Rad, USA). After imaging in the ChemiDoc MP in stain-free mode, the membranes were blocked with 1% blocking solution (Roche, USA) in room temperature for 1h, incubated with primary antibody (GABAA1, GABAB3, Clu, BDNF, Tau p-S396 (cat. no. ab109390), ERK1/2 (cat. no. ab184699), KCC2, GluA2, CREB) overnight at 4°C, and rinsed 2x for 10 min in TBST and 2x for 5 min in 0.5% blocking solution (Roche, USA). After incubating with secondary antibody (50 mU/mL, Roche, USA) for 1h at room temperature, the membranes were rinsed in TBST 3x for 5 min, incubated for 1 min in enhanced chemiluminescence solution (Roche, USA), and protein bands visualized with ChemiDoc MP Imaging System. The stain-free membrane image of total protein was used for loading control normalization. The targets of interest were functionally associated with: excitatory/glutamatergic neurotransmission (GluA2); inhibitory/GABAergic neurotransmission (GABAA1, GABAB3, KCC2); and, neuronal survival/plasticity/remodeling (BDNF, CREB, Clu, ERK1/2, Tau p-S396).

4. Experimental design

Experiment 1: the effect of age and GPR39 KO on declarative and procedural memory in male mice

A total of 66 mice divided into 6 experimental groups were used to evaluate the effects of aging and constitutive GPR39 KO on distinct forms of memory. The groups were as follows: 4–5 months old WT (*n*=15) and KO (*n*=7); 11–12 months old WT (*n*=14) and KO (*n*=11); 18–

20 months old WT (*n*=7) and KO (*n*=12). All mice were tested in a battery of 3 behavioral tasks measuring: episodic-like memory (ELM test), procedural memory (modified rota-rod test) and spatial memory(Morris water maze). The order of the tests was set to progress from the least to the most stressful (Fig. 5). The groups in *ex vivo* experiments were as follows: 4–5 months old WT (*n*=11) and KO (*n*=7); 11–12 months old WT (*n*=10) and KO (*n*=9); 18–20 months old WT (*n*=7) and KO (*n*=10).

Experiment 2: the effect of age and GPR39 KO on declarative and procedural memory in female mice

A total of 57 female mice divided into 6 experimental groups were used to evaluate the effects of aging and constitutive GPR39 KO on distinct forms of memory. The groups were as follows: 4–5 months old WT (*n*=10) and KO (*n*=9); 7–8 months old WT (*n*=8) and KO (*n*=9); 16–17 months old WT (*n*=11) and KO (*n*=10). All mice were tested in a battery of 2 behavioral tasks, measuring: episodic-like memory (ELM test) and procedural memory (modified rota-rod test). The order of the tests was set to progress from the least to the most stressful (Fig. 5). Hippocampal mRNA expression levels of the following targets were evaluated *ex vivo* only in old WT (*n*=11) and KO (*n*=10) mice, due to a loss of tissue from other age groups after equipment failure: *Bdnf, Mapt, Gpr39, Grin1, Grin2a, Grin2b.*

Experiments 3–7: the effects of acute treatment with memantine or TC-G 1008 on ELM and ELM consolidation interference (CI)

All of the acute pharmacological manipulation studies were based on a within-subject experimental design. Animals underwent 2 ELM tests (under either vehicle or drug treatment) separated by a 7-day washout period (Fig. 5). *Ip* injections were performed 30 minutes before the first exposition trial. Different sets of objects were used for each ELM test, with a counterbalanced order of treatments and of object sets. The tissue for *ex vivo* experiments was

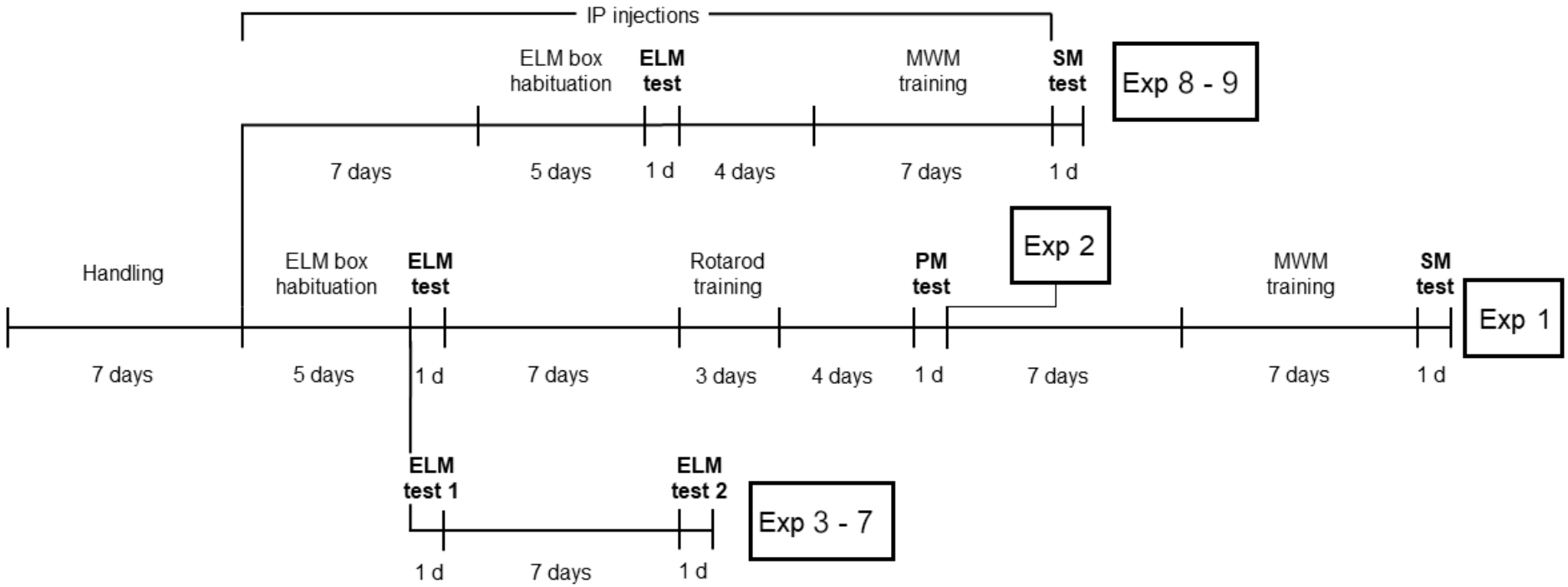

Fig. 5. Schematic representation of the experimental designs.

collected 30 min after an *ip* injection of either vehicle or drug, which was performed 7 days after the last ELM test. Animals were assigned to *ex vivo* treatment groups pseudo-randomly, so that the order of treatment during behavioral testing was counterbalanced.

The effect of TC-G 1008 was evaluated in old WT male (*Experiment 3*, age: 19 months, *n*=8) and female (*Experiment 4*, age: 16-17 months, *n*=10) mice in a standard ELM test. GPR39 agonist was also tested in the ELM CI version of the test in male WT mice (*Experiment 5*, age: 6–7 months, *n*=14). Both WT and GPR39 KO male animals participated in memantine-treatment experiments in either a standard ELM version (*Experiment 6*, WT: *n*=14; KO: *n*=14) or an ELM CI version (*Experiment 7*, WT: *n*=12; KO: *n*=14). All mice in the memantine experiments were 6–7 months old. Hippocampal mRNA expression levels of the following targets were evaluated *ex vivo* in 13 (tissue from one could not be collected, due to technical problems during dissection) animals from Experiment 5: *Bdnf, Clu, Creb1, Gabra5, Gabrb3, Gabrg2, Gpr39, Gpx1, Gria1, Gria2, Gria3, Gria4, Grin1, Grin2a, Grin2b, Gsk3b, Mapk1, Mapk3, Mapt, Mtor, Slc12a5*.

Experiment 8: the effects of chronic treatment with memantine or TC-G 1008 on ELM and SM in WT and GPR39 KO male mice

A total of 46 WT and 41 KO male mice (age: 5–6 months) were chronically injected with either a vehicle (WT: *n*=16; KO: *n*=14), memantine (WT: *n*=14; KO: *n*=14) or TC-G 1008 (WT: *n*=16; KO: *n*=13) and assessed in the ELM test, which was followed by the MWM procedure (Fig. 5). ELM was evaluated after 12 days, while SM was tested after 24 days of injections, in an off-drug state (i.e. no injections were made prior to memory tests and the daily treatments were continued only after the ELM test or the MWM training sessions). The GPR39 KO group treated with TC-G 1008 served as a negative control and was introduced into the design in order to verify the specificity of the GPR39 agonist. Hippocampal mRNA expression levels of the following targets were evaluated *ex vivo*: *Bdnf, Clu, Creb1, Gabra5, Gabrb3, Gabrg2, Gpr39, Gria1, Gria2, Gria3, Gria4, Grin1, Grin2a, Grin2b, Mapk1, Mapk3, Mapt, Mtor, Slc12a5*. The number of animals in *ex vivo* experiments was set to *n*=9 in all groups.

Experiment 9: the effects of chronic treatment with memantine or TC-G 1008 on ELM and SM in WT and BDNF HET male mice

A total of 35 WT and 33 BDNF HET male mice (age: 3–6 months) were chronically injected with either a vehicle (WT: *n*=12; HET: *n*=12), memantine (WT: *n*=10; HET: *n*=12) or

TC-G 1008 (WT: *n*=11; HET: *n*=11) and assessed in the ELM test, which was followed by the MWM procedure (Fig. 5). ELM was evaluated after 14 days, while SM was tested after 28 days of injections, in an off-drug state. Hippocampal levels of the following targets were evaluated *ex vivo*: mRNA - *Bdnf, Clu, Creb1, Gabra5, Gabrg2, Gpr39, Gria2, Grin1, Grin2a, Grin2b, Mapk1, Mapk3, Mapt, Mtor, Slc12a5*; proteins – BDNF, CREB, GABAA alpha-1, GluA2. The number of animals in Western Blot experiments was set to *n*=8 in all groups; and, *n*=9 in qRT-PCR, except for memantine WT and TC-G 1008 HET groups where *n*=8.

5. Drugs

Memantine hydrochloride was purchased from Cayman Chemical, USA, dissolved in 0.9% saline (Experiments 6 and 7) and administered at a dose of 5 mg/kg, 30 minutes before the first exposition trial in the ELM test. TC-G 1008 was purchased from Tocris, UK, suspended in 1% Tween 80 (Experiments 3 - 5) and injected at a dose of 10 mg/kg IP, 30 minutes before the first exposition trial in the ELM test. In Experiments 8 and 9, 1% Tween 80 in 0.9% saline solution served as the vehicle for both drugs, and *ip* injections were performed after the behavioral procedures, alternating injection sides (left *vs* right) daily. The volume was 5 ml/kg for all injections.

Since GPR39 KO mice are highly susceptible to kainite-induced epileptic seizures (Gilad *et al.*, 2015), the dose of memantine used in Experiment 6 was selected on the basis of studies showing its lack of an epileptogenic effect and no disturbance of cortical EEG in epilepsy-prone rats, in comparison with 10 or 20 mg/kg (Löscher and Hönack, 1990). Due to lack of effects of 5 mg/kg memantine in experiment 8, as well as no contraindications for higher dose usage in BDNF HET animals, 10 mg/kg of memantine was used in Experiment 9. The dose of TC-G 1008 was chosen on the basis of our previous studies (Młyniec *et al.*, 2016).

6. Statistical analyses

The 3 parameters from the ELM test were analyzed separately either by two-way ANOVA (Experiments 1, 2, 8, 9), mixed-model two-way ANOVA (Experiments 6 and 7) or repeated-measures *t*-tests (Experiments 3 - 5). The presence *vs* absence of ELM components was tested for each experimental group with one-sample *t*-tests against a theoretical value of 0.5 (chance level, i.e. lack of preference). Time to fall in the rotarod PM test was assessed independently in different age groups with a mixed-model two-way ANOVA.

A three-way ANOVA of swimming speed in MWM training revealed a significant effect of age in Experiment 1, and a significant effect of genotype in Experiment 9. Therefore, the MWM training data were analyzed with mixed-model two-way ANOVAs for different age groups (Experiment 1) or genotypes (Experiment 9) separately. Measures used in the SM probe test are independent of swimming speed (Vorhees and Williams, 2006), and were analyzed with two-way ANOVAs in all experiments. A three-way analysis of swimming speed during MWM training in Experiment 8 revealed no differences between experimental groups; thus, whenever possible, the training data were analyzed with mixed-model three-way ANOVAs. Percentage of time spent in the platform quadrant was compared with chance performance (25%) using one-sample *t*-tests in all MWM experiments.

Data from qRT-PCR experiments were analyzed with two-way ANOVAs (Experiments 1, 8, 9) or *t*-tests (Experiment 5). All analyses were carried out on delta Ct values i.e. the difference in number of cycles to reach the threshold between endogenous control gene (*Actb*) and the target gene measured in the same well. The threshold was set automatically by Applied Biosystems PCR software. Normalized values of band fluorescence from Western Blot experiments were analyzed with two-way ANOVAs.

Homogeneity of variance was tested with Levene's test, and normality of data distributions with the Shapiro–Wilk test. Data were inspected for the presence/absence of outliers with Grubb's test, and cleared of such data points. Data sets that violated the normality assumption and were positively skewed (skewness >1) were log transformed. Sphericity was evaluated with Mauchly's test, and a Greenhouse–Geisser correction was used for data not meeting this assumption. Post-hoc evaluation of ANOVAs was carried out using Sidak's correction. All data are presented as mean ± SEM. The *p*-values (two-tailed) were set to 0.05. Statistical analyses were performed using IBM SPSS Statistics 27, and graphs were created using GraphPad Prism 7.0.

Results

Experiment 1: the effect of age on ELM, PM and SM of adult, middle-aged and old WT and GPR39 KO male mice

ELM

We observed an impairment of integrated spatiotemporal memory in GPR39 KO mice (PR3, Genotype: $F_{(1,58)} = 7.604$, $p = 0.0078$), which was irrespective of animals' age (Age: $F_{(2,58)}$

= 0.79, NS; Age x Genotype: $F_{(2,58)}$ = 0.33, NS, Fig. 6). This effect was driven by adult and middle-aged WT mice, since only these 2 groups exhibited intact spatiotemporal memory (one-sample *t*-test, *adult WT*: $t_{(14)}$ = 2.77, p = 0.015; *middle-aged WT*: $t_{(12)}$ = 2.47, p = 0.029, Fig. 6).

We did not observe any effects of Age or Genotype on temporal order memory, or any interaction between these factors (Fig. 6; *PR1*: Age, $F_{(2,58)}$ = 2.08, NS; Genotype, $F_{(1,58)}$ = 0.24, NS; Age x Genotype, $F_{(2,58)}$ = 0,23, NS). No main effects or interaction were found for spatial memory (Fig. 6; *PR2*: Age, $F_{(2,58)}$ = 0,58, NS; Genotype, $F_{(1,58)}$ = 1,79, NS; Age x Genotype, $F_{(2,58)}$ = 0,69, NS, Fig. 6).

Two mice from the middle-aged group (1 WT and 1 KO) were excluded from the ELM analysis due to insufficient exploration of objects during the first 2 exposition trials. In the remaining animals there were no differences between the experimental groups in either total exploration time during the exposition trials, or speed and distance travelled (not shown).

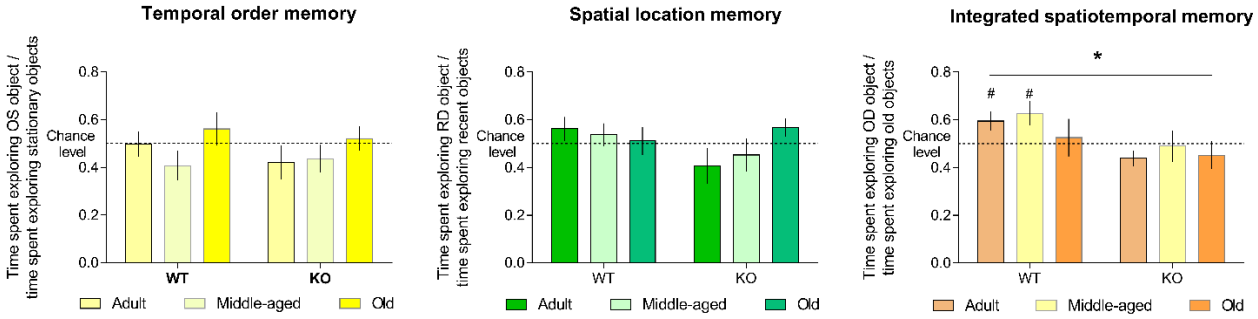

Fig. 6. GPR39 KO impairs spatiotemporal integration of ELM regardless of age in male C57BL/6J mice, which is similar to a spatiotemporal integration deficit of old WT mice. * - main effect of Genotype, p <0.05; # - one-sample *t*-test against chance preference level, p <0.05.

PM

All animals managed to learn the rotarod task and were included in the PM analysis. The statistics for the middle-aged and old groups were calculated on log-transformed data. We did not observe any effects of genotype on PM in any of the age groups (*adult mice*: Genotype, $F_{(1,20)}$ = 0.11, NS; Genotype x Retention, $F_{(1,20)}$ = 1.55, NS; *middle-aged mice*: Genotype, $F_{(1,23)}$ = 0.21, NS; Genotype x Retention, $F_{(1,23)}$ = 0.65, NS; *old mice*: Genotype, $F_{(1,17)}$ = 0.82, NS; Genotype x Retention, $F_{(1,17)}$ = 0.20, NS, Fig. 7). However, adult mice performed better after a retention-delay of 4 days (Fig.5; main effect of Retention: $F_{(1,20)}$ = 8.01, p = 0.01, Fig. 7), which was not the case for the other 2 groups (*middle-aged mice*: Day, $F_{(1,23)}$ = 0.44, NS; *old mice*: Day, $F_{(1,17)}$ = 1.51, NS, Fig. 7).

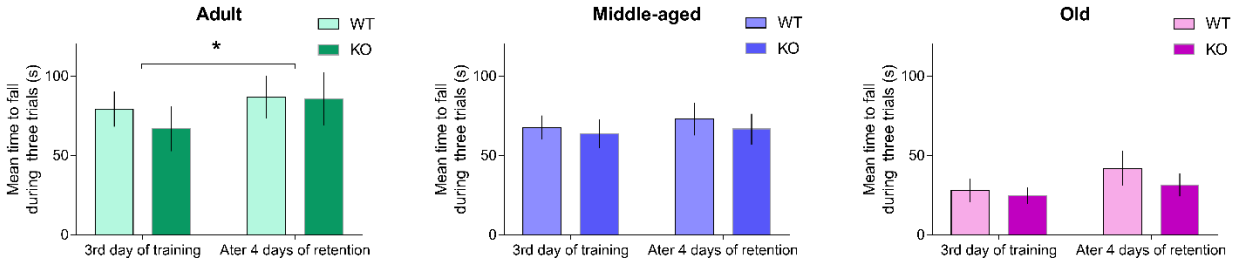

Fig. 7. Lack of effect of GPR39 KO on PM at 3 developmental stages in male C57BL/6J mice. Adult mice performed better after 4 days of retention regardless of genotype. * - main effect of retention, $p < 0.05$.

SM

During the SM probe test, GPR39 KO mice spent less time in the platform quadrant than WT littermates (main effect of Genotype, $F_{(1,61)} = 6.13$, $p = 0.016$, Fig. 8). Furthermore, all KO groups as well as old WT mice performed at chance level, with only adult and middle-aged WT animals spending more than 25% of the time in the correct quadrant (one-sample *t*-test: *adult WT*, $t_{(14)} = 3.15$, $p = 0.007$; *middle-aged WT*, $t_{(13)} = 2.25$, $p = 0.043$, Fig. 8). A trend towards a significant difference between WT and GPR39 KO mice was also seen in cumulative distance to the platform ($F_{(1,60)} = 3.23$, $p = 0.078$), but there were no differences between genotypes in the number of platform crossings ($F_{(1,60)} = 0.52$, $p = 0.476$, Fig. 8). Overall, this pattern of results suggests an SM impairment caused by GPR39 KO.

A three-way mixed-model ANOVA revealed that during the MWM learning, adult mice swam faster than middle-aged ($p = 0.026$) and old mice ($p = 0.04$, main effect of Age, $F_{(2,60)} = 3.1$, $p = 0.052$, not shown). Further two-way analyses showed a clear learning curve for adult and old mice regardless of their genotype (main effect of Day for: **1)** latency to reach the platform; *adult mice*: $F_{(3.02,60.3)} = 3.99$, $p = 0.01$; *old mice*: $F_{(6,102)} = 3.67$, $p = 0.002$; and **2)** cumulative distance from the platform; *adult mice*: $F_{(2.57,51.54)} = 3.99$, $p = 0.02$; *old mice*: $F_{(2.7,45.89)} = 6.07$, $p = 0.002$), with asymptotic performance beginning on Day 4. Middle-aged mice showed either a trend towards learning progress regardless of genotype (main effect of Day for latency to reach the platform: $F_{(2.91,66.99)} = 2.49$, $p = 0.069$) or significant learning (main effect of Day for cumulative distance from the platform: $F_{(2.38,54.77)} = 3.18$, $p = 0.04$). All of the groups learned the task, as evidenced by significant differences between training days 1 and 7 in latency to reach the platform (simple effect for Day 1 vs Day 7: *adult mice*, $p = 0.00$; *middle-aged mice*, $p = 0.02$; *old mice*, $p = 0.017$) and in cumulative distance (simple effect for Day 1 vs Day 7: *adult mice*, $p < 0.001$; *middle-aged mice*, $p = 0.06$; *old mice*, $p < 0.001$).

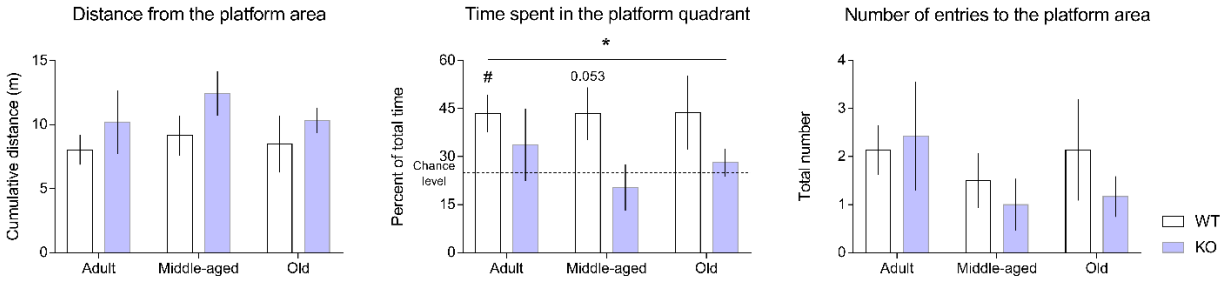

Fig. 8. GPR39 KO mice were able to locate the platform (no effect of genotype on the number of platform entries), but they spent significantly less time in the correct quadrant, and had a tendency to swim further away from the location of the platform (main effect of genotype on distance: p = 0.078), implying an SM impairment caused by GPR39 KO. * main effect of genotype, $p < 0.05$; # one-sample *t*-test against chance level, $p < 0.05$.

Hippocampal mRNA expression levels

Significant effects were observed in 8 out of the 22 tested targets, while the levels of *Gpr39* were too low to be appropriately amplified during PCR. Four of these targets displayed a similar pattern of effects of experimental manipulations on mRNA expression levels. Transcription of ***Creb1***, ***Gria2***, ***Mapk1***, *and* ***Mapt*** was lower in adult GPR39 KO compared to adult WT mice (simple effect of Genotype: ***Creb1***, p = 0.003; ***Gria2***, p = 0.019; ***Mapk1***, p = 0.02; ***Mapt***, p = 0.014, Fig. 9), and it remained unchanged with age in GPR39 KO animals, whereas significant downregulation was present in middle-aged and old WT mice compared to their adult conspecifics: ***Creb1*** (simple effect of Age: *adult vs middle-aged*, p<0.001; *adult vs old*, p = 0.011, Genotype x Age interaction: $F_{(2,47)} = 6.88$, p = 0.002, Fig 6A), ***Gria2*** (simple effect of Age: *adult vs middle-aged*, p = 0.021; *adult vs old*, p<0.001, Genotype x Age interaction: $F_{(2,48)} = 3.6$, p = 0.035, Fig 6B), ***Mapk1*** (simple effect of Age: *adult vs middle-aged*, p = 0.02; *adult vs old*, p = 0.074, Genotype x Age interaction: $F_{(2,47)} = 3.68$, p = 0.033, Fig 6C), ***Mapt*** (simple effect of Age: *adult vs middle-aged*, p = 0.061; *adult vs old*, p = 0.001, Genotype x Age interaction: $F_{(2,48)} = 7.58$, p = 0.001, Fig 6D). Additionally in case of the mRNA coding the Tau protein (***Mapt***), lower expression levels were observed in old WT compared to old GPR39 KO mice (simple effect of Genotype: p = 0.005, Fig 6D).

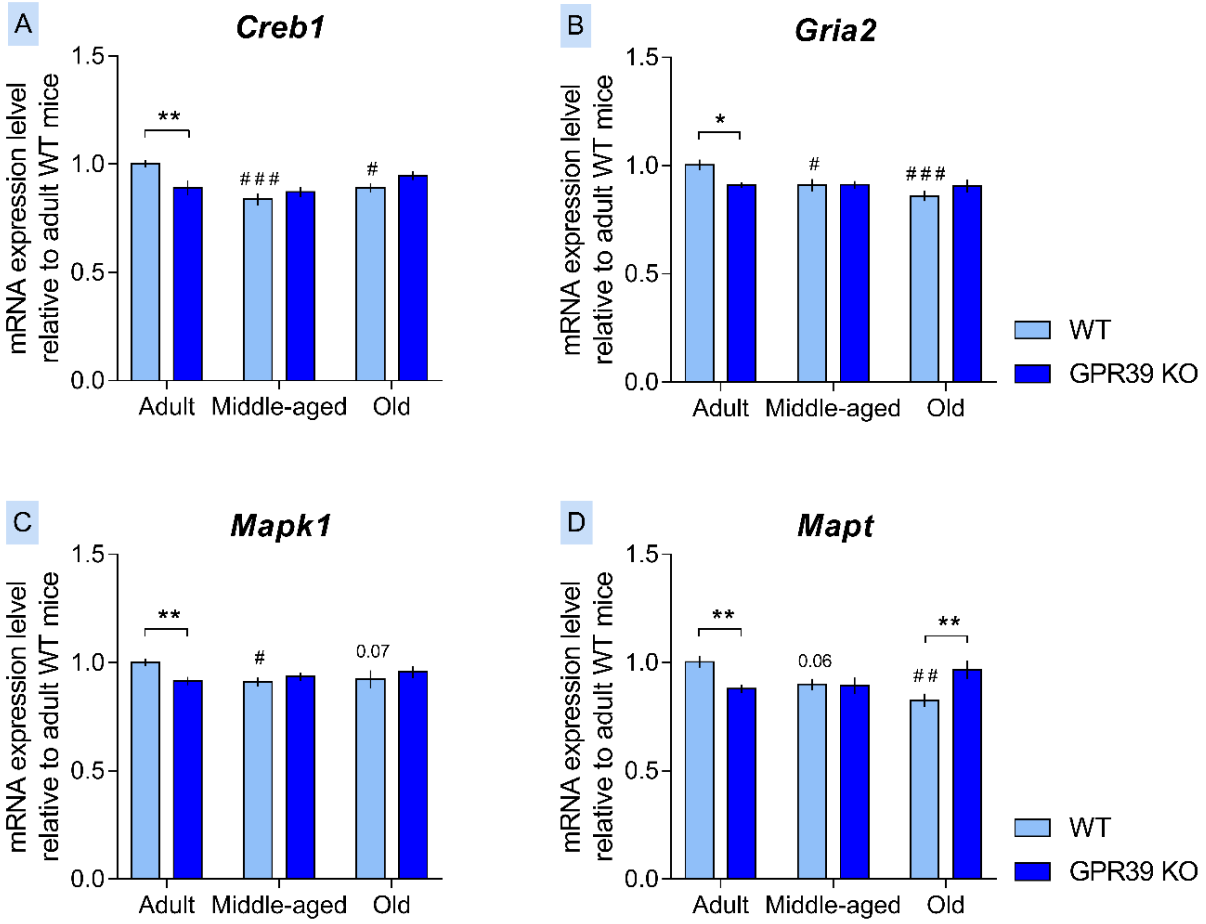

Fig. 9. Age-related transcription changes of *Creb1*, *Gria2*, *Mapk1*, and *Mapt* in the hippocampus depend on GPR39 and follow a similar pattern. The expression of *Creb1*, *Gria2*, *Mapk1*, and *Mapt* in GPR39 KO mice remains unchanged throughout development, while the transcription of the same genes drops with age in WT mice. This discrepancy is most pronounced in *Mapt*, where a reversal of the direction of GPR39 KO and WT expression levels differences is observed between adult and old age. * - simple effect of Genotype, $p<0.05$; # or *p*-values – simple effect of Age compared to adult WT group.

A significant Genotype x Age interaction was also found for 3 other targets (***Gabrb3***, $F_{(2,48)} = 12.06$, $p<0.001$; ***Gpx1***, $F_{(2,48)} = 3.44$, $p = 0.04$; ***Mtor***, $F_{(2,46)} = 5.36$, $p = 0.008$, Fig 7). A similar pattern of differences between GPR39 KO and WT mice was observed in the profile of age-related changes in mRNA expression levels for ***Gpx1*** and ***Mtor***. In WT animals, expression levels of both genes were lower in middle-aged compared to adult mice (simple effect of Age: ***Gpx1***, $p = 0.009$; ***Mtor***, $p = 0.051$, Fig. 9B and C), while in GPR39 KO mice the expression of both genes was elevated in old age compared to the remaining GPR39 KO age groups (simple effect of Age, *adult vs old*: **Gpx1**, $p = 0.01$; ***Mtor***, $p = 0.004$; *middle-aged vs old*: ***Gpx1***, $p = 0.003$; ***Mtor***, $p = 0.012$, Fig. 9B and C), and led to higher ***Mtor*** ($p = 0.011$), as well as ***Gpx1*** ($p = 0.028$) expression in old GPR39 KO compared to old WT mice. Additionally, a trend towards

lower ***Mtor*** expression in adult GPR39 KO compared to adult WT mice (p = 0.058) was observed. An opposite expression profile was present for the ***Gabrb3*** gene, which had higher expression levels in adult GPR39 KO compared to adult WT mice (simple effect of Genotype, p<0.001) and lower expression levels in old GPR39 KO compared to old WT mice (simple effect of Genotype, p = 0.007).

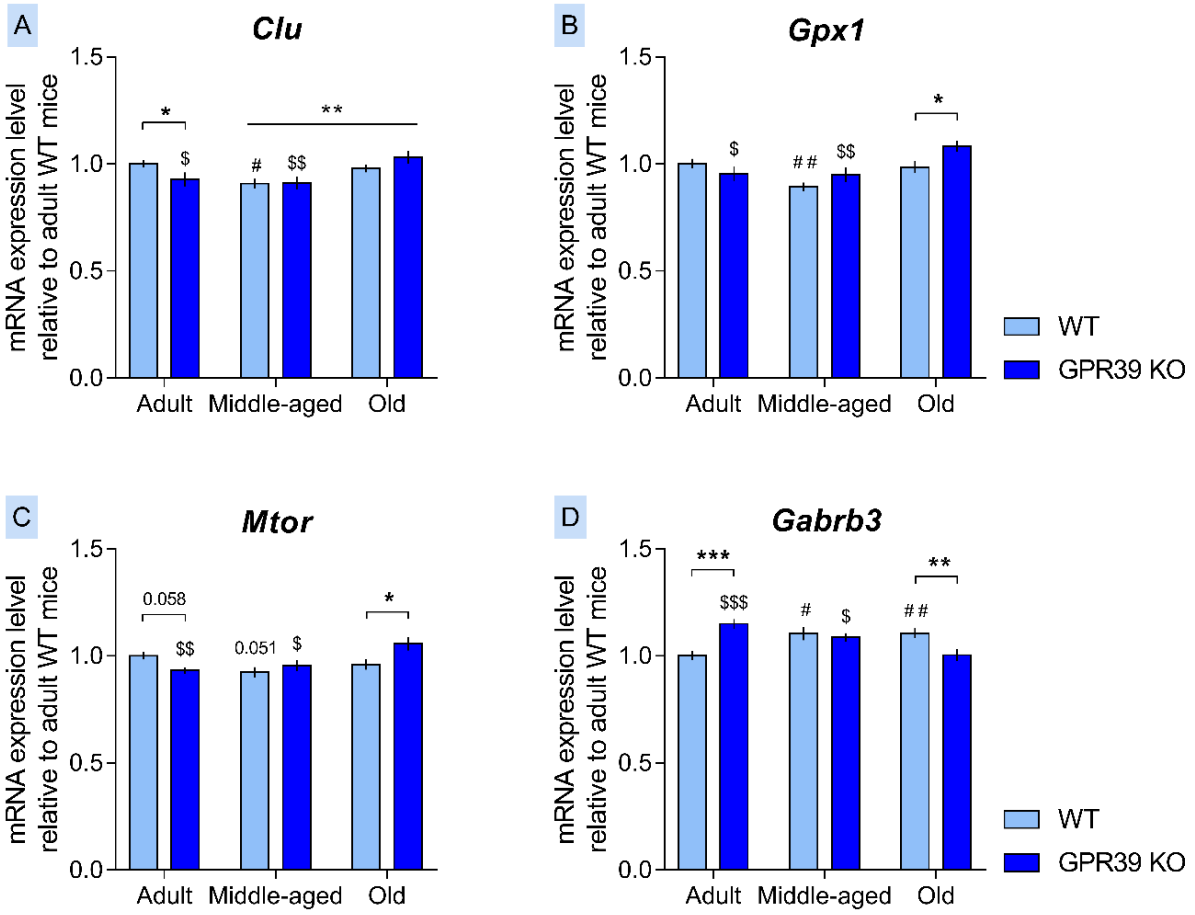

Fig. 10. The expression of *Gpx1* (B) and *Mtor* (C) is altered in old age only in GPR39 KO mice hippocampi, while in old WT mice it returns to adult-levels after a temporary drop in middle-age. The receptor's impact on age-related transcription changes is most pronounced with regard to *Gabrb3*, where lack of GPR39 causes a reversal of the direction of expression level differences between adult and old age (D). GPR39 KO affected *Clu* expression only in adult hippocampi. * - simple effect of Genotype or main effect of Age (A), p<0.05; # or *p*-values – simple effect of Age compared to adult WT group; $ - simple effect of Age compared to old GPR39 KO group.

A clear, age-related switch in ***Gabrb3*** expression was present in both GPR39 KO and WT mice, albeit in different directions and timing. While in GPR39 KO mice the levels of ***Gabrb3*** dropped in old age (simple effect of Age: *adult vs old*, p<0.001; *middle-aged vs old*, p = 0.054), in WT animals the levels of ***Gabrb3*** were elevated in middle- (p = 0.01) and old-age (p = 0.017) compared to adult age.

Lastly, ***Clu*** mRNA levels were lower in middle-aged compared to old mice, regardless of genotype (main effect of Age, $F_{(2,47)} = 7.53$, $p = 0.001$; post-hoc of *middle-aged vs old*, $p = 0.001$). A trend towards a significant Age x Genotype interaction ($F_{(2,47)} = 3.05$, $p = 0.057$) also revealed lower ***Clu*** levels in adult GPR39 KO, compared to adult WT mice ($p = 0.038$), a decrease of ***Clu*** levels in middle-aged WT compared to adult WT mice ($p = 0.014$), and an increase of ***Clu*** levels in old GPR39 KO mice compared to other two age groups of GPR39 KO animals (*adult vs old*, $p = 0.021$; *middle-aged vs old*, $p = 0.004$).

Hippocampal protein levels

A significant effect of Age was present with respect to Tau p-S396 ($F_{(2,48)} = 4.74$, $p = 0.013$), with more phosphorylated Tau in middle-aged compared to adult hippocampi ($p = 0.009$), regardless of genotype. A trend towards the same pattern of results was observed for beta 3 subunit of the GABAA receptor (main effect of Age: $F_{(2,45)} = 3.28$, $p = 0.047$; post hoc for adult vs middle-aged, $p = 0.068$), as well as an opposing pattern for KCC2, with less KCC2 in middle-aged compared to adult hippocampi (main effect of Age: $F_{(2,48)} = 3.14$, $p = 0.053$; post hoc for adult vs middle-aged, $p = 0.079$). No other differences in protein levels were detected.

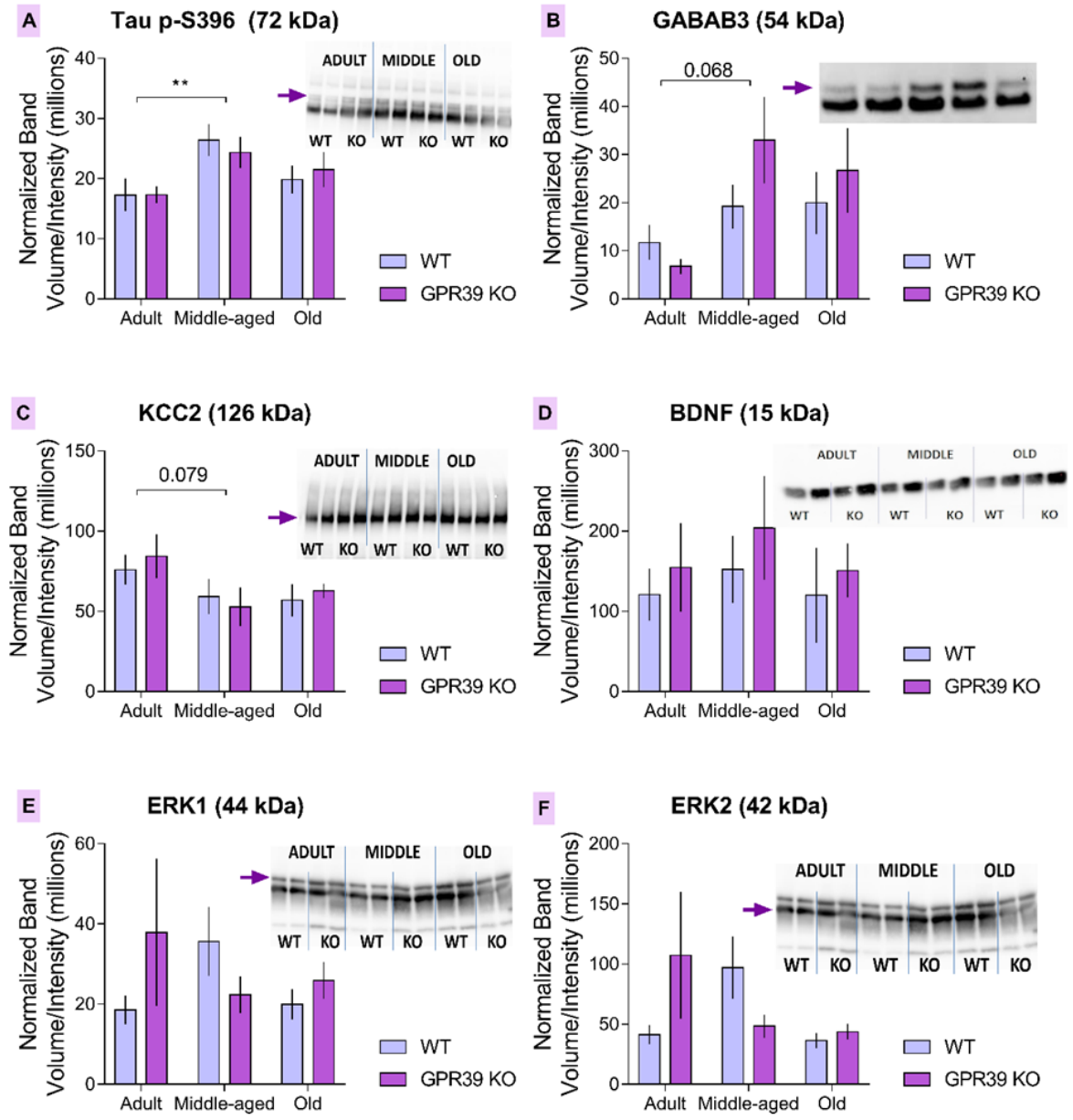

Fig. 11. The phosphorylation of Tau protein at serine 396 site is higher in middle-aged mice hippocampi compared to adult levels (A). A trend towards a similar pattern is observed with regard to beta 3 subunit of GABAA receptor (B), as well as an opposite pattern in the hippocampal levels of KCC2 protein (C). ** or *p*-values - main effect of Age, $p<0.01$.

Experiment 1

		WT						GPR39 KO					
Target		Adult		Middle		Old		Adult		Middle		Old	
mRNA	protein	mRNA	protein	mRNA	protein	mRNA	protein	mRNA	protein	mRNA	protein	mRNA	protein
Gpr39	GPR39	nd	NA	nd	NA	nd	NA	nd	NA	nd	NA	nd	NA
Creb1	CREB-1	–	NA	↓	NA	↓	NA	↓	NA	–	NA	–	NA
Slc12a5	KCC2	–	–	–	–	–	–	–	–	–	–	–	–
Bdnf	BDNF	–	–	–	–	–	–	–	–	–	–	–	–
Mapt	Tau p-S396	–	–	↓	↑	↓	–	↓	–	–	↑	–	–
Grin1	GluN1	–	NA	–	NA	–	NA	–	NA	–	NA	–	NA
Grin2a	GluN2A	–	NA	–	NA	–	NA	–	NA	–	NA	–	NA
Grin2b	GluN2B	–	NA	–	NA	–	NA	–	NA	–	NA	–	NA
Clu	Clusterin	–	–	↓	–	–	–	↓	–	–	–	–	–
Mtor	mTOR	–	NA	↓	NA	–	NA	↓	NA	–	NA	–	NA
Gria1	GluA1	–	NA	–	NA	–	NA	–	NA	–	NA	–	NA
Gria2	GluA2	–	NA	–	NA	–	NA	–	NA	–	NA	–	NA
Gria3	GluA3	–	NA	–	NA	–	NA	–	NA	–	NA	–	NA
Gria4	GluA4	–	NA	–	NA	–	NA	–	NA	–	NA	–	NA
Gabra5	GABAA-α5	–	–	–	–	–	–	–	–	–	–	–	–
Gabrb3	GABAA-β3	–	–	↑	↑	↑	–	↑	–	–	↑	–	–
Gabrg2	GABAA-γ2	–	NA	–	NA	–	NA	–	NA	–	NA	–	NA
Mapk1	ERK-2	–	–	–	–	–	–	–	–	–	–	–	–
Mapk3	ERK-1	–	–	↓	–	↓	–	–	–	–	–	–	–
Gsk3b	GSK3β	–	NA	–	NA	–	NA	–	NA	–	NA	–	NA
Gpx1	GPX1	–	NA	↓	NA	–	NA	–	NA	–	NA	–	NA

Table 1. Summary of the hippocampal mRNA expression and total protein levels in adult, middle-aged and old male WT and GPR39 KO mice. Black arrows: ↓ - downregulation or ↑ - upregulation compared to adult WT mice; *NA* – not available, *nd* – not detected; "–" – no significant effect compared to adult WT mice.

Experiment 2: the effect of age and GPR39 KO on declarative and procedural memory in female mice

ELM

No effects of either Age (Fig. 12, main effect of Age: *PR1*, $F_{(2,50)} = 0.01$, NS; *PR2*, $F_{(2,50)} = 0.42$, NS; *PR3*, $F_{(2,50)} = 0.14$, NS) or Genotype (Fig. 12, main effect of Genotype: *PR1*, $F_{(1,50)} = 0.9$, NS; *PR2*, $F_{(1,50)} = 0.03$, NS; *PR3*, $F_{(1,50)} = 0.38$, NS), nor an interaction of these factors (Fig. 12, Age x Genotype: *PR1*, $F_{(2,50)} = 1.69$, NS; *PR2*, $F_{(2,50)} = 1.64$, NS; *PR3*, $F_{(2,50)} = 2.49$, NS) were observed in female mice in all 3 of the components measured in the ELM test. One sample *t*-test revealed a trend towards spatiotemporal memory in adult GPR39 KO female mice ($t_{(8)} = 2.18$, p = 0.061, Fig. 12). One animal from the middle-aged WT group was excluded from ELM analysis due to insufficient exploration time during the test trial i.e. lack of data.

The interpretation of these results is confounded by a significant effect of Genotype on exploration time during the second exposition trial, when GPR39 KO animals spent more time exploring the objects ($F_{(2,51)} = 8.1$, p<0.001). Moreover, throughout the second trial GPR39 KO mice were more active, as evidenced by less time spent immobile ($F_{(2,51)} = 4.81$, p = 0.01), more distance travelled ($F_{(2,51)} = 6.05$, p = 0. 004) and higher mean speed ($F_{(2,51)} = 5.98$, p = 0.005).

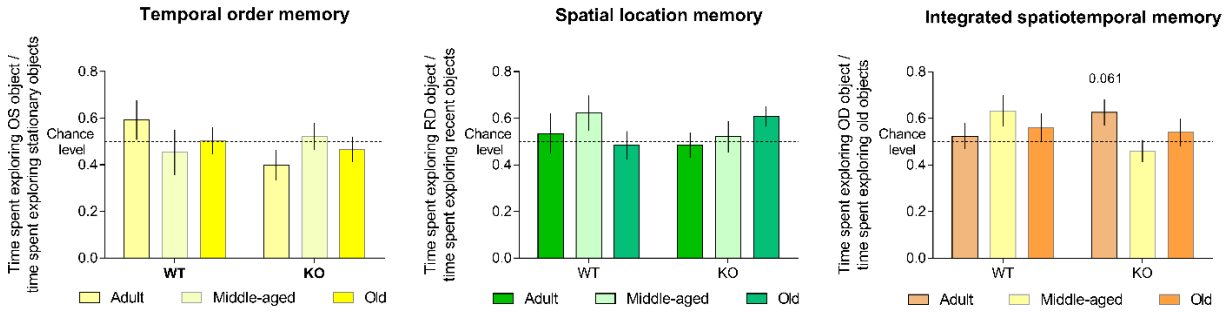

Fig. 12. Lack of effect of GPR39 KO on ELM at 3 developmental stages in female C57BL/6J mice. Adult GPR39 female mice displayed a trend towards spatiotemporal integration of ELM (one-sample *t*-test, p = 0.061).

PM

Similarly to male mice, we did not observe any effects of genotype on PM in any of the female age groups (*adult mice*: Genotype, $F_{(1,17)} = 2.95$, NS; Genotype x Retention, $F_{(1,17)} = 0.68$, NS; *middle-aged mice*: Genotype, $F_{(1,15)} = 0.01$, NS; Genotype x Retention, $F_{(1,15)} = 3.57$, NS; *old mice*: Genotype, $F_{(1,20)} = 0.03$, NS; Genotype x Retention, $F_{(1,20)} = 0.08$, NS, Fig.10). However, a pattern opposite to the one observed in male mice was present in females with regard to the effect of consolidation on PM at 3 developmental stages. There was no

improvement of performance in adult female mice (main effect of Retention: $F_{(1,17)} = 0.62$, NS. Fig.10), while both middle-aged and old females performed better after the 4-day retention delay (*middle-aged*: $F_{(1,15)} = 5.32$, $p = 0.036$; *old*: $F_{(1,20)} = 12.38$, $p = 0.002$, Fig.10). All animals managed to learn the rotarod task and were included in the PM analysis.

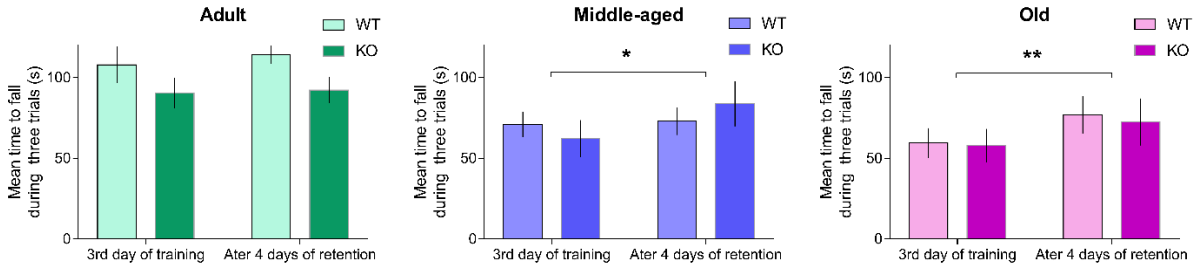

Fig. 13. Lack of effect of GPR39 KO on PM at 3 developmental stages in female C57BL/6J mice. Middle-aged and old female mice performed better after 4 days of retention regardless of genotype. * - main effect of retention, $p < 0.05$.

Hippocampal mRNA expression levels

As previously mentioned, the qRT-PCR *ex vivo* analyses were restricted to old female age group. We did not observe any differences between GPR39 KO and WT old female mice in either *Bdnf*, *Mapt*, *Grin1*, *Grin2a* or *Grin2b* expression levels (not shown), and the levels of *Gpr39* were too low to be appropriately amplified during PCR.

Experiment 3: the effect of acute TC-G 1008 on ELM of old WT male mice

In old WT male mice, acute administration of TC-G 1008 before the standard ELM task improved both the temporal (*PR1*, paired *t*-test: $t_{(6)} = 3.59$, $p = 0.012$, Fig. 14) and the spatial (*PR2*, paired *t*-test: $t_{(6)} = 3.09$, $p = 0.021$, Fig. 14) components, without an effect on the integrated spatiotemporal component (*PR3*, paired *t*-test: $t_{(6)} = 1.51$, NS, Fig. 14). One-sample *t*-tests confirmed that mice remembered when (*PR1*, $t_{(6)} = 2.93$, $p = 0.027$, Fig. 14) and where (*PR2*, $t_{(6)} = 2.60$, $p = 0.041$, Fig. 14) the objects were placed *only after* TG-G 1008 treatment (Fig. 14). One animal was excluded from the analysis due to insufficient exploration during the exposition trials after vehicle treatment.

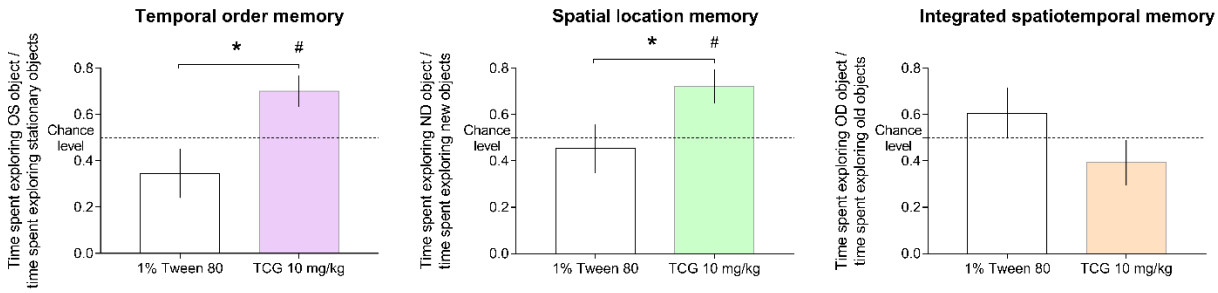

Fig. 14. GPR39 agonist (TC-G 1008) improves temporal and spatial components of ELM after acute injection in old male WT C57BL/6J mice. * - paired *t*-test, p <0.05; # - one-sample *t*-test against chance preference, p <0.05.

Experiment 4: the effect of acute TC-G 1008 on ELM of old WT female mice

In old WT female mice, acute administration of TC-G 1008 before the standard ELM task had no effect on both the temporal (*PR1*, paired *t*-test: $t_{(9)} = 0.53$, NS, Fig. 15) and the spatial (*PR2*, paired *t*-test: $t_{(9)} = 0.47$, NS, Fig. 15) components, but a weak trend toward an effect on the integrated spatiotemporal component was observed (*PR3*, Wilcoxon matched-pairs test: W = -35, p = 0.08, Fig. 15). One-sample *t*-tests and Wilcoxon test revealed that only after TC-G 1008 administration mice remembered when the objects were placed (*PR2*, $t_{(9)} = 3.46$, p = 0.007, Fig. 15) and displayed a trend towards spatiotemporal memory (*PR3*, W = -37, p = 0.065, Fig. 15). Interestingly, the weak effect on spatiotemporal memory was due to preference towards OS object over OD object after, which is a pattern observed in rats (Chao *et al.*, 2017).

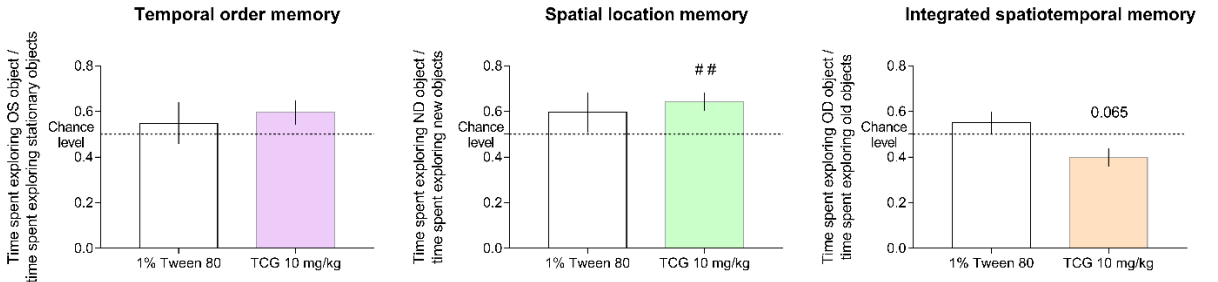

Fig. 15. Lack of clear effect of GPR39 agonist (TC-G 1008) on ELM components after acute injection in old female WT C57BL/6J mice. # # - one-sample *t*-test against chance preference, p <0.01; 0.065 – p-value of one-sample *t*-test against chance preference.

Experiment 5: the effect of acute TC-G 1008 on ELM CI of adult WT male mice

ELM CI

In adult WT male mice, acute administration of TC-G 1008 before the ELM CI task had no effect (Fig. 16, paired-samples *t*-tests, *PR1*, $t_{(11)} = 1.39$, NS; *PR2*, $t_{(11)} = 0.79$, NS; *PR3*, $t_{(11)} = 1.46$, NS). This group of mice did show a preference towards OS object over OD object after vehicle treatment (one-sample *t*-test, *PR3*, $t_{(11)} = 2.21$, $p = 0.049$, Fig. 16), a pattern which – as mentioned above - is usually observed in rats tested with a 60-minute ISI (Chao *et al.*, 2017). Two animals (one after vehicle and one after drug treatment) were excluded from the analyses, due to insufficient time of exploration during the test trial, i.e. lack of data.

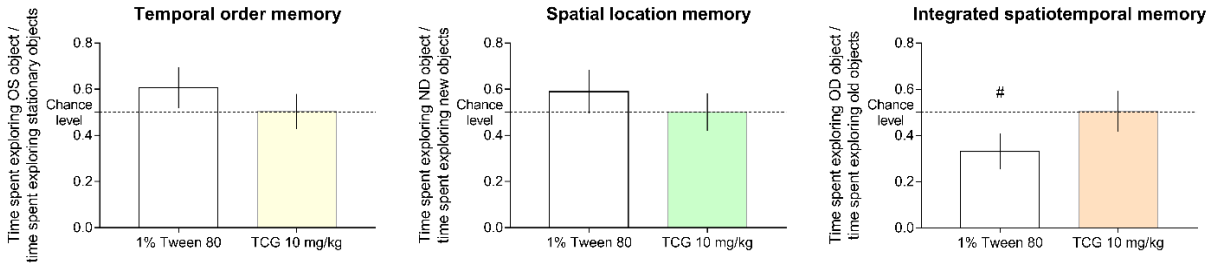

Fig. 16. Lack of effect of GPR39 agonist (TC-G 1008) on consolidation interference of ELM components after acute injection in adult male WT C57BL/6J mice. # - one-sample *t*-test against chance preference, $p < 0.05$.

Hippocampal mRNA expression levels

Significant effects were observed in 2 out of the 22 tested targets (*Gria2* and *Gabrb3*). Acute TC-G 1008 administration increased the expression levels of both ***Gria2*** ($t_{(11)} = 3.45$, $p = 0.005$, Fig. 17) and ***Gabrb3*** ($t_{(11)} = 2.42$, $p = 0.034$, Fig. 17) in adult WT hippocampus. The levels of *Gpr39* were too low to be appropriately amplified during PCR.

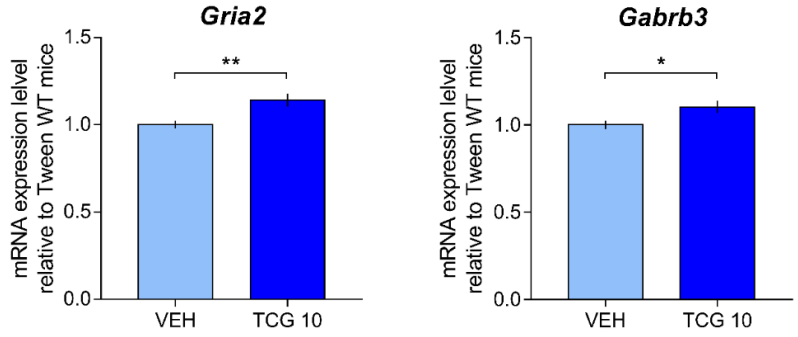

Fig. 17. Acute injection of GPR39 agonist (TC-G 1008) causes an upregulation of *Gria2* and *Gabrb3* mRNA transcription in adult male WT C57BL/6J mice. *; ** - unpaired *t*-test, $p < 0.05$; $p < 0.01$.

Experiment 6: the effect of acute memantine on ELM of adult WT and GPR39 KO male mice

In adult WT and KO male mice, acute administration of memantine before the standard ELM task had no effect on ELM (Fig. 18, main effect of Treatment, *PR1*, $F_{(1,23)}$ = 1.45, NS; *PR2*, $F_{(1,23)}$ = 2.27, NS; *PR3*, $F_{(1,23)}$ = 1.66, NS). There were also no differences between WT and KO animals (main effect of Genotype, *PR1*, $F_{(1,23)}$ = 0.17, NS; *PR2*, $F_{(1,23)}$ = 0.00, NS; *PR3*, $F_{(1,23)}$ = 1.85, NS), as well as no Treatment x Genotype interaction (*PR1*, $F_{(1,23)}$ = 0.05, NS; *PR2*, $F_{(1,23)}$ = 0.01, NS; *PR3*, $F_{(1,23)}$ = 0.00, NS, Fig. 18). We did not observe object preference in any of the groups/conditions. Data from 2 WT animals was not collected due to technical difficulties, and 1 WT mouse was excluded due to lack of exploratory behavior during the test trial after vehicle treatment.

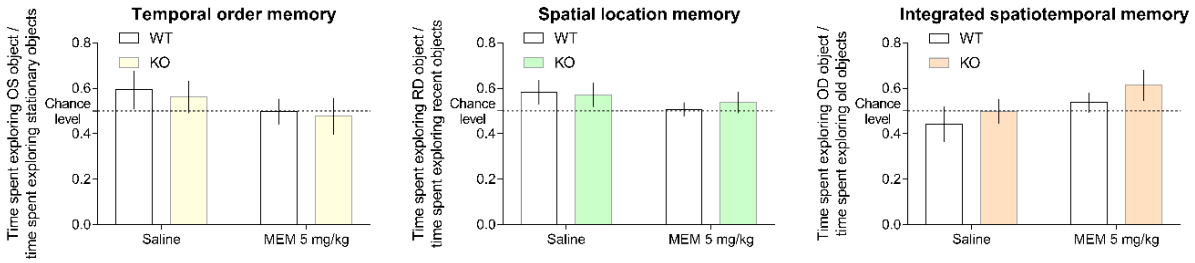

Fig. 18. Lack of effect of memantine on ELM components after acute injection in adult male GPR39 KO and WT C57BL/6J mice.

Experiment 7: the effect acute memantine on ELM CI of adult WT and GPR39 KO male mice

In adult WT and GPR39 KO male mice, acute administration of memantine had no effect in the ELM CI test (main effect of Treatment, *PR1*, $F_{(1,22)}$ = 2.28, NS; *PR2*, $F_{(1,22)}$ = 1.56, NS; *PR3*, $F_{(1,22)}$ = 0.02, NS; Treatment x Genotype interaction, *PR1*, $F_{(1,22)}$ = 0.18, NS; *PR2*, $F_{(1,22)}$ = 2.38, NS; *PR3*, $F_{(1,22)}$ = 0.11, NS, Fig. 19).

GPR39 KO mice differed from their WT littermates in *PR3* regardless of the drug treatment (main effect of Genotype, $F_{(1,22)}$ = 4.46, p = 0.046, Fig. 19); however, neither group displayed the spatiotemporal ELM component (one-sample *t*-tests, WT: $t_{(9)}$ = 1.67, NS; KO: $t_{(13)}$ = 0.86, NS, Fig. 19).

The only group of mice which showed a trend towards object preference were GPR39 KO mice after memantine treatment (one-sample *t*-test, *PR2*, $t_{(13)}$ = 2.1, p = 0.056, Fig. 19). There were no differences in measures of locomotor activity or exploration time during

exposition and test trails. Two WT mice were excluded from the analysis due to lack of exploratory behavior during the test trial after vehicle (1 animal) or memantine (1 animal) treatment.

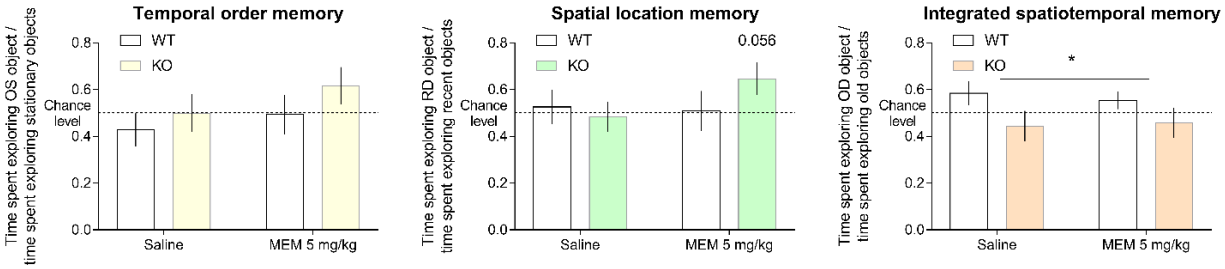

Fig. 19. Lack of effect of memantine on consolidation interference (CI) of ELM components after acute injection in adult male GPR39 KO and WT C57BL/6J mice. GPR39 KO mice differed in old object preference under CI condition, but the spatiotemporal component was absent in both groups. * - main effect of genotype, $p < 0.05$.

Experiment 8: the effects of chronic TC-G 1008 and memantine on ELM and SM adult WT and GPR39 KO mice

ELM

Although we did not observe any significant effects of 12 days of TG-G 1008 or memantine treatment on ELM, only memantine-treated groups showed spatial location memory (one-sample *t*-tests of PR2 for: *WT mice*, $t_{(12)} = 2.46$, $p = 0.03$; *KO mice*, $t_{(11)} = 2.67$, $p = 0.022$, Fig. 20). There were no differences in measures of locomotor activity or exploration time during exposition and test trails.

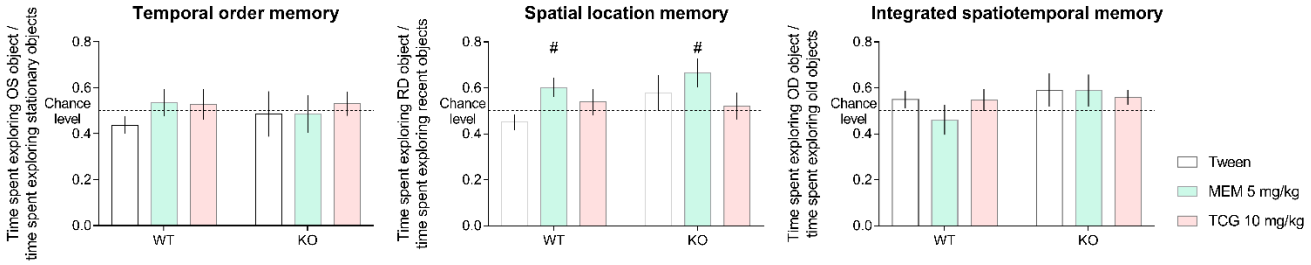

Fig. 20. Lack of significant group differences in the effect of 12 days of memantine or TG-G 1008 administration on ELM in adult GPR39 KO and WT C57BL/6J mice. Only memantine-treated groups displayed the spatial ELM component, with all other components absent regardless of treatment or genotype. # - one sample *t*-test against chance preference, $p < 0.05$.

SM

Chronic memantine treatment impaired SM in GPR39 KO in comparison with memantine-treated WT mice (Genotype x Treatment interaction in platform area crossings: $F_{(2,72)} = 3.66$, $p = 0.031$; simple effect in memantine groups: $p = 0.031$, Fig. 21). Moreover, KO animals had a tendency to spend less time than their WT littermates in the platform quadrant (main effect of Genotype: $F_{(1,72)} = 3.85$, $p = 0.054$, Fig. 21); however, only KO mice under memantine treatment performed at chance level in this regard (one-sample *t*-test: $t_{(13)} = 1.74$, NS, Fig. 21), which might have driven the main effect of Genotype. Main effect of Treatment was also observed with regard to distance from the platform area ($F_{(2,72)} = 3.86$, $p = 0.026$, Fig. 21), with memantine-caused impairment in comparison to TC-G 1008 ($p = 0.013$, Fig. 21). Although this effect was observed regardless of genotype, it was clearly driven by memantine-treated GPR39 KO group. Overall, this pattern of results implicates memantine-induced SM impairment in KO mice in the MWM.

A three-way mixed-model ANOVA revealed no differences between groups in swimming speed during MWM training (not shown). Neither genotype nor drug treatment affected the rate of MWM learning, as evidenced by no interaction between these factors and day of training in either latency to reach the platform or cumulative distance from it (Treatment x Genotype x Day: *latency*, $F_{(8.34,317.01)} = 0.839$, NS; *distance*, $F_{(6.69,254.38)} = 0.97$, NS; Treatment x Day: *latency*, $F_{(8.34,317.01)} = 1.23$, NS; *distance*, $F_{(6.69,254.38)} = 1.52$, NS; Genotype x Day: *latency*, $F_{(4.17,317.01)} = 1.13$, NS; *distance*, $F_{(3.35,254.38)} = 1.15$, NS).

All experimental groups learned the MWM task (main effect of Day for: **1)** *latency to reach the platform*, $F_{(4.17,317)} = 56.18$, $p<0.001$; *post hoc* for Day 1 vs Day 7: $p<0.001$; and **2)** *cumulative distance from the platform*: $F_{(3.35,254.38)} = 87.8$, $p<0.001$; *post hoc* for Day 1 vs Day 7: $p<0.001$). Five animals qualified as non-performers and were excluded during training (1 from vehicle WT and KO groups; 1 from TC-G 1008 KO; and 2 from memantine WT group).

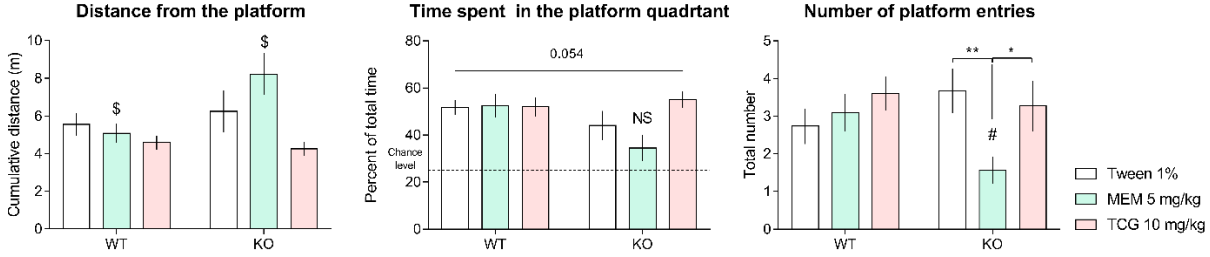

Fig. 21. GPR39 KO mice after 24 days of memantine treatment were less precise in locating the platform than memantine-treated WT mice (number of entries to the platform area: # - MEM WT *vs* MEM KO, $p < 0.05$) and

could not remember its general location (NS - chance level of platform quadrant exploration). $ - memantine *vs* TC-G 1008 post-hoc for main effect of Treatment, 0.054 = p-value for main effect of genotype.

Hippocampal mRNA expression levels

Significant differences in gene expression levels were found in 5 out of the 20 tested targets between GPR39 KO and WT mice treated chronically with TC-G 1008: ***Clu*** (simple effect of Genotype, p = 0.016, Genotype x Treatment, $F_{(2,48)} = 3.06$, p = 0.056, Fig. 22A), ***Creb1*** (p = 0.031; $F_{(2,48)} = 2.77$, p = 0.073, Fig. 22E), ***Gabrg2*** (p = 0.009; $F_{(2,46)} = 3.22$, p = 0.049, Fig. 22D), ***Gria3*** (p = 0.048; $F_{(2,48)} = 2.92$, p = 0.064, Fig. 22B), and ***Slc12a5*** (p = 0.008; $F_{(2,48)} = 4.13$, p = 0.022, Fig. 22C). In all cases the expression was lower in GPR39 KO hippocampi in response to the drug, compared to WT littermates.

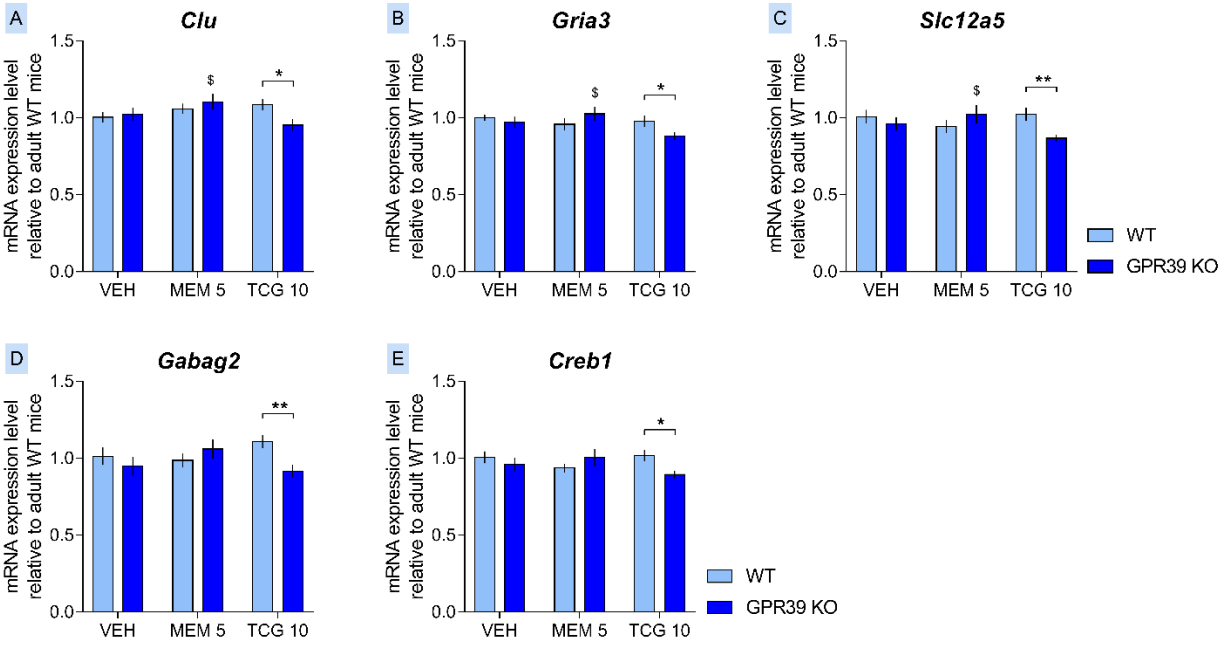

Fig. 22. TC-G 1008 may not be a selective agonist of GPR39, as the compound caused downregulation of transcription of 5 genes in hippocampi of GPR39 KO mice compared to TC-G 1008-treated WT littermates (A-E). *, ** - simple effect of Genotype for TC-G 1008, p<0.05, p<0.01; $ - simple effect of Treatment compared to TC-G 1008 GPR39 KO group, p<0.05.

The levels of ***Clu*** (simple effect of Treatment, p = 0.027, Fig. 22A), ***Gria3*** (p = 0.016, Fig. 22B), and ***Slc12a5*** (p = 0.031, Fig. 22C) were also lower in TC-G 1008-treated GPR39 KO mice compared to their KO littermates treated with memantine. Again**,** the gene expression levels of *Gpr39* were too low to be appropriately amplified during PCR.

Experiment 9: the effects of chronic treatment with memantine or TC-G 1008 on ELM and SM in WT and BDNF HET male mice

ELM

No effects of either Treatment, Genotype or an interaction of these factors on all 3 ELM components were present after 14 days of *ip* injections in WT and BDNF HET mice (Fig. 23). No preference for any object was observed in one sample *t*-tests. Three-way ANOVA of Treatment x Genotype x Trial of immobility during 2 exposition trials revealed that memantine-treated mice spent more time immobile during the first exposition trial, compared to vehicle-treated mice, regardless of genotype (simple effect of Treatment, p = 0.002; Trail x Treatment interaction: $F_{(2,62)} = 3.38$, p = 0.04), with vehicle-treated mice being more immobile during the second trial, compared to the first trial (p = 0.029). No differences were observed with regard to time spent exploring the objects. Three WT animals were excluded from ELM test analysis due to insufficient exploration time during the exposition trails – one from each drug treatment group.

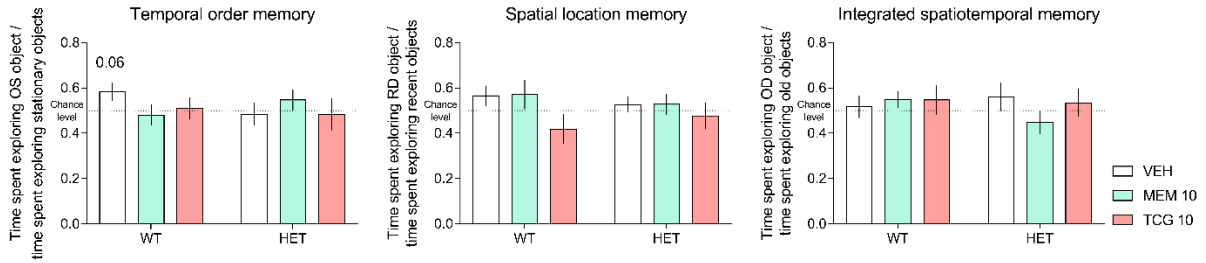

Fig. 23. Lack of effect of 14 days of memantine or TG-G 1008 administration on ELM in adult BDNF HET and WT C57BL/6J mice. p = 0.06 - one sample *t*-test against chance preference.

SM

BDNF HET mice spent less time in the platform quadrant than their WT littermates during the SM probe test (main effect of Genotype: $F_{(1,58)} = 4.49$, p = 0.038, Fig. 24), regardless of the drug treatment (main effect of Treatment: $F_{(2,58)} = 2.22$, NS; Treatment x Genotype interaction: $F_{(2,58)} = 0.09$, NS, Fig. 24). The difference was quantitative rather than qualitative, since all animals explored the correct quadrant at above chance levels (on sample *t*-tests: *vehicle* – **WT**, $t_{(10)} = 4.65$, p<0.001; **HET**, $t_{(11)} = 3.65$, p = 0.004; *memantine* - **WT**, $t_{(8)} = 4.47$, p = 0.002; **HET**, $t_{(10)} = 5.08$, p<0.001; *TC-G 1008*: **WT**, $t_{(9)} = 7.21$, p<0.001; **HET**, $t_{(10)} = 5.95$, p<0.001, Fig. 24). No further effects were present in either cumulative distance from the platform area or the number of platform area crossings during the probe test.

A three-way mixed-model ANOVA revealed that during the MWM training, BDNF HET mice swam faster than WT littermates (main effect of Genotype: $F_{(1,59)} = 8.07$, $p = 0.006$, not shown), and therefore latencies to reach the platform during the training could not be directly compared between genotypes. Further two-way mixed model ANOVAs showed a clear learning curve in both WT and BDNF HET mice, with asymptotic performance starting at day 3 of the 5-day training in both groups: **1)** main effect of Day for *latency to reach the platform*: **WT**, $F_{(4, 108)} = 59.46$, $p<0.001$, post hoc for Day 1 vs Day 5: $p<0.001$; **HET**, $F_{(4, 128)} = 45.68$, $p<0.001$, post hoc for Day 1 vs Day 5: $p<0.001$; **2)** *cumulative distance from the platform*: **WT**, $F_{(4, 108)} = 96.6$, $p<0.001$, post hoc for Day 1 vs Day 5: $p<0.001$; **HET**, $F_{(4, 128)} = 60.05$, $p<0.001$, post hoc for Day 1 vs Day 5: $p<0.001$. Three WT animals qualified as non-performers and were excluded during training – one from each drug treatment group.

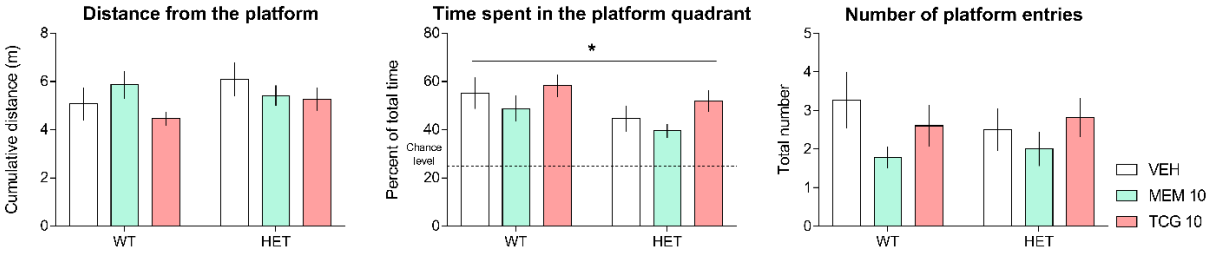

Fig. 24. Although BDNF HET mice remembered the location of the platform following a 24 h delay, they spent less time in the correct quadrant of the MWM pool than WT C57BL/6J mice, regardless of drug treatment. * - main effect of Genotype, $p<0.05$; one sample *t*-test of time spent in the platform quadrant against chance level: $p<0.05$ for all groups (not shown).

Hippocampal mRNA expression levels

The expression level of ***Mapk3*** was higher in BDNF HET compared to WT hippocampi, regardless of drug treatment (main effect of Genotype: $F_{(1,46)} = 4.08$, $p = 0.049$, Fig. 25B). Significant Genotype x Treatment interaction was also observed with regard to ***Mapk1*** ($F_{(2,45)} = 6.82$, $p = 0.003$, Fig. 25A), with higher expression in BDNF HET after vehicle treatment, compared to vehicle-treated WT littermates ($p = 0.024$). An opposing effect of TC-G 1008 depending on animals' genotype was observed, with downregulation in BDNF HET mice ($p = 0.037$) and upregulation in WT mice ($p = 0.055$) after chronic TC-G 1008, compared to vehicle-treated littermates of the same genotype.

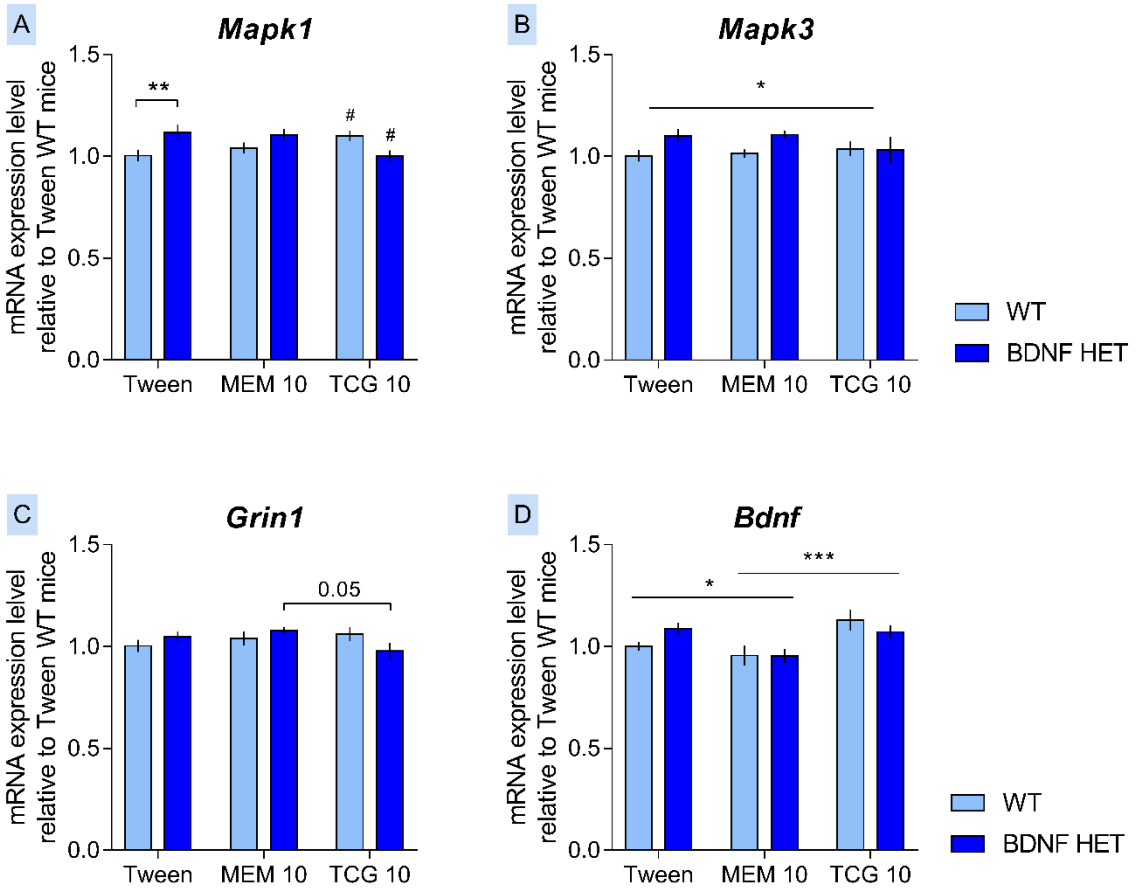

Fig. 25. BDNF HET knockout caused an upregulation of *Mapk3* transcription in the hippocampus (B), and affected the impact of chronic TC-G 1008 administration on hippocampal *Mapk1* mRNA levels (A). The transcription of *Bdnf* was attenuated by chronic memantine regardless of genotype (D), while *Grin1* displayed a tendency towards lower expression in TC-G 1008-treated BDNF HET mice, compared to their memantine-treated littermates (C). * - main or simple effect of Genotype or Treatment (C), $p<0.05$; # - simple effect of Treatment against VEH, $p<0.05$.

A strong trend towards lower expression of ***Grin1*** in BDNF HET mice treated with TC-G 1008, compared to memantine-treated BDNF HET mice, was also present ($p = 0.05$, Genotype x Treatment: $F_{(2,46)} = 3.05$, $p = 0.057$, Fig.22C). Although the BDNF protein translation was successfully attenuated in BDNF HET mice (see: next section), there were no differences in the initial transcription of the ***Bdnf*** gene (main effect of Genotype: $F_{(1,46)} = 0.15$, NS, Fig. 25D). However, chronic memantine treatment reduced ***Bdnf*** transcription in comparison to both vehicle- and TC-G 1008-treated groups, regardless of genotype (main effect of Treatment: $F_{(2,46)} = 8.13$, $p<0.001$; post hoc for *vehicle vs memantine*, $p = 0.033$; post hoc for *TC-G 1008 vs memantine*, $p<0.001$, Fig. 25D).

Hippocampal protein levels

The BDNF HET mice had lower BDNF protein levels in the hippocampi than their WT littermates (main effect of Genotype: $F_{(1,42)} = 9.73$, $p = 0.003$, Fig. 26A). A similar pattern was observed for the alpha 1 subunit of the GABAA receptor (main effect of Genotype: $F_{(1,42)} = 4.29$, $p = 0.045$, Fig. 26B). Lastly, memantine treatment caused a lowering of CREB protein levels compared to other treatment groups, irrespective of genotype (main effect of Treatment: $F_{(1,41)} = 6.6$, $p = 0.003$; post hoc for *vehicle vs memantine*, $p = 0.019$; post hoc for *TC-G 1008 vs memantine*, $p = 0.005$, Fig. 26C).

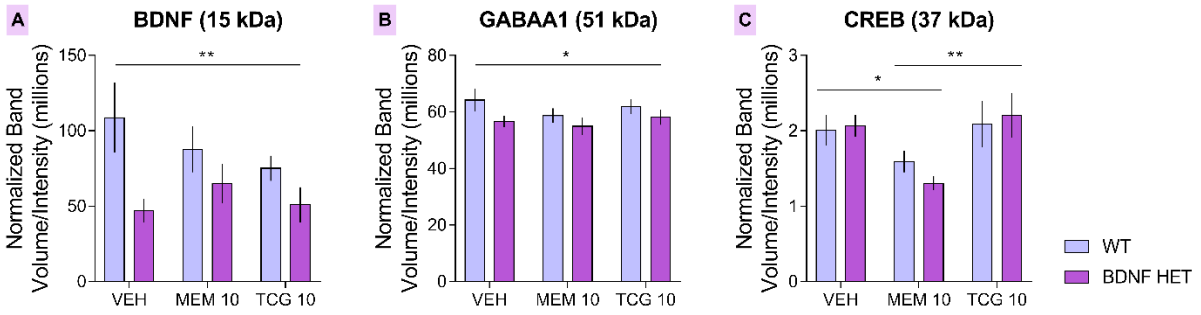

Fig. 26. BDNF HET mice had lower levels of mBDNF than WT mice in their hippocampi, but the expected twofold difference was observed only in vehicle-treated animals (A). An effect of the knockout was also observed for alpha1 subunit of the GABAA receptor (B), with lower protein levels in BDNF HET hippocampi. The cAMP-response element binding (CREB) expression factor was downregulated by chronic memantine, regardless of genotype (C), similarly to *Bdnf* mRNA expression (Fig. 25D). * - main effect of Genotype or *post hoc* for main effect of Treatment, $p<0.05$.

Experiment 9

		WT						BDNF HET					
Target		VEH		MEM		TC-G 1008		VEH		MEM		TC-G 1008	
mRNA	protein	mRNA	protein	mRNA	protein	mRNA	protein	mRNA	protein	mRNA	protein	mRNA	protein
Gpr39	GPR39	nd	NA	nd	NA	nd	NA	nd	NA	nd	NA	nd	NA
Bdnf	BDNF	–	–	↓	–	–	–	–	–	↓	–	–	–
Clu	Clusterin	–	NA	–	NA	–	NA	–	NA	–	NA	–	NA
Creb1	CREB-1	–	–	–	–	–	–	–	–	–	–	–	–
Gabra5	GABAA-α5	–	–	–	–	–	–	–	–	–	–	–	–
Gabrg2	GABAA-γ2	–	NA	–	NA	–	NA	–	NA	–	NA	–	NA
Gria2	GluA2	–	–	–	–	–	–	–	–	–	–	–	–
Grin1	GluN1	–	NA	–	NA	–	NA	–	NA	–	NA	–	NA
Grin2a	GluN2A	–	NA	–	NA	–	NA	–	NA	–	NA	–	NA
Grin2b	GluN2B	–	NA	–	NA	–	NA	–	NA	–	NA	–	NA
Mapk1	ERK-2	–	NA	–	NA	↑	NA	↑	NA	–	NA	↓	NA
Mapk3	ERK-1	–	NA	–	NA	–	NA	↑	NA	↑	NA	↑	NA
Mapt	Tau p-S396	–	NA	–	NA	–	NA	–	NA	–	NA	–	NA
Mtor	mTOR	–	NA	–	NA	–	NA	–	NA	–	NA	–	NA
Slc12a5	KCC2	–	NA	–	NA	–	NA	–	NA	–	NA	–	NA

Table 2. Summary of the hippocampal mRNA expression and total protein levels male WT and BDNF HET mice after chronic vehicle (VEH), memantine (MEM) or GPR39 agonist (TC-G 1008) treatment. *Black arrows*: ↓ - downregulation or ↑ - upregulation compared to adult WT mice; *green arrows*: compared to other treatment groups regardless of genotype; *red arrows*: compared to other genotype regardless of the treatment; *NA* – not available, *nd* – not detected; "–" – no significant effect.

Discussion

The hippocampus is one of the best-studied brain structures with regard to Zn^{2+}'s effects on neuronal activity, and a crucial hub for episodic memory, which is affected in early stages of AD continuum. The interaction between Zn^{2+} and Aβ causes rapid "double-edge sword"-like effects by disrupting zincergic neurotransmission and neuromodulation and - at the same time - exacerbating Aβ neuropathology. Therefore, Zn^{2+} supplementation – although necessary for the elderly - might not lead to desired outcomes in individuals suffering from Alzheimer's pathologic change. To circumvent this issue, direct activation of a zincergic GPR39 receptor could be a strategy worth pursuing, provided that the receptor was involved in regulating declarative memory.

The effects of GPR39 KO on memory

The question of whether the rodent form of episodic memory (ELM) is vulnerable to aging and whether GPR39 modulates ELM was addressed in Experiments 1-2 of this work. In male mice spatiotemporal integration of ELM was absent in old WT mice and remained intact in adult and middle-aged WT mice, while GPR39 KO caused a complete lack of spatiotemporal integration at all 3 developmental stages (Fig. 6). A similar pattern was present in the MWM test, with an impairment of spatial memory in all GPR39 KO age groups as well as in old WT male mice (Fig. 8).

Previous studies suggest a notion that the deleterious impact of a constitutive GPR39 KO on hippocampus-dependent declarative memory (i.e. both ELM and spatial memory) observed in male mice in Experiment 1 could be mediated by an activity-independent mechanism. Due to high metabolic demands and modest antioxidant defense, neurons are susceptible to oxidative insults and endoplasmatic reticulum stress, which play an important role in neurodegeneration (Cobley, Fiorello and Bailey, 2018). Pronounced ligand-independent activity of the GPR39 through $G_{12/13}$ – Rho kinase – serum response element–dependent transcription (Holst *et al.*, 2004) promotes neuroprotection in response to both of the abovementioned stressors in hippocampal neurons *in vitro* (Dittmer *et al.*, 2008). Although a relationship between age, genotype and antioxidant response - as measured by glutathione peroxidase 1 mRNA (*Gpx1*) levels in the hippocampi – was present in Experiment 1, it could not explain the ELM test results (Fig. 10B). It did however confirm that GPR39 modulates age-related changes in the gene expression an enzyme responsible for neutralization of H_2O_2, with

most prominent effect in old male mice, where lack of the receptor caused an upregulation of *Gpx1* compared to old WT littermates (Fig. 10B).

GPR39 also regulates the response to oxidative insults (H_2O_2) in an activity-dependent manner by promoting ERK1/2 phosphorylation and the expression of clusterin (Abramovitch-Dahan *et al.*, 2016) - a chaperone glycoprotein, mutations of which influence the progression of stages on AD continuum (Lacour *et al.*, 2017). Moreover, the prosurvival role of GPR39 has been shown to be experience-dependent, as GPR39 KO blocked an increase of survival rates of newborn granule cells in the subventricular zone of the dentate gyrus, caused by environmental enrichment in male mice (Chrusch, 2015). Numerous studies have shown that one of the mechanisms behind the neuroprotective effects of environmental enrichment on hippocampal neurons is an increase of antioxidant response, and that these effects are observed throughout the entire lifespan in rodents (Fernández *et al.*, 2004; Mármol *et al.*, 2015; Griñan-Ferré *et al.*, 2016; Kang *et al.*, 2016). Although plausible, this line of reasoning may however not be applicable to the effects of Experiment 1. Firstly, Chrusch (2015) also showed that GPR39 KO had no effect on the survival of granule cells in male mice housed in standard conditions (Chrusch, 2015), which was the case in Experiment 1. Secondly, changes in hippocampal clusterin (*Clu*) and ERK2 (*Mapk1*) mRNA levels, although modulated by animals' age and genotype, could not explain the ELM test results in Experiment 1, perhaps with the exception of adult mice, where GPR39 KO caused a downregulation of both genes (Fig. 10A; Fig. 9C). In fact, none of the observed differences in gene expression corresponded to ELM test results across both age and genotype factors, which may be due to the fact that before collecting the hippocampi, mice underwent two additional behavioral procedures (Fig. 5), and therefore only large and sustained effects could be captured in such experimental design. Having said that, it is worth noting that the MWM spatial memory (SM) test, which was performed as the last of the 3 tests (Fig. 5), yielded results analogous to ELM (Fig. 8). Combined with no effects of GPR39 KO on procedural memory (Fig. 7), which was assessed between ELM and MWM (Fig. 5), this pattern strongly suggests that GPR39 selectively modulates hippocampus-dependent declarative memory in male mice, although the molecular mechanisms behind this effect remain to be elucidated.

In female WT mice, spatiotemporal integration was absent regardless of the animals' age (Experiment 2, Fig. 12) suggesting sex differences exist with respect to ELM – at least as measured by the task used in this work. The same can be stated with regard to procedural memory, since the effects of retention delay were opposite in males and females in all 3 age groups (Fig. 4 and 10). Moreover, adult female GPR39 KO mice displayed a trend towards

presence of the spatiotemporal integration of ELM (Fig. 12), which was absent in adult male GPR39 KO mice (Fig. 6). We also observed that the effects of GPR39 agonist on ELM deficit of old WT female mice (Fig. 15) were weaker than in male conspecifics of similar age (Fig. 14), and affected only the spatial component of ELM. This pattern of results is consistent with lesser dependence of female hippocampi on zincergic neurotransmission (Lee *et al.*, 2004), and the fact that zinc acts as a positive allosteric modulator (PAM) of TC-G 1008 activity at GPR39 (Sato *et al.*, 2016). However, since we did not control for the stage of the estrous cycle at which behavioral testing was performed, it is impossible to interpret the observed sex differences in terms of hormone levels. Nevertheless, we replicated better performance of adult female from male WT mice in the rotarod test (Oliveira *et al.*, 2015), and extended these results by showing that – in contrast to male mice – PM of WT female mice does benefit from a retention delay at middle- and old-age developmental stages (Fig. 10). Importantly, GPR39 KO had no effect on PM regardless of animals' sex or age. The question of sex differences in MWM performance of WT and GPR39 KO mice remains open, but it is worth noting that studies on ZnT3 KO female mice suggest that – contrary to male mice – they do not show cognitive abnormalities in the test (Thackray, McAllister and Dyck, 2017).

Comparison of the effects of GPR39 KO with pharmacological activation of GPR39 on declarative memory

GPR39 KO affected spatiotemporal integration of ELM in male mice, while acute pharmacological activation of the receptor recovered temporal and spatial components of ELM, but had no effect on spatiotemporal integration in old male WT mice (Experiment 3, Fig. 14). Even after taking into account the different neurobiological consequences of constitutive *vs* ligand-dependent activity of GPR39 (discussed in: Rychlik and Mlyniec, 2019), the results from male mice may seem counterintuitive. Due to the lack of spatial and temporal components in male WT mice in Experiment 1 (which is a pattern sometimes observed in healthy mice in the ELM paradigm: Belblidia *et al.*, 2015), we do not know if GPR39 KO caused a selective spatiotemporal, or a global ELM impairment. A speculative explanation of the observed pattern may be derived from neuropsychological ELM studies of hippocampal CA1 and CA3 areas' contributions to ELM components in rodents. Disconnection of the mPFC and CA3 area impairs all 3 ELM components (De Souza Silva *et al.*, 2016), while disconnection of mPFC and the CA1 area, which is *downstream* to CA3 in information processing (Fig. 2 and 3), disrupts only spatiotemporal integration and spares the temporal and spatial components (Chao *et al.*, 2017).

Processing of information by the CA3 area is therefore a *sine qua non* condition for all ELM components, while the CA1 area seems solely responsible for spatiotemporal integration. The presence of spatiotemporal integration in adult and middle-aged WT mice in Experiment 1 indicates that the functionality of both areas was preserved in these animals, even though the temporal and spatial components were absent. Two CA1-independent components were selectively improved by acute pharmacological activation of GPR39 in Experiment 3, and - at the same time - had no effect on CA1-dependent spatiotemporal integration (Fig. 14). This pattern suggests a CA3-driven effect of GPR39 pharmacological activation, and would also indicate a global ELM impairment in GPR39 KO animals in Experiment 1. Indeed, a recent study revealed that in mice exposed to a strong, acute stressor (forced swimming), GPR39 KO causes hyperactivity of mPFC, CA3 and CA1 areas (Sah, Kharitonova and Mlyniec, 2021) – pointing to the possibility of a global disruption of a network involved in ELM caused by GPR39 KO, but future studies are needed to elaborate this matter.

Contrary to the effect of acute treatment (Experiment 3), chronic TC-G 1008 administration (Experiments 8 and 9) did not rescue ELM (or SM) when animals were in an "off-drug" state (i.e. ~24 h after last injection). Desensitization of the GPR39 in response to chronic agonist treatment could explain this discrepancy; however, it has been previously shown that both acute and repeated administration of TC-G 1008 exert similar behavioral effects in an one-trial forced swimming test in mice (Starowicz *et al.*, 2019). Therefore, another explanation of the contrasting results observed in the present study could be that pharmacological modulation of declarative memory *via* GPR39 relies on endogenous task-dependent Zn^{2+} release. At the high concentrations (~100 μM) observed during synaptic transmission in the hippocampus (Assaf and Chung, 1984), Zn^{2+} acts as a PAM for TC-G 1008 through the GPR39-Gαq-PLC pathway (Sato *et al.*, 2016), which is primarily involved in GPR39-dependent regulation of hippocampal neurons' activity (Besser *et al.*, 2009; Chorin *et al.*, 2011). PAM activity of the ion could therefore explain why TC-G 1008 affected ELM only when the compound was administered immediately before a memory test. The memory trace measured in the ELM task decays after an interval of >2h from the 2nd exposition trial in mice (Belblidia *et al.*, 2015) and GPR39-Gαq-PLC activation leads to the release of Ca^{2+} from endoplasmatic reticulum stores and ERK1/2 phosphorylation (Chorin *et al.*, 2011), both of which act as second messengers in the intracellular processes necessary for long-term memory formation (Xia and Storm, 2012). Thus, in future studies it would be interesting to see whether acute GPR39 activation delays the ELM time decay, potentially leading to long-term ELM in

mice. However, results of this study strongly suggest use of drugs with verified selectivity – an issue discussed in the next paragraph.

Sato *et al.* (2016) conducted a drug-receptor specificity assay to determine which of the G protein coupled receptors are activated by TC-G 1008 (and two novel GPR39 agonists) in the presence of Zn^{2+} (Sato *et al.*, 2016). The authors concluded, that all three compounds "are highly specific agonists at GPR39" (*ibidem*). However, concerns have been raised about selectivity of GPR39 agonists, and a need to test these compounds in GPR39 KO animals has been emphasized (Grunddal *et al.*, 2021). Although no behavioral effects of chronic TC-G 1008 at a dose of 10 mg/kg were present in the present study (Experiment 8), the compound caused a downregulation of 5 of the 20 genes assessed in hippocampi of adult GPR39 KO male mice compared to their WT littermates under the same treatment (Fig. 22). All of the affected genes represented mechanisms previously associated with GPR39, such as inhibitory (*Slc12a5* and *Gabag2*, Fig. 22C and D) or excitatory (*Gria3*, Fig. 22B) neurotransmission, synaptic plasticity (*Creb1*, Fig. 22E) and neuronal survival (*Clu*, Fig. 22A). This result calls for caution in interpreting the effects of pharmacological manipulations of GPR39 in this, as well as other studies utilizing TC-G 1008 and other known, but unverified, GPR39 agonists as a tool compound.

The possible impact of stress

Acute TC-G 1008 treatment did not exert any effect on ELM when consolidation of memory was disrupted in WT adult male mice in Experiment 5 (Fig. 16). The ELM CI paradigm was developed in order to confirm a promnesic, rather than a stress-resiliency-promoting, activity profile of drugs (Zlomuzica *et al.*, 2007). The rationale was that since the stress of *ip* injections disrupts ELM (Kart-Teke *et al.*, 2006), a drug effect in sub-optimal learning conditions would clearly indicate that cognitive functions were manipulated pharmacologically. Using a one-trial forced swimming test in mice, it has previously been shown that – in contrast to Zn^{2+} – acute TC-G 1008 modulates stress reactivity for up to 24h post injection; and, that chronic TC-G 1008 also decreases passive stress-coping in this test (Starowicz *et al.*, 2019). Combined with the lack of TC-G 1008 effect in the ELM CI paradigm in Experiment 5 and the failure to replicate the presence of spatiotemporal integration in adult male WT mice after chronic vehicle treatment (possibly due to chronic *ip* injection stress) in Experiments 8 and 9, it therefore seems probable that better performance of old WT mice in standard ELM after TC-G 1008 treatment in Experiment 3 was mediated by an interaction with affective and hormonal factors. Indeed, TC-G 1008 has recently been shown to be neuroprotective against

corticosterone-induced injury in a mouse hippocampal cell line (Mo *et al.*, 2020). However, first effects of the drug on mRNA expression, as well as of corticosterone on cell viability, were observed after at least 12h of incubation in preliminary time-course studies, and therefore all assays were performed with a 24h incubation period (*ibidem*), which poses the question of whether neuroprotection against stress is an explanation applicable to the ELM experimental setup, where the final test was performed 3.5h after the injection. The use of information obtained *in vitro* to explain *in vivo* results is further complicated by the fact that acute injection of 10 mg/kg TC-G 1008 caused an upregulation of 2 genes responsible for excitatory (*Gria2*, Fig. 17) and inhibitory (*Gabrb3*, Fig. 17) neurotransmission after 0.5h in adult WT mice. Moreover, the GPR39-CREB-BDNF pathway, which was responsible for neuroprotection *in vitro* (Mo *et al.*, 2020) was unaffected by acute TC-G 1008 injection. Therefore, the question of whether the beneficial effect of the drug on ELM of old WT mice in Experiment 3 was *via* stress-resiliency or procognitive effects remains unresolved.

Stress-resiliency should also be altered by chronic TC-G 1008 treatment in Experiments 8 and 9 in the ELM test, as well as the MWM task, which has been shown to be sensitive to the animals' affective state (Hölscher, 1999). Yet, chronic drug treatment did not change neither SM nor ELM in both experiments. Since consolidation of episodic-like contextual fear memory is mediated by the CA1 area, rather than the CA3 area (Daumas *et al.*, 2005), an alternative explanation of Experiment 3 results could be the aforementioned specificity of the locus of action of TC-G 1008 in the CA3 area. Notably, the CA1 area alone is also responsible for incremental spatial learning (Nakashiba *et al.*, 2008), which is affected by complete depletion of synaptic Zn^{2+} in adult mice (Adlard *et al.*, 2010), but was undisturbed in GPR39 KO animals in the MWM in Experiments 1 and 8, and remained unchanged by GPR39 agonist in Experiments 8 and 9.

GPR39 KO and hyperactivity in the CA3

The lack of incremental learning deficits combined with selective impairment of SM retrieval in MWM in GPR39 KO mice in Experiments 1 and 8 resembles previously reported effects of higher basal glutamate release (i.e. excitability) in the CA3 area of old WT mice (Hascup *et al.*, 2017). GPR39 is responsible for ~25% of the metabotropic signaling-induced increase of intracellular Ca^{2+} levels in CA3 neurons in response to mossy fibers stimulation, which leads to ERK1/2 phosphorylation in pyramidal neurons (Besser *et al.*, 2009). This affects the intrinsic excitability of these cells by upregulating the potassium-chloride co-transporter (KCC2), that maintains the inhibitory effect of $GABA_A$ receptor activation (Chorin *et al.*, 2011).

It is also known, that the hippocampus remains hyperactive in GPR39 KO mice after an acute stressor (Sah, Kharitonova and Mlyniec, 2021) and successful postsynaptic inhibition of hippocampal pyramidal neurons is necessary for the preservation of memory in aging animals (Tran, Gallagher and Kirkwood, 2018). Therefore, hyperactivity of the hippocampus might have contributed to the MWM results observed in GPR39 KO adult mice in Experiments 1 and 8. Further support for this hypothesis stems from the fact that 5 mg/kg of memantine administered for 24 days caused a SM deficit only in adult GPR39 KO mice in Experiment 8 (no effect of 5 mg/kg of memantine on WT mice in the MWM was reproduced from a previous study, Saab *et al.*, 2011). A higher dose of 25 mg/kg of memantine administered for 7 days has been shown to weaken the inhibitory effect of $GABA_A$ activation by downregulating KCC2 in the hippocampus (Molinaro *et al.*, 2009). Therefore, the selective SM impairment in memantine-treated GPR39 KO mice in Experiment 8 would be consistent with a synergistic effect on the decreased inhibitory potential of hippocampal neurons, perhaps due to excessive loss of KCC2. The *ex vivo* gene expression studies do not confirm this hypothesis, as downregulation of *Slc12a5* (the gene encoding KCC2) was present only in GPR39 KO mice after chronic TC-G 1008 (but not memantine) treatment (Fig. 22C), and SM remained intact in this group (Fig. 24). Furthermore, no clear alternative mechanistic explanation of the behavioral results of Experiment 8 stems from gene expression molecular experiments (Fig. 22).

The effects of memantine on ELM

No significant effects of acute extrasynaptic NMDAR antagonism caused by memantine on ELM or ELM CI, nor its modulation by GPR39 KO, were observed in Experiments 6 and 7 (Fig. 18 and 19). Previous ELM studies showed that an acute dose of 15 mg/kg D-cycloserine (NMDAR partial agonist) rescues the CA3-dependent "when?" and "where?" components under normal conditions in rats (Kart-Teke *et al.*, 2006), similarly to TC-G 1008 in old WT mice in the present study (Experiment 3). The promnesic effect of 20 mg/kg D-cycloserine on all components was also present in the ELM CI test in mice, although with the use of only a single object in the exposition trials (Zlomuzica *et al.*, 2007). Notwithstanding the different pharmacodynamics and testing setup, the use of a low dose (5 mg/kg) could be a factor contributing to the lack of effect of acute memantine found in the current studies. The presence of a spatial component of ELM only in adult WT and GPR39 KO mice chronically treated with 5 mg/kg memantine in Experiment 8, and a trend towards the presence of the same component in adult GPR39 KO mice after acute memantine administration in Experiment 7, indeed

suggested that the drug could impact ELM at higher doses. This hypothesis was tested in Experiment 9, where 10 mg/kg of memantine was used in a chronic schedule. The complete lack of effect of a higher dose of the drug on ELM (Fig. 23) or SM (Fig. 24) corroborated previous findings, and possibly corresponds to the fact that the proposed mechanism of procognitive effects of memantine (Matsunaga *et al.*, 2018) requires simultaneous overactivation of both synaptic and extrasynaptic NMDARs, with the latter being attenuated by the drug (Zhou *et al.*, 2013). Although NMDAR overactivation cannot be excluded in the current studies, no effects of either GPR39 KO or BDNF HET manipulations were present with respect to the expression of the 3 NMDAR subunits tested *ex vivo* (i.e. *Grin1*, *Grin2a* and *Grin2b*). The only effect observed suggests that in BDNF HET hippocampi memantine has an opposite mode of regulating *Grin1* expression to that of TC-G 1008 (Fig. 22C).

GPR39, CREB and BDNF

Previous *in vivo* KO studies suggested that GPR39 regulates the levels of BDNF *via* the CREB expression factor (Mlyniec *et al.*, 2015), and pharmacological activation approach (with the use of TC-G 1008) in CD-1 mice yielded contradictory results, showing either higher hippocampal BDNF protein levels (Młyniec *et al.*, 2016) or no effect of the drug (Starowicz *et al.*, 2019). Here, neither hippocampal BDNF mRNA nor protein levels were affected by GPR39 KO (Experiment 1) or TC-G 1008 (Experiments 3, 8 and 9). Given the well-recognized interaction of stress with BDNF (Notaras and van den Buuse, 2020) it is possible that these differences stem from the fact that the procedures used in current studies were less stressful compared to previous studies. Nevertheless, the involvement of GPR39 in the regulation of CREB was replicated in the current study with respect to adult male mice, in which GPR39 KO caused a downregulation of *Creb1* (Fig. 9A), but only when the animals were not exposed to chronic injection stress (Fig. 22E). In the latter conditions, TC-G 1008 also caused a downregulation of *Creb1*, but only in GPR39 KO mice (Fig. 22E), suggesting that the action of the drug is not selective for GPR39, and therefore may explain the previously mentioned inconsistencies in hippocampal BDNF levels (Młyniec *et al.*, 2016; Starowicz *et al.*, 2019), which are regulated by CREB.

BDNF is consistently found to be decreased in serum (Ng *et al.*, 2019; Xie *et al.*, 2020) and cerebrospinal fluid (Du *et al.*, 2018) of AD patients at advanced stages of the disease. Here - similarly to previous studies (Gururajan, Hill and van den Buuse, 2015; Grech *et al.*, 2018) – decreased levels of the protein in BDNF HET mice (Fig. 26A) did not cause deficits in an object

novelty recognition paradigm (Fig. 23), but impacted spatial memory in the MWM (Fig. 24). Moreover, the effect was a quantitative difference, rather than loss of function in BDNF HET mice, possibly due to compensatory mechanisms, which are expected to be engaged in constitutive KO models. One candidate for such a mechanism is higher sensitivity of hippocampal neurons and changes in their oscillatory activity maintained by the GABAergic interneurons (Buzsáki, 2001), that are known to affect SM in the MWM test in mice (Wang *et al.*, 2020). Both of these might have been modulated in Experiment 9 by the downregulation of the alpha 1 subunit of the $GABA_A$ receptor in BDNF HET hippocampi (Fig. 26B). This hypothesis is supported by the fact that $GABA_A$ activity in the hippocampus negatively regulates ERK1/2 phosphorylation, dendritic spine formation and spatial memory (Zheng *et al.*, 2009; Yoon *et al.*, 2015), all of which are functions shared with BDNF. Notably, both of the genes encoding ERK kinases (i.e. *Mapk1* and *Mapk3*) were upregulated in vehicle-treated BDNF HET hippocampi (Fig. 25A and B) lending further support to this idea. Lastly, it is worth noting that chronic memantine at a dose of 10 mg/kg caused a downregulation of CREB protein (Fig. 26C), and CREB-dependent *Bdnf* transcription (Fig. 25D), which is in stark contrast to the impact of the drug in chronic stress models, where memantine has an opposite effect on CREB and BDNF (Takahashi *et al.*, 2018; Mishra, Hidau and Rai, 2021). This further underscores the abovementioned close interaction between stress and BDNF.

Conclusions and future directions

Since the interaction of Zn^{2+} with Aβ promotes neurodegeneration, the aim of this work was to establish whether a Zn^{2+}-sensing GPR39 modulates memory, as direct targeting of the receptor could circumvent potential problems raised by Zn^{2+} supplementation in AD-prone individuals. The obtained results strongly suggest that GPR39 plays a role in declarative memory in rodents, however the lack of effect of prolonged pharmacological intervention directed at the receptor in both healthy and neurologically impaired (BDNF HET) mice calls for further investigation of the GPR39 as an add-on treatment target in AD continuum.

Given the well-recognized bidirectional PAM activity of Zn^{2+} and GPR39 agonists (Sato *et al.*, 2016) and pathway specificity of constitutive *vs* ligand-mediated activity of GPR39 (Rychlik and Mlyniec, 2019), an interesting direction would be to develop neutral antagonists of GPR39 and compare their action to agonist compounds. Following the example of this and other works (Thackray, McAllister and Dyck, 2017; McAllister *et al.*, 2020; Grunddal *et al.*, 2021) care should be undertaken in future studies to use tool compounds with verified

selectivity, assess their action at different developmental stages in both sexes, and with well-controlled environmental stressors, as these factors modulate the effects of GPR39 manipulations.

Highlights

- GPR39 modulates declarative, but not procedural memory in mice.
- ELM is can be manipulated pharmacologically *via* GPR39 activation in male, rather than female mice.
- Acute GPR39 activation does not rescue ELM when consolidation of memory is challenged.
- Chronic GPR39 activation does not affect declarative memory of male mice.
- GPR39 can interact with the action of chronic, but not acute NMDAR noncompetitive antagonist – memantine.
- The biological effects of TC-G 1008 may not be a restricted to GPR39.

References

Abramovitch-Dahan, C. *et al.* (2016) 'Amyloid β attenuates metabotropic zinc sensing receptor, mZnR/GPR39, dependent Ca2+, ERK1/2 and Clusterin signaling in neurons', *Journal of Neurochemistry*, pp. 221–233. doi: 10.1111/jnc.13760.

Adlard, P. A. *et al.* (2010) 'Cognitive Loss in Zinc Transporter-3 Knock-Out Mice: A Phenocopy for the Synaptic and Memory Deficits of Alzheimer's Disease?', *Journal of Neuroscience*, 30(5), pp. 1631–1636. doi: 10.1523/JNEUROSCI.5255-09.2010.

Aizenman, E. (2019) 'Zinc Signaling in the Life and Death of Neurons', in *Zinc Signaling*. Singapore: Springer Singapore, pp. 165–185. doi: 10.1007/978-981-15-0557-7_9.

Alberdi, E. *et al.* (2010) 'Amyloid β oligomers induce Ca2+ dysregulation and neuronal death through activation of ionotropic glutamate receptors', *Cell Calcium*. Elsevier Ltd, 47(3), pp. 264–272. doi: 10.1016/j.ceca.2009.12.010.

An, W. L. *et al.* (2005) 'Mechanism of zinc-induced phosphorylation of p70 S6 kinase and glycogen synthase kinase 3β in SH-SY5Y neuroblastoma cells', *Journal of Neurochemistry*. J Neurochem, 92(5), pp. 1104–1115. doi: 10.1111/j.1471-4159.2004.02948.x.

Anderson, C. T. *et al.* (2015) 'Modulation of extrasynaptic NMDA receptors by synaptic and tonic zinc', *Proceedings of the National Academy of Sciences*, 112(20), pp. E2705–E2714.

doi: 10.1073/pnas.1503348112.

Andreini, C. *et al.* (2006) 'Zinc through the three domains of life', *Journal of Proteome Research*, 5(11), pp. 3173–3178. doi: 10.1021/pr0603699.

Assaf, S. Y. and Chung, S. H. (1984) 'Release of endogenous Zn2+ from brain tissue during activity', *Nature*. Nature Publishing Group, 308(5961), pp. 734–736. doi: 10.1038/308734a0.

Belblidia, H. *et al.* (2015) 'Time decay of object, place and temporal order memory in a paradigm assessing simultaneously episodic-like memory components in mice', *Behavioural Brain Research*. Elsevier B.V., 286, pp. 80–84. doi: 10.1016/j.bbr.2015.02.043.

Bero, A. W. *et al.* (2011) 'Neuronal activity regulates the regional vulnerability to amyloid-?? 2 deposition', *Nature Neuroscience*, 14(6), pp. 750–756. doi: 10.1038/nn.2801.

Bero, A. W. *et al.* (2012) 'Bidirectional Relationship between Functional Connectivity and Amyloid- Deposition in Mouse Brain', *Journal of Neuroscience*. Society for Neuroscience, 32(13), pp. 4334–4340. doi: 10.1523/JNEUROSCI.5845-11.2012.

Besser, L. *et al.* (2009) 'Synaptically Released Zinc Triggers Metabotropic Signaling via a Zinc-Sensing Receptor in the Hippocampus', *Journal of Neuroscience*, 29(9), pp. 2890–2901. doi: 10.1523/JNEUROSCI.5093-08.2009.

Birinyi, A. *et al.* (2001) 'Zinc co-localizes with GABA and glycine in synapses in the lamprey spinal cord', *Journal of Comparative Neurology*. Wiley-Blackwell, 433(2), pp. 208–221. doi: 10.1002/cne.1136.

Burnet, F. M. (1981) 'A POSSIBLE ROLE OF ZINC IN THE PATHOLOGY OF DEMENTIA', *The Lancet*. Elsevier, 317(8213), pp. 186–188. doi: 10.1016/S0140-6736(81)90062-3.

Burnham, S. C. *et al.* (2019) 'Application of the NIA-AA Research Framework: Towards a Biological Definition of Alzheimer's Disease Using Cerebrospinal Fluid Biomarkers in the AIBL Study', *The journal of prevention of Alzheimer's disease*, 6(4), pp. 248–255. doi: 10.14283/jpad.2019.25.

Busche, M. A. and Konnerth, A. (2015) 'Neuronal hyperactivity - A key defect in Alzheimer's disease?', *BioEssays*. John Wiley and Sons Inc., pp. 624–632. doi: 10.1002/bies.201500004.

Bush, A. I. *et al.* (1994) 'Rapid induction of Alzheimer Aβ amyloid formation by zinc',

Science, 265(5177), pp. 1464–1467. doi: 10.1126/science.8073293.

Buzsáki, G. (2001) 'Hippocampal GABAergic interneurons: A physiological perspective', *Neurochemical Research*. Neurochem Res, pp. 899–905. doi: 10.1023/A:1012324231897.

Ceccom, J. *et al.* (2014) 'A specific role for hippocampal mossy fiber's zinc in rapid storage of emotional memories', *Learning and Memory*. Cold Spring Harbor Laboratory Press, 21(5), pp. 287–297. doi: 10.1101/lm.033472.113.

Chao, O. Y. *et al.* (2017) 'Interaction between the medial prefrontal cortex and hippocampal CA1 area is essential for episodic-like memory in rats', *Neurobiology of Learning and Memory*. Elsevier Inc., 141, pp. 72–77. doi: 10.1016/j.nlm.2017.03.019.

Chao, O. Y. *et al.* (2020) 'The medial prefrontal cortex - hippocampus circuit that integrates information of object, place and time to construct episodic memory in rodents: Behavioral, anatomical and neurochemical properties', *Neuroscience and Biobehavioral Reviews*. Elsevier, 113(February), pp. 373–407. doi: 10.1016/j.neubiorev.2020.04.007.

Cheignon, C. *et al.* (2018) 'Oxidative stress and the amyloid beta peptide in Alzheimer's disease', *Redox Biology*. Elsevier, pp. 450–464. doi: 10.1016/j.redox.2017.10.014.

Chen, N. N. *et al.* (2019) 'Long-Term Effects of Zinc Deficiency and Zinc Supplementation on Developmental Seizure-Induced Brain Damage and the Underlying GPR39/ZnT-3 and MBP Expression in the Hippocampus', *Frontiers in Neuroscience*. Frontiers Media S.A., 13, p. 920. doi: 10.3389/fnins.2019.00920.

Chorin, E. *et al.* (2011) 'Upregulation of KCC2 Activity by Zinc-Mediated Neurotransmission via the mZnR/GPR39 Receptor', *Journal of Neuroscience*, 31(36), pp. 12916–12926. doi: 10.1523/JNEUROSCI.2205-11.2011.

Chrusch, M. (2015) 'The Role of Synaptic Zinc in Experience-Dependent Plasticity', p. 231. doi: 10.11575/PRISM/28358.

Cline, E. N. *et al.* (2018) 'The Amyloid-β Oligomer Hypothesis: Beginning of the Third Decade.', *Journal of Alzheimer's disease : JAD*, 64(s1), pp. S567–S610. doi: 10.3233/JAD-179941.

Cobley, J. N., Fiorello, M. L. and Bailey, D. M. (2018) '13 reasons why the brain is susceptible to oxidative stress', *Redox Biology*. Elsevier B.V., pp. 490–503. doi: 10.1016/j.redox.2018.01.008.

Cox, B. M. *et al.* (2019) 'Acquisition of temporal order requires an intact CA3 commissural/associational (C/A) feedback system in mice', *Communications Biology*. Springer US, 2(1). doi: 10.1038/s42003-019-0494-3.

Datki, Z. *et al.* (2020) 'Alzheimer risk factors age and female sex induce cortical Aβ aggregation by raising extracellular zinc', *Molecular Psychiatry*. Springer Nature, 25(11), pp. 2728–2741. doi: 10.1038/s41380-020-0800-y.

Daumas, S. *et al.* (2005) 'Encoding, consolidation, and retrieval of contextual memory: Differential involvement of dorsal CA3 and CA1 hippocampal subregions', *Learning and Memory*. Cold Spring Harbor Laboratory Press, 12(4), pp. 375–382. doi: 10.1101/lm.81905.

Dede, A. J. O. and Smith, C. N. (2016) 'The Functional and Structural Neuroanatomy of Systems Consolidation for Autobiographical and Semantic Memory', in *Brain Imaging in Behavioral Neuroscience*, pp. 119–150. doi: 10.1007/7854_2016_452.

DeGrado, T. R. *et al.* (2016) 'First PET Imaging Studies With ^{63} Zn-Zinc Citrate in Healthy Human Participants and Patients With Alzheimer Disease', *Molecular Imaging*, 15, p. 153601211667379. doi: 10.1177/1536012116673793.

Dere, E. *et al.* (2008) 'Episodic-like and procedural memory impairments in histamine H1 Receptor knockout mice coincide with changes in acetylcholine esterase activity in the hippocampus and dopamine turnover in the cerebellum', *Neuroscience*. IBRO, 157(3), pp. 532–541. doi: 10.1016/j.neuroscience.2008.09.025.

Dere, E., Huston, J. P. and De Souza Silva, M. A. (2005a) 'Episodic-like memory in mice: Simultaneous assessment of object, place and temporal order memory', *Brain Research Protocols*, 16(1–3), pp. 10–19. doi: 10.1016/j.brainresprot.2005.08.001.

Dere, E., Huston, J. P. and De Souza Silva, M. A. (2005b) 'Integrated memory for objects, places, and temporal order: Evidence for episodic-like memory in mice', *Neurobiology of Learning and Memory*, 84(3), pp. 214–221. doi: 10.1016/j.nlm.2005.07.002.

Deshpande, A. *et al.* (2009) 'A Role for Synaptic Zinc in Activity-Dependent A Oligomer Formation and Accumulation at Excitatory Synapses', *Journal of Neuroscience*, 29(13), pp. 4004–4015. doi: 10.1523/JNEUROSCI.5980-08.2009.

Dittmer, S. *et al.* (2008) 'The constitutively active orphan G-protein-coupled receptor GPR39 protects from cell death by increasing secretion of pigment epithelium-derived growth factor', *Journal of Biological Chemistry*, 283(11), pp. 7074–7081. doi: 10.1074/jbc.M704323200.

Du, Y. *et al.* (2018) 'Postmortem Brain, Cerebrospinal Fluid, and Blood Neurotrophic Factor Levels in Alzheimer's Disease: A Systematic Review and Meta-Analysis', *Journal of Molecular Neuroscience*. Springer New York LLC, 65(3), pp. 289–300. doi: 10.1007/s12031-018-1100-8.

Ebenezer, I. (2015) *Neuropsychopharmacology and Therapeutics*. Oxford: John Wiley & Sons, Ltd.

Economou, A., Routsis, C. and Papageorgiou, S. G. (2015) 'Episodic Memory in Alzheimer Disease, Frontotemporal Dementia, and Dementia With Lewy Bodies/Parkinson Disease Dementia', *Alzheimer Disease & Associated Disorders*, 30(1), pp. 47–52. doi: 10.1097/wad.0000000000000089.

Ennaceur, A., Neave, N. and Aggleton, J. P. (1997) 'Spontaneous object recognition and object location memory in rats: The effects of lesions in the cingulate cortices, the medial prefrontal cortex, the cingulum bundle and the fornix', *Experimental Brain Research*, 113(3), pp. 509–519. doi: 10.1007/PL00005603.

Eom, K. *et al.* (2019) 'Intracellular Zn2+ signaling facilitates mossy fiber input-induced heterosynaptic potentiation of direct cortical inputs in hippocampal CA3 pyramidal cells', *Journal of Neuroscience*. Society for Neuroscience, 39(20), pp. 3812–3831. doi: 10.1523/JNEUROSCI.2130-18.2019.

Ernfors, P., Lee, K. F. and Jaenisch, R. (1994) 'Mice lacking brain-derived neurotrophic factor develop with sensory deficits', *Nature*. Nature, 368(6467), pp. 147–150. doi: 10.1038/368147a0.

Extance, K. and Goudie, A. J. (1981) 'Inter-animal olfactory cues in operant drug discrimination procedures in rats', *Psychopharmacology*. Springer-Verlag, 73(4), pp. 363–371. doi: 10.1007/BF00426467.

Fernández, C. I. *et al.* (2004) 'Environmental enrichment-behavior-oxidative stress interactions in the aged rat: Issues for a therapeutic approach in human aging', in *Annals of the New York Academy of Sciences*. New York Academy of Sciences, pp. 53–57. doi: 10.1196/annals.1297.012.

Foster, E. M. *et al.* (2019) 'Clusterin in Alzheimer's disease: Mechanisms, genetics, and lessons from other pathologies', *Frontiers in Neuroscience*. Frontiers Media S.A., p. 164. doi: 10.3389/fnins.2019.00164.

Frederickson, C. J. *et al.* (2006) ‘Concentrations of extracellular free zinc (pZn)ein the central nervous system during simple anesthetization, ischemia and reperfusion’, *Experimental Neurology*. Academic Press, 198(2), pp. 285–293. doi: 10.1016/j.expneurol.2005.08.030.

Frederickson, C. J. and Moncrieff, D. W. (1994) ‘Zinc-containing neurons.’, *Biological signals*. Switzerland, 3(3), pp. 127–139.

Gilad, D. *et al.* (2015) ‘Homeostatic regulation of KCC2 activity by the zinc receptor mZnR/GPR39 during seizures’, *Neurobiology of Disease*, 81, pp. 4–13. doi: 10.1016/j.nbd.2014.12.020.

Glenner, G. G. and Wong, C. W. (1984) ‘Alzheimer’s disease: Initial report of the purification and characterization of a novel cerebrovascular amyloid protein’, *Biochemical and Biophysical Research Communications*. Academic Press, 120(3), pp. 885–890. doi: 10.1016/S0006-291X(84)80190-4.

Granzotto, A., Canzoniero, L. M. T. and Sensi, S. L. (2020) ‘A Neurotoxic Ménage-à-trois: Glutamate, Calcium, and Zinc in the Excitotoxic Cascade’, *Frontiers in Molecular Neuroscience*. Frontiers Media S.A., p. 225. doi: 10.3389/fnmol.2020.600089.

Grech, A. M. *et al.* (2018) ‘Sex-dependent effects of environmental enrichment on spatial memory and brain-derived neurotrophic factor (BDNF) signaling in a developmental “two-hit” mouse model combining bdnf haploinsufficiency and chronic glucocorticoid stimulation’, *Frontiers in Behavioral Neuroscience*. Frontiers Media S.A., 12. doi: 10.3389/fnbeh.2018.00227.

Griñan-Ferré, C. *et al.* (2016) ‘Environmental enrichment modified epigenetic mechanisms in SAMP8 mouse hippocampus by reducing oxidative stress and inflammaging and achieving neuroprotection’, *Frontiers in Aging Neuroscience*. Frontiers Media S.A., 8(OCT). doi: 10.3389/fnagi.2016.00241.

Grunddal, K. V. *et al.* (2021) ‘Selective release of gastrointestinal hormones induced by an orally active GPR39 agonist’, *Molecular Metabolism*. Elsevier GmbH, 49(March), p. 101207. doi: 10.1016/j.molmet.2021.101207.

Gururajan, A., Hill, R. A. and van den Buuse, M. (2015) ‘Brain-derived neurotrophic factor heterozygous mutant rats show selective cognitive changes and vulnerability to chronic corticosterone treatment’, *Neuroscience*. Elsevier Ltd, 284, pp. 297–310. doi: 10.1016/j.neuroscience.2014.10.009.

Hardy, J. A. and Higgins, G. A. (1992) ‘Alzheimer’s disease: The amyloid cascade hypothesis’, *Science*. Science, pp. 184–185. doi: 10.1126/science.1566067.

Hardy, J. and Selokoe, D. (2002) ‘The Amyloid Hypothesis of Alzheimer ’s Disease’, *Science’s Compass*, 297(5580), pp. 353–357.

Hascup, K. N. *et al.* (2017) ‘Enhanced cognition and hypoglutamatergic signaling in a growth hormone receptor knockout mouse model of successful aging’, *Journals of Gerontology - Series A Biological Sciences and Medical Sciences*, 72(3), pp. 329–337. doi: 10.1093/gerona/glw088.

Hedden, T. *et al.* (2013) ‘Meta-analysis of amyloid-cognition relations in cognitively normal older adults’, *Neurology*. American Academy of Neurology, 80(14), pp. 1341–1348. doi: 10.1212/WNL.0b013e31828ab35d.

Hölscher, C. (1999) ‘Stress impairs performance in spatial water maze learning tasks’, *Behavioural Brain Research*. Behav Brain Res, 100(1–2), pp. 225–235. doi: 10.1016/S0166-4328(98)00134-X.

Holst, B. *et al.* (2004) ‘Common structural basis for constitutive activity of the ghrelin receptor family’, *Journal of Biological Chemistry*. American Society for Biochemistry and Molecular Biology, 279(51), pp. 53806–53817. doi: 10.1074/jbc.M407676200.

Holst, B. *et al.* (2007) ‘GPR39 signaling is stimulated by zinc ions but not by obestatin’, *Endocrinology*, 148(1), pp. 13–20. doi: 10.1210/en.2006-0933.

Holst, B. *et al.* (2009) ‘G protein-coupled receptor 39 deficiency is associated with pancreatic islet dysfunction’, *Endocrinology*, 150(6), pp. 2577–2585. doi: 10.1210/en.2008-1250.

Hu, J. Y. *et al.* (2017) ‘Pathological concentration of zinc dramatically accelerates abnormal aggregation of full-length human Tau and thereby significantly increases Tau toxicity in neuronal cells’, *Biochimica et Biophysica Acta - Molecular Basis of Disease*. Elsevier B.V., 1863(2), pp. 414–427. doi: 10.1016/j.bbadis.2016.11.022.

Huang, Y. Z. *et al.* (2008) ‘Zinc-Mediated Transactivation of TrkB Potentiates the Hippocampal Mossy Fiber-CA3 Pyramid Synapse’, *Neuron*. Cell Press, 57(4), pp. 546–558. doi: 10.1016/j.neuron.2007.11.026.

Ingelsson, M. *et al.* (2004) ‘Early Aβ accumulation and progressive synaptic loss, gliosis, and tangle formation in AD brain’, *Neurology*. Wolters Kluwer Health, Inc. on behalf of the American Academy of Neurology, 62(6), pp. 925–931. doi:

10.1212/01.WNL.0000115115.98960.37.

Inoue, N. and Watanabe, S. (2014) 'Effects of reversible deactivation of mossy fibers in the dentate-CA3 system on geometric center detection task in mice: Functional separation of spatial learning and its generalization to new environment', *Physiology and Behavior*. Elsevier Inc., 131, pp. 75–80. doi: 10.1016/j.physbeh.2014.04.015.

Jack, C. R. *et al.* (2016) 'A/T/N: An unbiased descriptive classification scheme for Alzheimer disease biomarkers', *Neurology*. Lippincott Williams and Wilkins, pp. 539–547. doi: 10.1212/WNL.0000000000002923.

Jack, C. R. *et al.* (2018) 'NIA-AA Research Framework: Toward a biological definition of Alzheimer's disease', *Alzheimer's and Dementia*. Elsevier Inc., 14(4), pp. 535–562. doi: 10.1016/j.jalz.2018.02.018.

Jutten, R. J. *et al.* (2021) 'Identifying Sensitive Measures of Cognitive Decline at Different Clinical Stages of Alzheimer's Disease', *Journal of the International Neuropsychological Society*. Cambridge University Press, 27(5), pp. 426–438. doi: 10.1017/S1355617720000934.

Kabogo, D. *et al.* (2010) 'β-Amyloid-related peptides potentiate K+-evoked glutamate release from adult rat hippocampal slices', *Neurobiology of Aging*. Elsevier, 31(7), pp. 1164–1172. doi: 10.1016/j.neurobiolaging.2008.08.009.

Kalappa, B. I. *et al.* (2015) 'AMPA receptor inhibition by synaptically released zinc', *Proceedings of the National Academy of Sciences*, (Cv), p. 201512296. doi: 10.1073/pnas.1512296112.

Kang, H. *et al.* (2016) 'Alteration of Energy Metabolism and Antioxidative Processing in the Hippocampus of Rats Reared in Long-Term Environmental Enrichment', *Developmental Neuroscience*. S. Karger AG, 38(3), pp. 186–194. doi: 10.1159/000446772.

Kart-Teke, E. *et al.* (2006) 'Wistar rats show episodic-like memory for unique experiences', *Neurobiology of Learning and Memory*, 85(2), pp. 173–182. doi: 10.1016/j.nlm.2005.10.002.

Kesner, R. P. (2016) 'Exploration of the Neurobiological Basis for a Three-System, Multiattribute Model of Memory', in *Hippocampus*, pp. 325–359. doi: 10.1007/7854_2016_454.

Klunk, W. E. *et al.* (2004) 'Imaging Brain Amyloid in Alzheimer's Disease with Pittsburgh Compound-B', *Annals of Neurology*. John Wiley and Sons Inc., 55(3), pp. 306–319. doi: 10.1002/ana.20009.

Knopman, D. S., Petersen, R. C. and Jack, C. R. (2019) 'A brief history of "Alzheimer disease": Multiple meanings separated by a common name', *Neurology*, 92(22), pp. 1053–1059. doi: 10.1212/WNL.0000000000007583.

Lacour, A. *et al.* (2017) 'Genome-wide significant risk factors for Alzheimer's disease: Role in progression to dementia due to Alzheimer's disease among subjects with mild cognitive impairment', *Molecular Psychiatry*, 22(1), pp. 153–160. doi: 10.1038/mp.2016.18.

Lambert, M. P. *et al.* (1998) 'Diffusible, nonfibrillar ligands derived from Aβ1-42 are potent central nervous system neurotoxins', *Proceedings of the National Academy of Sciences of the United States of America*. National Academy of Sciences, 95(11), pp. 6448–6453. doi: 10.1073/pnas.95.11.6448.

Leal, S. L. and Yassa, M. A. (2015) 'Neurocognitive Aging and the Hippocampus across Species', *Trends in Neurosciences*, 38(12), pp. 800–812. doi: 10.1016/j.tins.2015.10.003.

Leal, S. L. and Yassa, M. A. (2018) 'Integrating new findings and examining clinical applications of pattern separation', *Nature Neuroscience*. Springer US, 21(2), pp. 163–173. doi: 10.1038/s41593-017-0065-1.

Lee, Joo Yong *et al.* (2004) 'Estrogen Decreases Zinc Transporter 3 Expression and Synaptic Vesicle Zinc Levels in Mouse Brain', *Journal of Biological Chemistry*. Elsevier, 279(10), pp. 8602–8607. doi: 10.1074/jbc.M309730200.

Lee, M. C. *et al.* (2018) 'Zinc ion rapidly induces toxic, off-pathway amyloid-β oligomers distinct from amyloid-β derived diffusible ligands in Alzheimer's disease', *Scientific Reports*. Springer US, 8(1), pp. 1–16. doi: 10.1038/s41598-018-23122-x.

Lisman, J. and Redish, A. D. (2018) 'How the hippocampus contribites to mempory, navigation and Cognition', *Nature Neuroscience*, 20(11), pp. 1434–1447. doi: 10.1038/nn.4661.Viewpoints.

Löscher, W. and Hönack, D. (1990) 'High doses of memantine (1-amino-3,5-dimethyladamantane) induce seizures in kindled but not in non-kindled rats', *Naunyn-Schmiedeberg's Archives of Pharmacology*, 341(5), pp. 476–481. doi: 10.1007/BF00176343.

Lu, Y.-M. *et al.* (2000) 'Endogenous Zn2+ is required for the induction of long-term potentiation at rat hippocampal mossy fiber-CA3 synapses', *Synapse*, 38(2), pp. 187–197. doi: 10.1002/1098-2396(200011)38:2<187::AID-SYN10>3.0.CO;2-R.

Lüscher, C. *et al.* (2012) 'NMDA Receptor-Dependent Long-Term Potentiation and Long-

Term Depression (LTP / LTD)', *Cold Spring Harbor perspectives in biology*. Cold Spring Harbor Laboratory Press, 4(6), pp. 1–15. doi: 10.1101/cshperspect.a005710.

Mármol, F. *et al.* (2015) 'Anti-oxidative effects produced by environmental enrichment in the hippocampus and cerebral cortex of male and female rats', *Brain Research*. Elsevier, 1613, pp. 120–129. doi: 10.1016/j.brainres.2015.04.007.

Matsunaga, S. *et al.* (2018) 'The efficacy and safety of memantine for the treatment of Alzheimer's disease', *Expert Opinion on Drug Safety*. Taylor and Francis Ltd, 17(10), pp. 1053–1061. doi: 10.1080/14740338.2018.1524870.

Maurer, K., Volk, S. and Gerbaldo, H. (1997) 'Auguste D and Alzheimer's disease', *Lancet*. Elsevier B.V., pp. 1546–1549. doi: 10.1016/S0140-6736(96)10203-8.

McAllister, B. B. *et al.* (2020) 'Brain-derived Neurotrophic Factor and TrkB Levels in Mice that Lack Vesicular Zinc: Effects of Age and Sex', *Neuroscience*. IBRO, 425, pp. 90–100. doi: 10.1016/j.neuroscience.2019.11.009.

McAllister, B. B. and Dyck, R. H. (2017) 'Zinc transporter 3 (ZnT3) and vesicular zinc in central nervous system function', *Neuroscience and Biobehavioral Reviews*, pp. 329–350. doi: 10.1016/j.neubiorev.2017.06.006.

McCollum, L. E. *et al.* (2021) 'Oh brother, where art tau? Amyloid, neurodegeneration, and cognitive decline without elevated tau', *NeuroImage: Clinical*, 31. doi: 10.1016/j.nicl.2021.102717.

McKhann, G. M. *et al.* (2011) 'The diagnosis of dementia due to Alzheimer's disease: Recommendations from the National Institute on Aging-Alzheimer's Association workgroups on diagnostic guidelines for Alzheimer's disease', *Alzheimer's and Dementia*, 7(3), pp. 263–269. doi: 10.1016/j.jalz.2011.03.005.

Mishra, S. K., Hidau, M. K. and Rai, S. (2021) 'Memantine treatment exerts an antidepressant-like effect by preventing hippocampal mitochondrial dysfunction and memory impairment via upregulation of CREB/BDNF signaling in the rat model of chronic unpredictable stress-induced depression', *Neurochemistry International*. Elsevier Ltd, 142. doi: 10.1016/j.neuint.2020.104932.

Mitchell, J. B. and Laiacona, J. (1998) 'The medial frontal cortex and temporal memory: Tests using spontaneous exploratory behaviour in the rat', *Behavioural Brain Research*, 97(1–2), pp. 107–113. doi: 10.1016/S0166-4328(98)00032-1.

Mlyniec, K. *et al.* (2015) ‘GPR39 (zinc receptor) knockout mice exhibit depression-like behavior and CREB/BDNF down-regulation in the hippocampus’, *International Journal of Neuropsychopharmacology*, 18(3), pp. 1–8. doi: 10.1093/ijnp/pyu002.

Młyniec, K. *et al.* (2016) ‘Potential antidepressant-like properties of the TC G-1008, a GPR39 (zinc receptor) agonist’, *Journal of Affective Disorders*. Elsevier, 201, pp. 179–184. doi: 10.1016/j.jad.2016.05.007.

Mo, F. *et al.* (2020) ‘GPR39 protects against corticosterone-induced neuronal injury in hippocampal cells through the CREB-BDNF signaling pathway’, *Journal of Affective Disorders*. Elsevier B.V., 272(March), pp. 474–484. doi: 10.1016/j.jad.2020.03.137.

Mo, Z. Y. *et al.* (2009) ‘Low micromolar zinc accelerates the fibrillization of human Tau via bridging of Cys-291 and Cys-322’, *Journal of Biological Chemistry*. American Society for Biochemistry and Molecular Biology, 284(50), pp. 34648–34657. doi: 10.1074/jbc.M109.058883.

Mocchegiani, E. *et al.* (2013) ‘Zinc: Dietary intake and impact of supplementation on immune function in elderly’, *Age*. Springer, 35(3), pp. 839–860. doi: 10.1007/s11357-011-9377-3.

Molinaro, G. *et al.* (2009) ‘Memantine treatment reduces the expression of the K+/Cl- cotransporter KCC2 in the hippocampus and cerebral cortex, and attenuates behavioural responses mediated by GABAAreceptor activation in mice’, *Brain Research*. Elsevier B.V., 1265, pp. 75–79. doi: 10.1016/j.brainres.2009.02.016.

Moscoso, A. *et al.* (2019) ‘Staging the cognitive continuum in prodromal Alzheimer’s disease with episodic memory’, *Neurobiology of Aging*. Elsevier Inc, 84, pp. 1–8. doi: 10.1016/j.neurobiolaging.2019.07.014.

Nakashiba, T. *et al.* (2008) ‘Transgenic inhibition of synaptic transmission reveals role of CA3 output in hippocampal learning’, *Science*, 319(5867), pp. 1260–1264. doi: 10.1126/science.1151120.

Ng, T. K. S. *et al.* (2019) ‘Decreased serum brain-derived neurotrophic factor (BDNF) levels in patients with Alzheimer’s disease (AD): A systematic review and meta-analysis’, *International Journal of Molecular Sciences*. MDPI AG. doi: 10.3390/ijms20020257.

Nicoll, R. A. and Schmitz, D. (2005) ‘Synaptic plasticity at hippocampal mossy fibre synapses’, *Nature Reviews Neuroscience*. Nature Publishing Group, pp. 863–876. doi: 10.1038/nrn1786.

Notaras, M. and van den Buuse, M. (2020) 'Neurobiology of BDNF in fear memory, sensitivity to stress, and stress-related disorders', *Molecular Psychiatry*. Springer Nature, pp. 2251–2274. doi: 10.1038/s41380-019-0639-2.

O'Keefe, J. and Nadel, L. (1978) *The Hippocampus as a Cognitive Map, Philosophical Studies*. Oxford: Oxford University Press.

Oliveira, C. V. de *et al.* (2015) 'Evaluation of potential gender-related differences in behavioral and cognitive alterations following pilocarpine-induced status epilepticus in C57BL/6 mice', *Physiology and Behavior*. Elsevier Inc., 143, pp. 142–150. doi: 10.1016/j.physbeh.2015.03.004.

Pan, E. *et al.* (2011) 'Vesicular Zinc Promotes Presynaptic and Inhibits Postsynaptic Long-Term Potentiation of Mossy Fiber-CA3 Synapse', *Neuron*. Elsevier Inc., 71(6), pp. 1116–1126. doi: 10.1016/j.neuron.2011.07.019.

Pan, E., Zhao, Z. and McNamara, J. O. (2019) 'LTD at mossy fiber synapses onto stratum lucidum interneurons requires TrkB and retrograde endocannabinoid signaling', *Journal of Neurophysiology*. American Physiological Society, 121(2), pp. 609–619. doi: 10.1152/jn.00669.2018.

Pei, J. J. *et al.* (2006) 'P70 S6 kinase mediates tau phosphorylation and synthesis', *FEBS Letters*. No longer published by Elsevier, 580(1), pp. 107–114. doi: 10.1016/j.febslet.2005.11.059.

Perez-Rosello, T. *et al.* (2013) 'Synaptic Zn2+ Inhibits Neurotransmitter Release by Promoting Endocannabinoid Synthesis', *Journal of Neuroscience*. Society for Neuroscience, 33(22), pp. 9259–9272. doi: 10.1523/JNEUROSCI.0237-13.2013.

Perez-Rosello, T. *et al.* (2015) 'Tonic zinc inhibits spontaneous firing in dorsal cochlear nucleus principal neurons by enhancing glycinergic neurotransmission', *Neurobiology of Disease*. Elsevier B.V., 81(10), pp. 14–19. doi: 10.1016/j.nbd.2015.03.012.

Podcasy, J. L. and Epperson, C. N. (2016) 'Considering sex and gender in Alzheimer disease and other dementias', *Dialogues in Clinical Neuroscience*. Les Laboratoires Seriver, 18(4), pp. 437–446. doi: 10.31887/dcns.2016.18.4/cepperson.

Portbury, S. D. and Adlard, P. A. (2017) 'Zinc signal in brain diseases', *International Journal of Molecular Sciences*, 18(12). doi: 10.3390/ijms18122506.

Prince, M. *et al.* (2015) *World Alzheimer Report 2015. The global impact of dementia: an*

analysis of prevalence, incidence, cost and trends., London: Alzheimer's Disease International.

Ritchey, M., Libby, L. A. and Ranganath, C. (2015) 'Cortico-hippocampal systems involved in memory and cognition', in Shane, O. and Tsanov, M. (eds) *The Connected Hippocampus*. Elsevier, pp. 45–64. doi: 10.1016/bs.pbr.2015.04.001.

Ruediger, S. *et al.* (2011) 'Learning-related feedforward inhibitory connectivity growth required for memory precision', *Nature*. Nature Publishing Group, 473(7348), pp. 514–518. doi: 10.1038/nature09946.

Rychlik, M. and Mlyniec, K. (2019) 'Zinc-mediated Neurotransmission in Alzheimer's Disease: A Potential Role of the GPR39 in Dementia', *Current Neuropharmacology*, 18(1), pp. 2–13. doi: 10.2174/1570159x17666190704153807.

Saab, B. J. *et al.* (2011) 'Memantine affects cognitive flexibility in the morris water maze', *Journal of Alzheimer's Disease*, 27(3), pp. 477–482. doi: 10.3233/JAD-2011-110650.

Sah, A., Kharitonova, M. and Mlyniec, K. (2021) 'Neuronal correlates underlying the role of the zinc sensing receptor (GPR39) in passive-coping behaviour', *Neuropharmacology*. Elsevier BV, 198, p. 108752. doi: 10.1016/j.neuropharm.2021.108752.

Sato, S. *et al.* (2016) 'Discovery and characterization of novel GPR39 agonists allosterically modulated by zinc', *Molecular Pharmacology*, 90, pp. 726–737. doi: 10.1124/mol.116.106112.

Schacter, D. L. (1987) 'Implicit Memory: History and Current Status', *Journal of Experimental Psychology: Learning, Memory, and Cognition*, pp. 501–518. doi: 10.1037/0278-7393.13.3.501.

Schrag, M. *et al.* (2011) 'Iron, zinc and copper in the Alzheimer's disease brain: A quantitative meta-analysis. Some insight on the influence of citation bias on scientific opinion', *Progress in Neurobiology*. Prog Neurobiol, pp. 296–306. doi: 10.1016/j.pneurobio.2011.05.001.

Schultz, C. and Engelhardt, M. (2014) 'Anatomy of the hippocampal formation', *The Hippocampus in Clinical Neuroscience*, 34, pp. 6–17. doi: 10.1159/000360925.

Sekeres, M. J., Winocur, G. and Moscovitch, M. (2018) 'The hippocampus and related neocortical structures in memory transformation', *Neuroscience Letters*. Elsevier Ireland Ltd, 680, pp. 39–53. doi: 10.1016/j.neulet.2018.05.006.

Selkoe, D. J. and Hardy, J. (2016) ‘The amyloid hypothesis of Alzheimer’s disease at 25 years’, *EMBO Molecular Medicine*, 8(6), pp. 595–608. doi: 10.15252/emmm.201606210.

Sindreu, C. B. *et al.* (2003) ‘Boutons containing vesicular zinc define a subpopulation of synapses with low AMPAR content in rat hippocampus’, *Cerebral Cortex*, 13(8), pp. 823–829. doi: 10.1093/cercor/13.8.823.

De Souza Silva, M. A. *et al.* (2016) ‘Evidence for a specific integrative mechanism for episodic memory mediated by AMPA/kainate receptors in a circuit involving medial prefrontal cortex and hippocampal CA3 region’, *Cerebral Cortex*, 26(7), pp. 3000–3009. doi: 10.1093/cercor/bhv112.

Sowa-Kućma, M. *et al.* (2008) ‘Antidepressant-like activity of zinc: Further behavioral and molecular evidence’, *Journal of Neural Transmission*. J Neural Transm (Vienna), 115(12), pp. 1621–1628. doi: 10.1007/s00702-008-0115-7.

Squire, L. R. (1992) ‘Declarative and nondeclarative memory: Multiple brain systems supporting learning and memory’, *Journal of Cognitive Neuroscience*. J Cogn Neurosci, pp. 232–243. doi: 10.1162/jocn.1992.4.3.232.

Starowicz, G. *et al.* (2019) ‘Long-lasting antidepressant-like activity of the GPR39 zinc receptor agonist TC-G 1008’, *Journal of Affective Disorders*. Elsevier B.V., 245(June 2018), pp. 325–334. doi: 10.1016/j.jad.2018.11.003.

Sugar, J. and Moser, M. B. (2019) ‘Episodic memory: Neuronal codes for what, where, and when’, *Hippocampus*, 29(12), pp. 1190–1205. doi: 10.1002/hipo.23132.

Sun, X. Y. *et al.* (2012) ‘Synaptic released zinc promotes tau hyperphosphorylation by inhibition of Protein Phosphatase 2A (PP2A)’, *Journal of Biological Chemistry*. J Biol Chem, 287(14), pp. 11174–11182. doi: 10.1074/jbc.M111.309070.

Takahashi, K. *et al.* (2018) ‘Memantine ameliorates depressive-like behaviors by regulating hippocampal cell proliferation and neuroprotection in olfactory bulbectomized mice’, *Neuropharmacology*. Elsevier Ltd, 137, pp. 141–155. doi: 10.1016/j.neuropharm.2018.04.013.

Takeda, A. *et al.* (2015) ‘Influx of extracellular Zn^{2+} into the hippocampal CA1 neurons is required for cognitive performance via long-term potentiation’, *Neuroscience*. IBRO, 304, pp. 209–216. doi: 10.1016/j.neuroscience.2015.07.042.

Takeda, A. *et al.* (2017) ‘Extracellular Zn^{2+} Is Essential for Amyloid $\beta_{1–42}$ -Induced

Cognitive Decline in the Normal Brain and Its Rescue', *The Journal of Neuroscience*, 37(30), pp. 7253–7262. doi: 10.1523/JNEUROSCI.0954-17.2017.

Tamano, H., Nishio, R. and Takeda, A. (2017) 'Involvement of intracellular Zn 2 1 signaling in LTP at perforant pathway – CA1 pyramidal cell synapse', (March), pp. 777–783. doi: 10.1002/hipo.22730.

Texidó, L. *et al.* (2011) 'Amyloid β peptide oligomers directly activate NMDA receptors', *Cell Calcium*. Churchill Livingstone, 49(3), pp. 184–190. doi: 10.1016/j.ceca.2011.02.001.

Thackray, S. E., McAllister, B. B. and Dyck, R. H. (2017) 'Behavioral characterization of female zinc transporter 3 (ZnT3) knockout mice', *Behavioural Brain Research*. Elsevier B.V., 321, pp. 36–49. doi: 10.1016/j.bbr.2016.12.028.

Tran, T., Gallagher, M. and Kirkwood, A. (2018) 'Enhanced postsynaptic inhibitory strength in hippocampal principal cells in high-performing aged rats', *Neurobiology of Aging*. Elsevier Inc., 70, pp. 92–101. doi: 10.1016/j.neurobiolaging.2018.06.008.

Tsanov, M. (2015) 'Septo-hippocampal signal processing', in, pp. 103–120. doi: 10.1016/bs.pbr.2015.04.002.

Tulving, E. (1983) *Elements of Episodic Memory*. Cambridge: Oxford University Press.

Vergnano, A. M. *et al.* (2014) 'Zinc dynamics and action at excitatory synapses', *Neuron*, 82(5), pp. 1101–1114. doi: 10.1016/j.neuron.2014.04.034.

Villemagne, V. L. *et al.* (2011) 'Longitudinal assessment of Aβ and cognition in aging and Alzheimer disease', *Annals of Neurology*. Wiley-Blackwell, 69(1), pp. 181–192. doi: 10.1002/ana.22248.

Villemagne, V. L. *et al.* (2014) 'In vivo evaluation of a novel tau imaging tracer for Alzheimer's disease', *European Journal of Nuclear Medicine and Molecular Imaging*. Springer Verlag, 41(5), pp. 816–826. doi: 10.1007/s00259-013-2681-7.

Vorhees, C. V. and Williams, M. T. (2006) 'Morris water maze: Procedures for assessing spatial and related forms of learning and memory', *Nature Protocols*, 1(2), pp. 848–858. doi: 10.1038/nprot.2006.116.

Wang, H. *et al.* (2020) 'Enriched Environment and Social Isolation Affect Cognition Ability via Altering Excitatory and Inhibitory Synaptic Density in Mice Hippocampus', *Neurochemical Research*. Springer, 45(10), pp. 2417–2432. doi: 10.1007/s11064-020-03102-

2.

Wang, P. and Wang, Z. Y. (2017) ‘Metal ions influx is a double edged sword for the pathogenesis of Alzheimer’s disease’, *Ageing Research Reviews*. Elsevier B.V., 35, pp. 265–290. doi: 10.1016/j.arr.2016.10.003.

Wang, Z. *et al.* (2002) ‘Inhibitory zinc-enriched terminals in the mouse cerebellum: Double-immunohistochemistry for zinc transporter 3 and glutamate decarboxylase’, *Neuroscience Letters*, 321(1–2), pp. 37–40. doi: 10.1016/S0304-3940(01)02560-5.

Xia, Z. and Storm, D. R. (2012) ‘Role of signal transduction crosstalk between adenylyl cyclase and MAP kinase in hippocampus-dependent memory’, *Learning and Memory*. Learn Mem, pp. 369–374. doi: 10.1101/lm.027128.112.

Xie, B. *et al.* (2020) ‘Evaluation of the diagnostic value of peripheral BDNF levels for Alzheimer’s disease and mild cognitive impairment: results of a meta-analysis’, *International Journal of Neuroscience*. Taylor and Francis Ltd, pp. 218–230. doi: 10.1080/00207454.2019.1667794.

Xiong, Y. *et al.* (2013) ‘Zinc induces protein phosphatase 2A inactivation and tau hyperphosphorylation through Src dependent PP2A (tyrosine 307) phosphorylation’, *Neurobiology of Aging*. Elsevier, 34(3), pp. 745–756. doi: 10.1016/j.neurobiolaging.2012.07.003.

Xu, Y. *et al.* (2018) ‘Comparing the neuropsychological profiles of mild dementia with Lewy bodies and mild Alzheimer’s disease’, *Psychogeriatrics*. John Wiley & Sons, Ltd (10.1111), 18(1), pp. 64–71. doi: 10.1111/psyg.12293.

Yassa, M. A. and Stark, C. E. L. (2011) ‘Pattern separation in the hippocampus’, *Trends in Neurosciences*, 34(10), pp. 515–525. doi: 10.1016/j.tins.2011.06.006.

Yasuda, S. *et al.* (2007) ‘Isolation of Zn2+ as an endogenous agonist of GPR39 from fetal bovine serum.’, *Journal of receptor and signal transduction research*, 27(4), pp. 235–46. doi: 10.1080/10799890701506147.

Yoo, M. H. *et al.* (2016) ‘Autism phenotypes in ZnT3 null mice: Involvement of zinc dyshomeostasis, MMP-9 activation and BDNF upregulation’, *Scientific Reports*. Nature Publishing Group, 6(June), pp. 1–15. doi: 10.1038/srep28548.

Yoon, D. H. *et al.* (2015) ‘Regulation of dopamine D2 receptor-mediated extracellular signal-regulated kinase signaling and spine formation by GABAA receptors in hippocampal

neurons', *Neuroscience Letters*. Elsevier Ireland Ltd, 586, pp. 24–30. doi: 10.1016/j.neulet.2014.12.010.

Zhao, Q. *et al.* (2018) 'Val66Met Polymorphism in BDNF Has No Sexual and APOE ε4 Status-Based Dimorphic Effects on Susceptibility to Alzheimer's Disease: Evidence From an Updated Meta-Analysis of Case–Control Studies and High-Throughput Genotyping Cohorts', *American Journal of Alzheimer's Disease and other Dementias*. SAGE Publications Inc., 33(1), pp. 55–63. doi: 10.1177/1533317517733037.

Zheng, G. *et al.* (2009) 'γ-aminobutyric acidA (GABAA) receptor regulates ERK1/2 phosphorylation in rat hippocampus in high doses of Methyl Tert-Butyl Ether (MTBE)-induced impairment of spatial memory', *Toxicology and Applied Pharmacology*. Toxicol Appl Pharmacol, 236(2), pp. 239–245. doi: 10.1016/j.taap.2009.01.004.

Zhou, X. *et al.* (2013) 'NMDA receptor-mediated excitotoxicity depends on the coactivation of synaptic and extrasynaptic receptors', *Cell Death and Disease*. Nature Publishing Group, 4(3), pp. e560-11. doi: 10.1038/cddis.2013.82.

Zlomuzica, A. *et al.* (2007) 'NMDA receptor modulation by D-cycloserine promotes episodic-like memory in mice', *Psychopharmacology*, 193(4), pp. 503–509. doi: 10.1007/s00213-007-0816-x.